MODELING OF HYDRODYNAMICS AND SEDIMENTATION IN A STRATIFIED RESERVOIR: TAHTALI RESERVOIR, IZMIR

A Thesis Submitted to
The Graduate School of Engineering and Sciences of
İzmir Institute of Technology
in Partial Fulfillment of the Requirements for the Degree of

MASTER SCIENCE

in Civil Engineering

by
Anıl ÇALIŞKAN

July 2008
İZMİR

We approve the thesis of **Anıl ÇALIŞKAN**

Assist. Prof. Dr. Şebnem ELÇİ
Supervisor

Prof. Dr. Gökmen TAYFUR
Committee Member

Assoc. Prof. Dr. Sevinç ÖZKUL
Committee Member

4 July 2008
Date

Prof. Dr. Gökmen TAYFUR
Head of the Department of
Civil Engineering

Prof. Dr. M. Hasan BÖKE
Dean of the Head of the Graduate
School

ACKNOWLEDGEMENTS

I am very grateful for the encouragement, guidance, understanding, and support of my advisor, Şebnem ELÇİ, for keeping me focused in my research throughout this study. Thanks to the many people at IYTE Department of Civil Engineering who helped me in anyway in this project.

Part of this thesis consisted of field measurements in Lake Tahtalı. It's a pleasure to thank to IZSU (Izmir Water and Sewage Administration) for providing the boat and the personnel of IZSU who helped us in the field. This study would not be possible without the support of European Union (Project number 28292) and The Scientific and Technical Research Council of Turkey (TUBİTAK Project number 104Y321).

Many thanks to my colleagues Ramazan AYDIN, Aslı BOR, and Pelin SELÇUK for their help, also thanks to Nisa YILMAZ for having good times during coffee breaks.

I owe a lot to my friends and my brother Andaç for all their good company, continuous support and interest in what I do. Finally, I would like to thank my mother and father for their boundless love and for all they have done for me.

ABSTRACT

MODELING OF HYDRODYNAMICS AND SEDIMENTATION IN A STRATIFIED RESERVOIR: TAHTALI RESERVOIR, IZMIR

The main goal of this study was to investigate the hydrodynamics of a stratified reservoir for different flow and weather conditions through numerical modeling. This study also investigated the effects of selective withdrawal, climate change, and sediment deposition on hydrodynamics. A three-dimensional numerical model, Environmental Fluid Dynamics Code (EFDC) has been selected in the present study to model the hydrodynamics in the lake. The study site was selected as the main pool of Tahtali Reservoir providing 40% of the water used in the city of İzmir (Population: 3.4 million by 2000). Applied numerical model was validated by monthly observations of water velocity and temperature profiles.

Field measurements were performed from July 2006 to September 2007 in the lake and in two rivers (Şaşal and Tahtali). The water velocity measurements in the lake were made using a 1.5-MHz acoustic Doppler current profiler. For water temperature and quality measurements, a hand-held water quality meter with a depth sensor were used for both lake and river measurements. Furthermore, a weather station was set up by the lake in order to collect accurate data for wind conditions in the study site.

The numerical model predicted the observed velocity profiles and temperature time series satisfactorily. Possible reasons for discrepancies were investigated. Numerical model results indicated that water velocities were strongly dominated by the wind data and correct measurement of wind stress on the lake surface is necessary for accurate prediction of velocities in the water column. Withdrawal of the water at the bottom outlet was found to be the most effective choice encouraging the mixing of the water column. Possible climate change impacts modeled numerically indicated that the thermocline depths were lowered in the water column causing the deterioration of water quality. Sedimentation thickness was estimated via numerical modeling and the long term erosion rate was calculated by USLE method. Modeling the sedimentation zones provided valuable information on the capacity of the reservoir. The results of this study can be used to guide the further investigations in the lake including modeling of water quality for better management practices.

ÖZET

TABAKALAŞMANIN OLUŞTUĞU BARAJ GÖLLERİNDE HİDRODİNAMİĞİN ve KATI MADDE BİRİKİMİNİN MODELLENMESİ: TAHTALI BARAJ GÖLÜ, İZMİR

Bu çalışmada, yaz aylarında hava sıcaklıklarındaki artış ile birlikte yoğun tabakalaşmaya maruz kalmış bir baraj gölünün hidrodinamiği, nümerik model kullanarak incelenmiştir. Su çekilme etkileri ve beklenen iklim değişikliklerinin tabakalaşma üzerindeki etkisi araştırılmış ve parçacıkların taşınımı ile birikme yerleri de modellenmiştir. Nümerik model olarak, 3 boyutlu bir program olan EFDC (Çevresel Akışkanlar Dinamiği Kodu) kullanılmıştır. Çalışma alanı olarak, İzmir ilinin % 40'ının içme suyunun karşılayan Tahtalı Baraj Gölü seçilmiştir. Uygulanan nümerik model, aylık akım hızı ve su sıcaklığı ölçümleri ile doğrulanmıştır.

Arazi ölçümleri, Temmuz 2006 ile Eylül 2007 tarihleri arasında yapılmıştır. Akım hızı, sıcaklık profili ve derinlik ölçümlerinde, akustik metot ile çalışan aletler tercih edilmiştir. Çalışmada kullanılacak olan meteorolojik veriyi toplamak üzere, göl kenarına meteoroloji istasyonu kurulmuştur. Kullanılan nümerik model, akım ve sıcaklık profillerini başarılı bir şekilde tahmin etmiştir. Oluşan farklılıkların sebepleri de araştırılmıştır. Çıkan nümerik model sonuçları, akım hızlarının rüzgâr şiddetinden önemli ölçüde etkilendiğine ve hassas rüzgâr ölçümlerinin model sonuçlarını çok daha doğru bir noktaya taşıyacağına işaret etmiştir. Su çekilme etkisinin araştırılması sonucunda, en alttaki kapaktan su çekilmesinin, su sütununda en fazla karışımı yarattığı saptanmıştır. Olası iklim değişikliği modellenerek, hava sıcaklıklarındaki artışın su sütunundaki tabakalaşmayı arttıracağı ve sonuç olarak göl su kalitesini düşüreceği saptanmıştır. Parçacık taşınımı ve birikme yerleri, nümerik model yardımi ile araştırılmış ve havzada uzun dönemde oluşan erozyon miktarı da USLE metodu ile hesaplanmıştır.

Yapılan bu çalışma, ileride yapılacak olan su kalitesi ile ilgili modelleme çalışmalarına ışık tutacaktır ve sürdürülebilir havza yönetimi için rehber oluşturacaktır.

TABLE OF CONTENTS

LIST OF FIGURES

Figure **Page**

LIST OF TABLES

CHAPTER 1

INTRODUCTION

Sustainable management of water resources is vital. Thus; both the quality and the quantity of water resources are very important and should be maintained to meet the needs of both environment and the living-beings. The hydrodynamic structure of a lake is affected by different meteorological factors such as short-wave solar radiation, inflows and outflows, rain, evaporation, precipitation, and wind. Wind, source of kinetic energy for mixing, is the major controlling factor in a lake. Strong winds cause mixing and decrease the intensity of stratification in lakes. Temperature is also one of the important parameters affecting the vertical structure of the water column and leading to stratification. Inflows are important especially for the life expectancy of reservoirs by carrying sediments into the lake. The hydrodynamic processes in a lake are shown in Figure 1.1. These processes are studied through both numerical modeling and field measurements here.

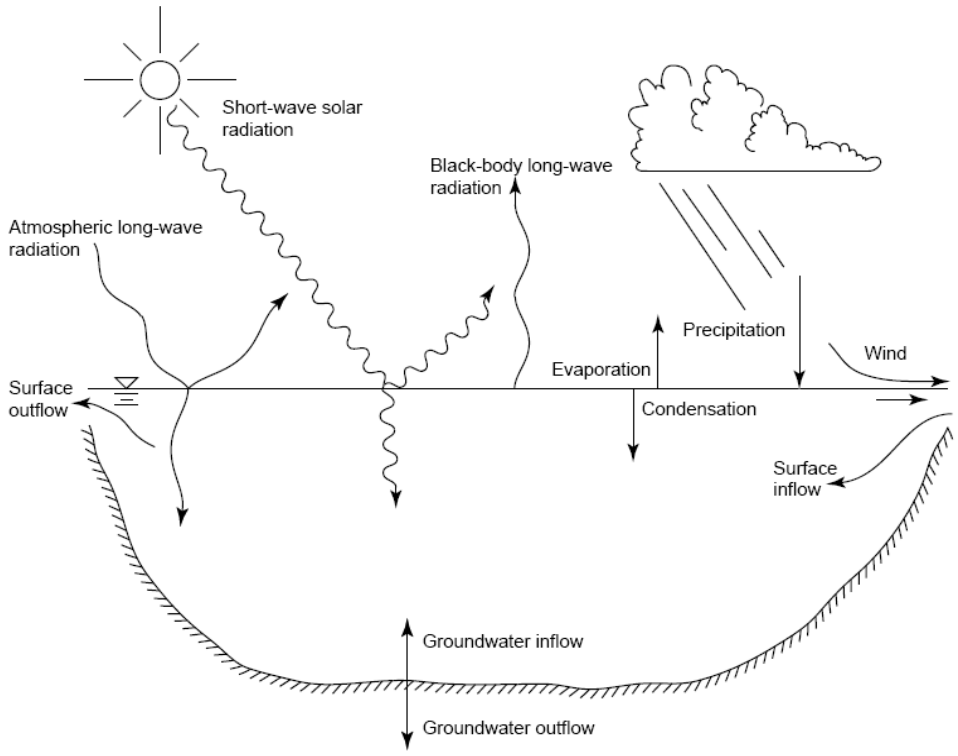

Figure 1.1. Schematic of the energy inputs to a lake

(Source: Fischer, et al. 1979)

The main goal of this research is to examine the effects of hydrologic, atmospheric, and topologic factors on hydrodynamic structure of Lake Tahtali through numerical modeling and physical measurements. Having achieved this goal, several other topics were investigated including; the effect of selective water withdrawal by water intake on stratification structure of the water column; the effect of climate change on stratification; and the deposition of sediments within the lake.

The complexities of the hydrodynamic processes in a reservoir suggest the use of numerical modeling approaches to provide a description of circulation, mixing and density stratification for better management strategies to meet the desired requirements. Hydrodynamic models use reservoir geometry, inflows, withdrawals, and meteorological data to simulate water levels, flow velocities, and temperatures. In a reservoir, wind-generated surface stresses, buoyancy or density forcing, turbulent momentum and mass transport should all be simulated by the model. A validated numerical model simulating hydrodynamic processes in Lake Tahtali would be very valuable for future contamination and sediment transport studies in the lake. A 3–D hydrodynamic model; Environmental Fluid Dynamics Code (EFDC) developed by Hamrick (1996) has been selected to model the hydrodynamics of Lake Tahtali to simulate velocity and temperature profiles due to wind forcing and inflows/outflows, and results were compared to the measured velocity and temperature data. Many reservoirs, including Tahtali, are located along major river beds necessitating including all three dimensions of flow in the analysis of hydrodynamics. Thus 1-D models are insufficient in this sense, and a 3-D hydrodynamic model was utilized in this study.

Selective withdrawal of water from intake of water supply reservoirs has been commonly used as reservoir management strategy to meet the downstream water quality demands. When water is released from hypolimnion in stratified reservoirs, anoxic water can result in poor water quality since it might contain dissolved iron, manganese, sulfide, ammonium and phosphate (Dortch 1997). In this study, temperature and velocity profiles are modeled using four different outlets located along the intake structure; and the best outlet level for water withdrawal encouraging mixing and thus improving water quality is discussed.

Climate change effects on hydrodynamics were also examined through numerical modeling. The results of climate change scenarios modeled by Dokuz Eylul University Water Resources Research Center for projection of climate in Menderes,

Izmir (belonging to years 2050, and 2100) were used as an input to the numerical model. In this study, these projections were utilized in the numerical model to predict water temperatures of the reservoir in the future.

Management of soil and water resources is one of the most critical environmental issues facing many countries, developing countries in particular, due to its wide range of impacts on water supply, water quality, flood control, soil erosion, irrigation, tourism, reservoir management and fishing, etc. It is necessary to predict effects of sedimentation and loss of storage capacity for better operation of the reservoirs. For this reason, transport of sediments by the rivers to the lake and the sedimentational zones in the lake were also modeled in this study. The sedimentation patterns were estimated utilizing numerical model and also compared to preliminary estimates of watershed sediment yield which derived from USLE – Universal Soil Loss Equation.

The study was carried out in Lake Tahtali, Turkey, which is a very important drinking water supply reservoir, providing 40% of the water used in the city of Izmir (Population: ~ 3.4 million by 2000). Influence of stratification on water quality and hydrodynamics was investigated in this research since the lake is strongly stratified in summer.

This thesis includes ten chapters. Chapter 1 aims to present a brief introductory background to the research subject. Previous relevant studies regarding numerical modeling of reservoirs are reviewed in Chapter 2. In Chapter 3, the study site is described including the location and geometry, and the hydrology of the region. The numerical model chosen to model the hydrodynamics, the governing and the boundary conditions of the numerical model used in the study, and the testing of the model are described in Chapter 4. Chapter 5 discusses the modeling of hydrodynamics in Lake Tahtali. Field data collection strategy in Lake Tahtali, instrumentation, and the comparison of the numerical model results with the field measurements is discussed in Chapter 6. In Chapter 7, effects of selective withdrawal on hydrodynamics are discussed. The effects of climate change on hydrodynamics are described in Chapter 8. In Chapter 9, modeling of sediment transport and deposition, and a method to predict the long term soil erosion is presented with the comparisons of the modeled and the calculated deposition rates and zones. Finally, in Chapter 10, the main results and the conclusions of the study are summarized.

CHAPTER 2

LITERATURE REVIEW

The previous research studies on stratified lake hydrodynamics included development of numerical schemes for heat transport and application of existing numerical models to water systems. Hydrodynamics in the lake including transport of heat, effects of selective water withdrawal, effect of climate change, and transport of sediments were modeled in this study. This chapter presents a literature review of similar studies conducted in the world.

2.1. Studies on Modeling of Heat Transport

Temperature is the major controlling factor on hydrodynamics of lakes by forming different density gradients in vertical. Numerical models provide description for the effects of heat transport on hydrodynamic structure of lakes. There are different studies carried out about the effects of temperature on hydrodynamics in literature.

Many studies in literature have investigated hydrodynamics of water systems to provide a description of the flow fields through numerical modeling in lakes, rivers, and estuaries (Johnson, et al. 1993, Appt, et al. 2004, Blumberg, et al. 1999, Jin, et al. 2000, Yang, et al. 2000, Rueda and Schladow 2003, Falconer, et al. 1991). EFDC, CH3D, DYRESM, ECOM, SI3D-L are the widely used numerical models in the studies discussed above.

Ottosson and Abrahamsson 1998 presented a numerical approach for simulation of heat transport in epilimnion and hypolimnion of the water column, which was later used as a sub-model in many models concerning lake ecosystems (Appelgren, et al. 1996, Monte, et al. 1997). The temperature model was calibrated based on the available empirical data from eleven Swedish lakes and one Italian lake. For practical use, the simulation of retention of caesium in lake water was presented, using the temperature model as a sub-model**.** The starting point for this work is an approach to model water temperatures (Håkanson 1996). In this study, the model predicted epilimnetic temperatures in these lakes very well. However, the results for the hypolimnetic

temperatures were not as good. It was concluded that it was because the data were collected from different depths for different years, so this situation increased the difficulty of deciding which empirical data should be used for the hypolimnetic temperature. The water retention time simulations for the caesium from the lake overestimated the caesium concentrations in the lake.

Rueda and Schladow 2003 investigated the dynamics of Clear Lake, California using a three-dimensional (3D) hydrodynamic model. Rueda et al. (2003) conducted the field experiment part of this study. The numerical model (SI3D-L) uses an accurate and efficient semi-implicit finite difference algorithm for the hydrodynamic equations based on the continuity equation for incompressible fluids, the Reynolds-averaged form of the Navier-Stokes equations for momentum, the transport equation for temperature, and an equation of state relating temperature to fluid density. The research has been focused on the internal circulation in the lake. Clear Lake was contaminated with mercury and investigating its circulation was important to understand the redistribution of mercury throughout the water body. The simulations indicated that the interaction of stratification, periodic wind forcing, and Coriolis effects (Earth's rotation) drove the circulation in the lake. The temperature results were gathered from three different stations and the velocities were recorded at one station. The simulation results were in agreement with the observations conducted in the lake.

Jin et al. (2000) applied a three-dimensional hydrodynamic and heat transport model for Lake Okeechobee located in South Florida. Lake Okeechobee is a large, shallow subtropical lake with a surface area of 1,730 km^2 and it is the second largest freshwater lake in the United States. The Environmental Fluid Dynamics Code (EFDC) was used in this study. They compared EFDC to another code, Estuarine Coastal and Ocean Model (ECOM). A 28-days calibration was conducted utilizing measured bathymetry, rainfall, relative humidity, total solar radiation, wind speed, inflow, and outflow data. Precipitation, air temperature, relative humidity, and solar radiation data were collected at three in-lake stations every 15 minutes. Wind data were collected at four in-lake stations every 15 minutes. EFDC model simulated water surface elevations, velocities, and temperatures. They pointed out that wind was the major factor driving circulation with also temperature being important. Inflows and outflows had only localized effects, due to the lake's large surface area. Comparisons between the

measurements and the simulation results showed that the model predicted the observed trends about vertical mixing and lake wide circulation patterns reasonable accurate.

Schladow and Thompson (2000) investigated the winter thermal structure of Lake Tahoe, in the Sierra Nevada Mountains of California and Nevada for four winters (from 1996 to 1999) using thermistor chains. Lake Tahoe has 35 km length and 19 km width with an average depth of 301 m. It is the second deepest lake in the United States and the eleventh deepest in the world. An energetic internal wave spectrum was observed in the lake. The deepest vertical mixing resulted from intense storm events and dynamic responses within the lake. Deep mixing was more intense in 1998 and 1999 due to higher winds and weaker initial stratification conditions. During the four years, bottom temperatures ranged between 4.84°C to 5.09°C. A one-dimensional (1D) lake model DLM was used to simulate mixed layer deepening for two years. Long term monitoring of parameters including Secchi depth, primary conductivity, and nutrient concentrations has provided invaluable information about the hydrodynamic structure of Lake Tahoe. The information about these parameters helped the water clarity dynamics, and how pollutants affected water clarity. The overall model results of the vertical temperature structures agreed well with the measured data.

Another study was carried out by Bell et al. (2006) where a one-dimensional two-layer lake model was used to simulate the daily temperature and oxygen profiles of Lake Bassenthwaite (an English Lake) in response to changes in wind, air temperature and radiation. Lake Bassenthwaite has a surface area of 5.2 km^2, and a mean depth of 5.3 m. Stratification is intermittent and strongly influenced by the velocity of the wind in this lake. Vertical variations in water temperature and the concentration of oxygen were recorded by a sonde and the transparency of the water was measured using a white Secchi disk. The model has been tested over an 8-year period from 1991 to 1999 utilizing daily weather data and fortnightly observations of chlorophyll a and Secchi depth. The simulated and observed oxygen profiles were in reasonable agreement.

Cesare et al. (2006) investigated the circulation in stratified lakes due to flood-induced turbidity currents. The impact of river born turbidity currents was investigated in Lake Lugano located between Italy and Switzerland under varying conditions using data measured at the inflow river and inside the lake, together with a three-dimensional numerical model (CDF) of the lake. Due to its vast volume compared to the tributaries' inflow volume, the theoretical water renewal time was estimated to be around 12 years.

The observed temperature profile indicated a strong stratification by the end of the summer. The thermocline located between 10 and 20 m with a sharp drop in temperature from 24°C to 5.5°C. It was observed that the strong thermal stratification could not prevent the development of bottom turbidity currents during major flood events resulting in the destabilizing of the water column due to the warmer river water and the water uplift induced by the hydrodynamic impact of the current.

In a research conducted by Patterson et al. (1984), vertical temperature and salinity structures of Wellington Reservoir (Western Australia) and Kootenay Lake (British Columbia) were simulated using field data and one-dimensional numerical model (DYRESM) with good results. They calculated Wedderburn number; a value used to understand the relative importance of surface stirring and shear production. For Wellington Reservoir, it was calculated $W>10$ most of the period whereas calculated $W<3$ for Kootenay Lake.

Hondzo and Stefan (1991) made simulations on stratification in Calhon, Elmo, and Holland lakes in U.S.A. and observed that summer stratification was getting harder as years pass due to the increase in air temperatures.

2.2. Studies on Modeling of Sediment Transport

Sediment transport in water systems is important affecting water quality and the life expectancies of the reservoirs. Thus, it's one of the most important factors that should be well assessed in design of reservoirs.

There are many studies in literature conducted to investigate the effective volume of the reservoirs (Arnold, et al. 1987, Lo 1994). Studies about sediment transport mainly investigated hydrodynamic processes and their driving forces to understand how sediments are transported, deposited, and resuspended in water systems through numerical modeling and surveying of reservoirs (Sheng 1984, Blumberg and Mellor 1987, Krone 1962, Mehta, et al. 1989).

Jin and Ji (2005) carried out a study on the validation and application of a hydrodynamic sub-model of Lake Okeechobee environmental model (LOEM) modified from the environmental fluid dynamics code (EFDC). The model simulated the sediment resuspension and transport due to the wind driven current and waves. The model investigated how and under what conditions the sediment was transported and

resuspended in shallow waters. The LOEM simulated the phosphorus concentrations in the lake in a 1 year validation from 1999 to 2000. The model results were used to predict the impact of sediment transport under different management scenarios and environmental conditions such as water levels and storm events. The velocity and the profile data were collected by Acoustic Doppler Current Profilers at four stations. They reported that the critical bottom shear stress for sediment deposition and resuspension were the most important parameters for the modeling of sediment transport. The critical stress of 0.18 N/m^2, a settling velocity of $1x10^{-5}$ m/s was used for sediment. A spectral wind-wave model SWAN was used to compute the significant wave height and the period. The model results of water elevation matched the observed data. This model was also used to estimate light extinction coefficient. Data of Secchi depth, light extinction coefficient, and total suspended solids were used for the empirical formula that was incorporated into the LOEM. The LOEM was also used to estimate the total phosphorus (TP) flux between the bay and open water.

Elci et al. (2007) described the erosion and deposition of cohesive sediments in a thermally stratified reservoir. Hartwell Lake, Georgia is a 227 km^2 hydropower reservoir with a maximum depth of 50 m. Sedimentation in the reservoir was modeled using a three-dimensional numerical model for different wind, inflow and outflow conditions. The reservoir was periodically strongly stratified, so the effect of thermal stratification on stratification patterns was investigated. They pointed out that although sedimentation in a reservoir is often modeled considering only the deposition of sediments delivered by tributaries, the sediments eroding from the shorelines could have significant effects to the sedimentation in the lake.

2.3. Studies on Selective Withdrawal

Water supply reservoirs are thermally stratified in summer months. Selective water withdrawal by intakes is very important by causing mixing and affecting the quality of water in lakes. So, the effect of selective withdrawal should be investigated to make the quality of water in the reservoirs better. This kind of studies conducted in literature would be useful in reservoir management (Brooks and Koh 1965, Elwin and Slotta 1969). The theories about withdrawal effect have also been discussed in several experimental papers (Debler 1959, Walesh and Monkmeyer 1970).

Recent research about selective water withdrawal included the study conducted by Casamitjana et al. (2003) where the effects of water withdrawal level in stratification patterns of a reservoir were presented using a 1-D lake model. The lake model is the Dynamic Layer Model (DLM). Two outlets were considered in the study. The model predicted the experimental temperature obtained in these months. The model was used to simulate the possible withdrawal scenarios. They indicated that the thermocline occurred at the depth where water was withdrawn.

In another study, Bonnet et al. 2000 stated that the vertical thermal structure clearly depended on the outlet level. If the lower outlet was used in summer, the thermocline became deeper. They simulated the hydrodynamic and thermal structure of an artificial lake located in France. The maximum depth of the reservoir was 45 m with a surface area of $7x10^6$ m^2. The residence time was relatively short in springtime (less than 3 months). It increased in summertime by decreasing of inflow when the water quality of the reservoir was less influenced by the river. The withdrawal period was generally between July and September. One-dimensional (1-D) numerical model was developed as a basis for an ecological water quality model. The model also discussed the effects of inflows and outflows. One-year data were used for calibration whereas the data collected over the other two years were used for the validation of the model. The model fitted the measured data well. The largest discrepancy between the measured and modeled temperatures was at the beginning of the simulation period (mid-April). The calculated temperatures were too low, indicating that the heat balance at this time was not very well estimated.

The effect of long internal waves on the quality of water withdrawn from a stratified reservoir was investigated by Anohin et al. (2006). The study site is Lake Burragorang, a long (57 km) canyon-shaped reservoir, located in Australia. The theory of selective withdrawal was discussed. Wind is an important feature influencing the dynamics of the canyon. Sensors to measure temperature, conductivity, turbidity, and pH were installed inside the main outflow pipelines, recording water quality parameters of the withdrawn water. The seasonal variation of wind speed and direction over the lake was also observed. Due to wind forcing, basin-scale seiches were generated at the thermocline after storm events. The increased stratification led to decreased internal wave activity. Lake number was calculated to quantify the internal wave activity. As a result, the data showed that, on a seasonal scale, basin-scale internal waves had a strong

effect on the temperature of the outflows. Wind-driven circulation observed in the surface layer had little or no effect on the temperature of the withdrawn water.

Another study based on the effect of withdrawal on water quality was conducted by Dortch (1997). The relationship of selective withdrawal and water quality was also discussed. Water quality treatment techniques were presented. Mathematical modeling was utilized to evaluate the effects on water quality of reservoir management options. Outflow management can be consist of controlling the outflow rate, outlet location and timing of releases, and treating the release, such as aeration. In-reservoir treating techniques were discussed including: destratification; hypolimnetic aeration/oxygenation; underwater dam; pool drawdown; dilution; phosphorus inactivation; sediment removal; harvesting; biological controls; herbidices and algicides. Hydraulic or pneumatic pumping can be used to disrupt or prevent stratification.

The effects of withdrawal on hydrodynamic structure of stratified reservoir were studied by Mahony and Pritchard (1981). They made a series of laboratory experiments to describe the features of the flow field. The tank was filled up with the stratified brine solution. A flow-control valve was adjusted to give the flow rate required for the experiment. The results of five experiments conducted indicated that the main horizontal motions were confined to a thin layer near the level of the outlet orifice, and the maximum velocities were observed near the lower lip of the outlet slot. Maximum velocities started to decrease with the distance from the outlet. The photographs indicated a recirculation at this zone and the width of withdrawal layer formed in a uniform structure.

2.4. Studies on Effect of Climate Change on Reservoir Hydrodynamics

In literature, previous studies exist describing the effect of climate change on hydrodynamic processes and the application of numerical hydrodynamic models to lakes and reservoirs. The potential effects of climate change were investigated from the analyses how biological components of lakes may respond (Hill and Magnuson 1990, Shuter and Post 1990, Meisner 1990, Minns and Moore 1992), and from the analyses indicating that most of the lakes act as a source of CO_2 because they are supersaturated relative to the atmosphere (Cole, et al. 1994). Several studies have conducted to

understand how climate change affects lake systems (Stefan and Fang 1994, McLain, et al. 1994)

De Stasio et al. (1996) used a 10-year record of the thermal characteristics of four lakes at the North-Temperature Lakes Long-Term Ecological Research site in Wisconsin (Trout, Sparkling, Crystal, and Mendota Lakes) to validate simulations of lake physics utilizing a reservoir simulation model. A one-dimensional physics based lake numerical model; DYRESM was used for water temperature and salinity scenarios with $1xCO_2$ and $2xCO_2$ climate conditions from the day of ice breakup to the date of ice formation. Lake morphometry and daily meteorological data were used as an input to the numerical model. A series of horizontal layers of variable thickness were simulated. They investigated the lake thermal structure, fish and plankton habitat availability, and habitat overlap between planktivorous fish and their pray as measures of the fate of climatic signals as they are transmitted through lake systems. Simulations for cool, warm, and intermediate years were rerun with a doubling of CO_2. Model results indicated an increase in epilimnetic temperatures between 1-7^{o}C, and an earlier stratification was observed which lasted longer.

In another study conducted by Leon et al. (2005), heat fluxes and temperature distributions to and from lakes especially during the thermally stratified ice-free periods were investigated applying a 3-D ELCOM (Estuary and Lake Computer Model) model. The numerical model was integrated with a regional climate model (CRCM). Large Canadian lakes such as Lake Erie, Lake Ontario and Great Slave Lake that have different morphometry over contrasting climatic regions were selected as study sites. Output data of ELCOM model were exported to be used as input for the next time step in the other model (CRCM). As a result, the 3-D hydrodynamic model was successfully applied to Lake Erie and connected the 3-D model results with the CRCM model.

Tucker and Slingerland (1997) investigated the efforts to understand the connection between climate change and drainage basin response using nine different climate change scenarios for different runoff, and critical shear stress required for sediment transport. The sensitivity of basins that are controlled by threshold flow erosion to climate change is analyzed using a physically based model of drainage basin evolution. The GOLEM model simulates basin evolution under the action of weathering processes, hillslope transport, and fluvial bedrock erosion and sediment transport. An increase in runoff intensity will lead to rapid expansion of the channel network, with the

resulting increase in sediment supply initially generating aggradation along the main network, followed by downcutting as the sediment supply tapers off. By contrast, a decrease in runoff intensity will lead to a retraction of the active channel network and a much more gradual geomorphic response.

In the study of Matzinger et al. (2007), it was observed that the expected increase in air temperatures as a result of climate change would prevent mixing in the lake meaning less dissolved oxygen in water.

In another study made in large Italian lakes showed that increasing air temperatures would lengthen the reservoir's retention time (Ambrosetti, et al. 2003).

CHAPTER 3

STUDY SITE

This study was carried out in Lake Tahtali (Figure 3.1), Izmir, Turkey. It was selected as study site because Tahtali Reservoir is a very important water resource providing drinking water for the city of Izmir. The lake experienced dense stratification during summer months and as a result of this stratification, the habitants are under the risk of bad drinking water quality. Another reason for this selection was the boat provided by IZSU during the field measurements to access the different parts of the lake.

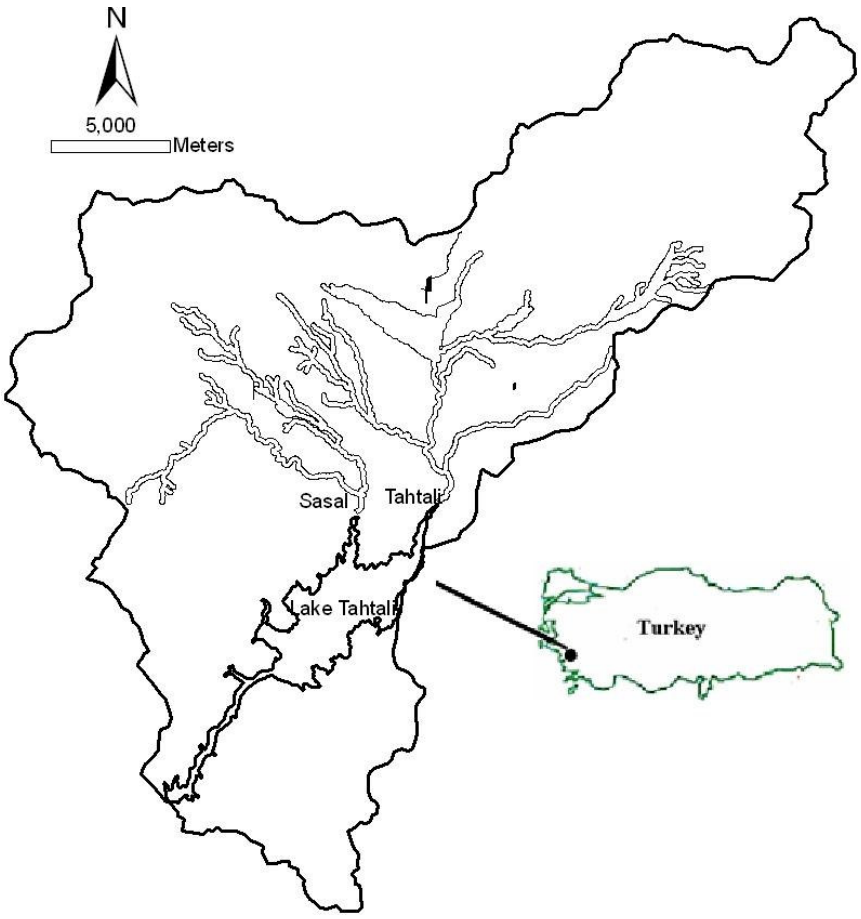

Figure 3.1. Map of study area: Tahtali Basin

3.1. Location and Geometry

The observations were conducted in Tahtali Reservoir, Menderes, Turkey (38º08' N, 27º06' E). Tahtali Dam was projected as a rockfill dam and completed in 1996 to supply fresh water to Izmir, the third largest metropolitan area with over 3 million populations.

Tahtali Reservoir has a surface area of 20 km^2, a mean depth of 15 m, with a maximum depth of 27 m corresponding to the time when the mean water level was 60 m. The capacity of the dam is 175 million m^3 and it generates monthly 5 million m^3 water in total with an average water of 3 m^3/s. The dam is currently operated by IZSU (Izmir Water and Sewage Administration)

3.2. Hydrology

The major inflows are from North via Sasal Stream and Tahtali Stream. Sasal Stream contributes 25% whereas Tahtali Stream contributes 75% to the total inflow. The discharges of the other four streams are negligible. Monthly average discharges due to inflows from two rivers, measured by DSI (General Directorate of State Hydraulic Works) are available in Figure 3.2. Soil granulometry of rivers and the lake are illustrated in Figure 3.3 indicating soil type as silty clay. Soil characteristics of the lake (Figure 3.4) belong to year 1995 shows that Tahtali River carried more alluvial soils when compared to Sasal. The site is exposed to the full force of wind blowing mostly from East as well as from North. The average annual wind speed is 3 m/s as recorded at the weather station. Long term average data of precipitation and water temperature in Menemen, Izmir are illustrated in Figure 3.5. The seasonal variation of water level, water withdrawal, evaporation and rainfall measured in 2006 are illustrated in Figure 3.6. Water elevation has increased after rain events occurred in January, February and March. The locale has a Mediterranean climate, with average annual temperatures for the warmest month July at 28ºC and for the coldest month January at 8ºC. Stratification in the lake starts in April and decrease by the end of September.

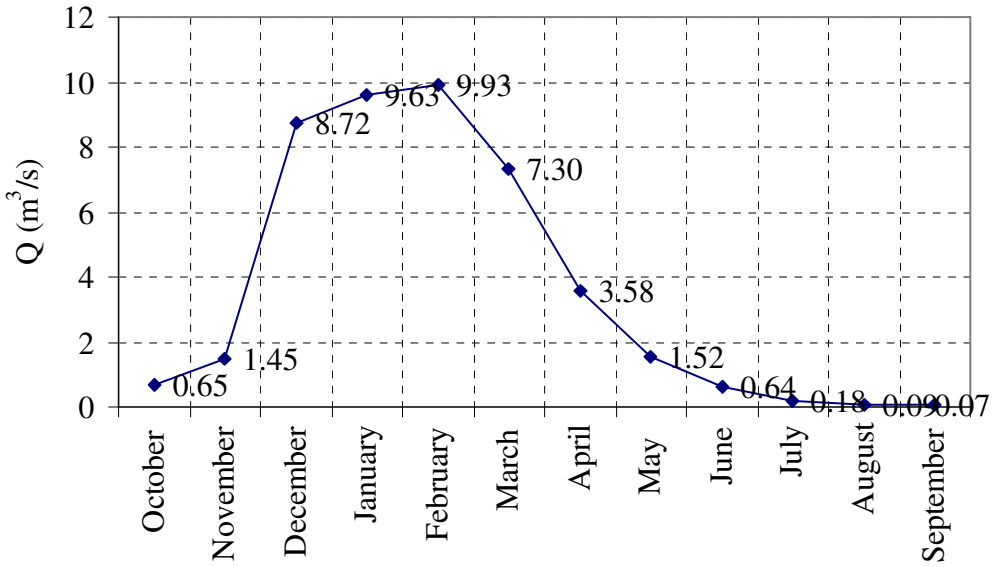

Figure 3.2. Lake Tahtali long term average discharges measured by General Directorate of State Hydraulic Works

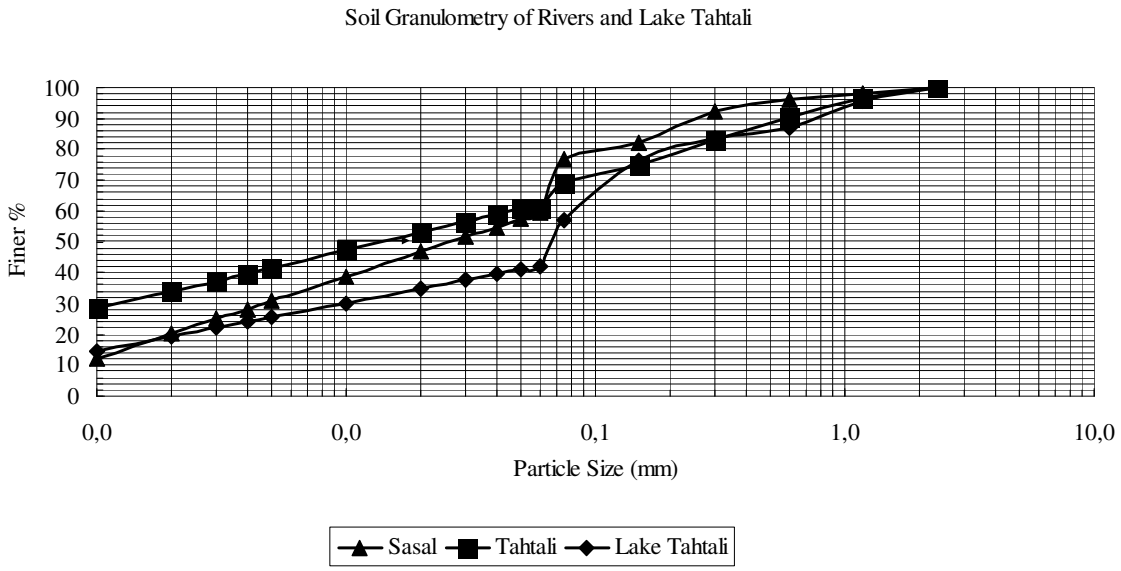

Figure 3.3. Soil Granulometry of rivers (Şaşal; Tahtali) and Lake Tahtali

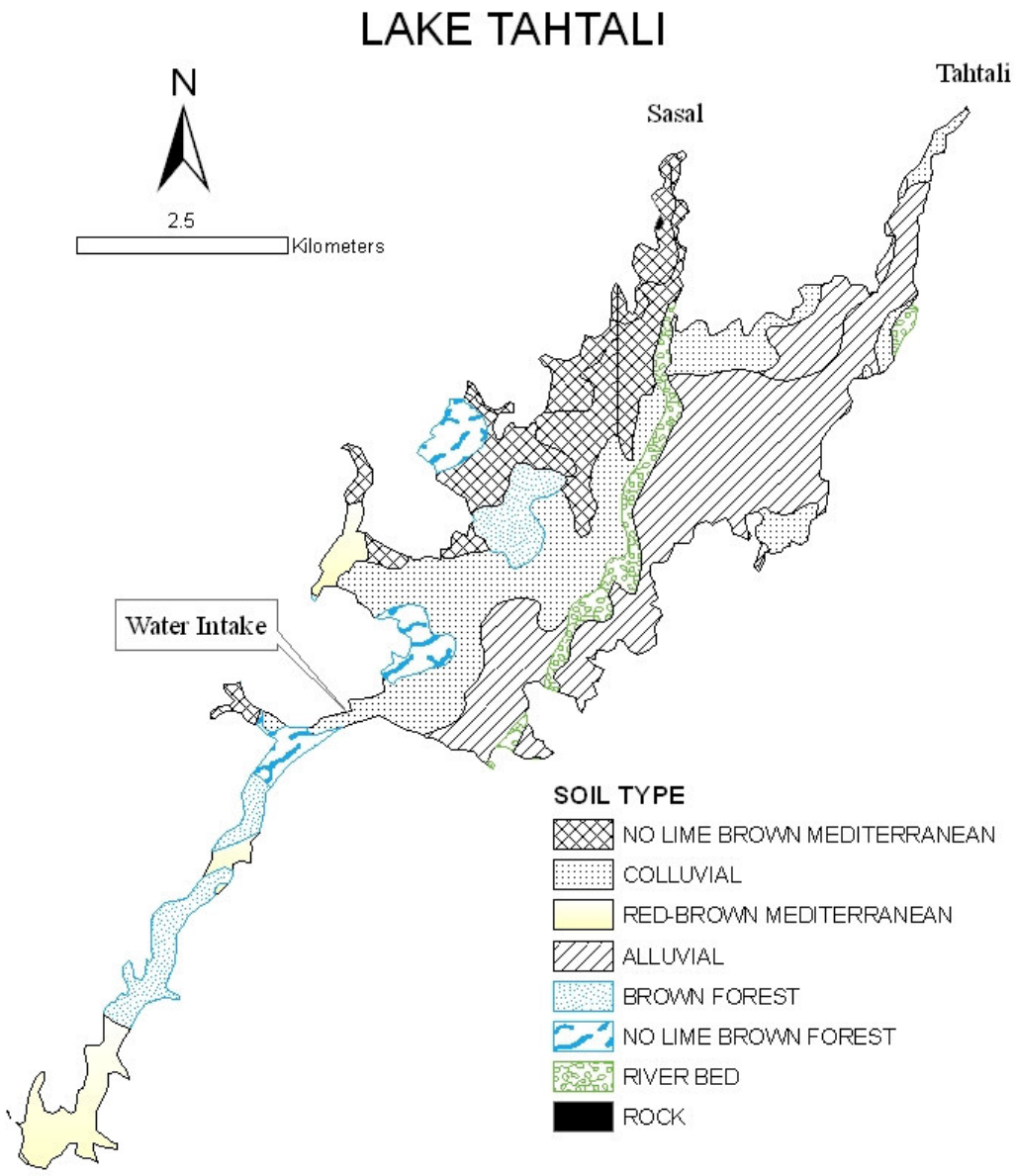

Figure 3.4. Map of Lake Tahtali showing soil characteristics of the area in 1995 and the location of water intake structure

The withdrawal point is at Southwest location in the lake from the deepest area corresponding to 27 m. There's a water intake structure in the lake constructed as reinforced concrete. The water is provided as drinking water for the city of Izmir after being treated. Water is generally withdrawn from hypolimnetic layer with an average flow rate of 3 m^3/s. The retention time of the reservoir is 2.5 years calculated based on

the volume of the lake and outflow rate as compared to the retention times of 3 months in Villerest reservoir (Rueda, et al. 2003), 191 years in Lake Superior, 2.6 years in Lake Erie, and 6 years in Lake Ontario.

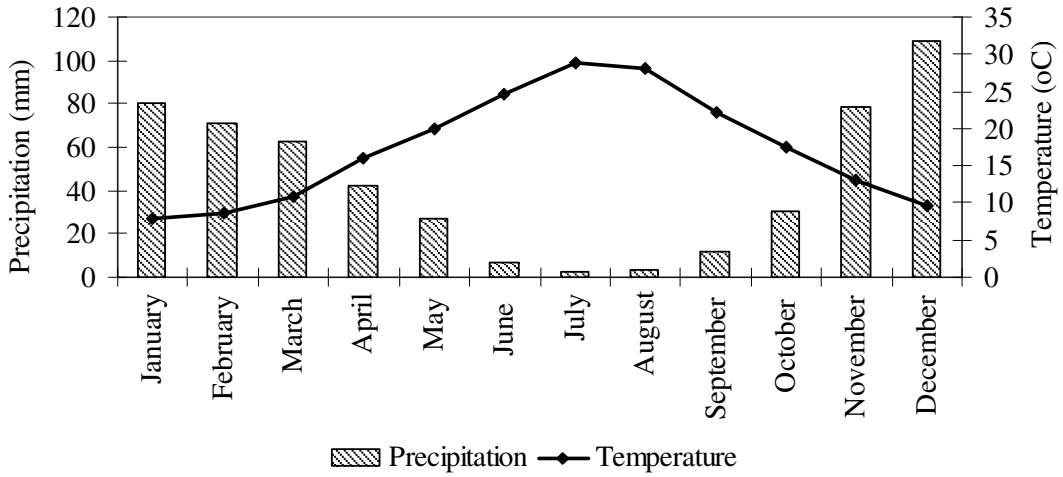

Figure 3.5. Long term average data of precipitation and rain values for Menemen, İzmir

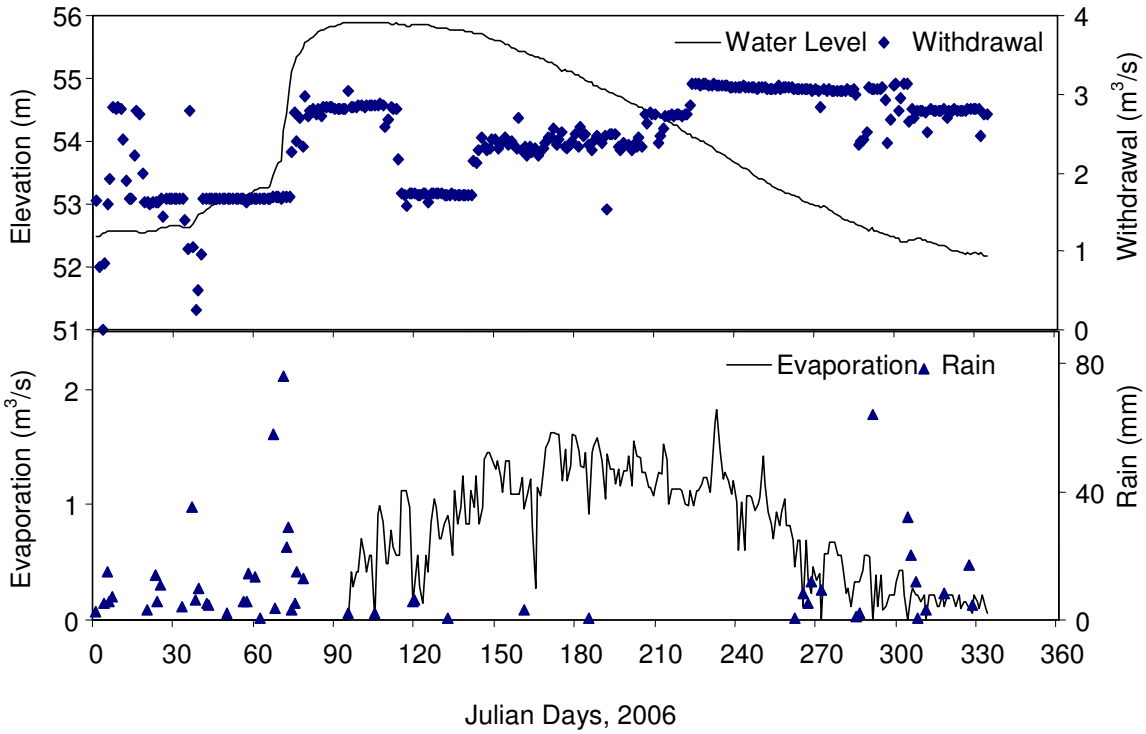

Figure 3.6. Time series of water level, withdrawal, evaporation, and rainfall measured in Lake Tahtali during 2006

CHAPTER 4

HYDRODYNAMICS AND SEDIMENT TRANSPORT MODEL

In recent years, numerical models are widely used since the complexities of the hydrodynamic processes in a reservoir necessitate the use of numerical modeling approaches that provide accurate description of mixing within a water body. Numerical models can simulate different scenarios and cost less when compared to physical models. For these reasons, a numerical model was utilized in this study to describe the hydrodynamic processes in Lake Tahtali. The Environmental Fluid Dynamics Code (EFDC) was selected for this purpose. EFDC is a widely used and tested numerical model developed by Hamrick (1996) that can simulate flow processes in all three dimensions in rivers, lakes, reservoirs, estuaries, wetlands and coastal regions fully time varying including density variation. The EFDC model was originally developed at Virginia Institute of Marine Science for estuarine and coastal applications. In addition to hydrodynamics, salinity, and temperature transport simulation capabilities, EFDC is capable of simulating cohesive and non-cohesive sediment transport, near-field and far-field discharge dilution from multiple sources, the transport and fate of toxic contaminants in water and sediment phases (EPA 2006).

4.1. Governing and Boundary Equations

The EFDC numerical model uses a finite difference scheme based on hydrostatic hydrodynamic equations and transport equations in vertical and horizontal coordinate systems which may be Cartesian or curvilinear-orthogonal. EFDC is coded in FORTRAN77, and it is PC compatible. The source code is 52124 lines broken into 145 subroutines. An implicit integration scheme is used to solve the governing mass-balance equations. Various options can be used in EFDC including “centered in time and space” and, “forward in time and upwind in space” schemes. Figure 4.1 shows the numerical model grid generated for Lake Tahtali. The numerical model grid was generated due to

the –x and -y coordinates extracted from the digitized maps of the basin belong to year 1995 using natural neighbor method in ArcMap and Surfer programs. At the beginning, the depth of the contour lines belong to the basin was not specified in the attributes table in ArcMap, so each contour line at 5 m depth intervals was scanned and exported as different shape files including the boundary shape file corresponding to 60 m elevation (water surface). These shape files were opened in Surfer and the coordinates were extracted in text format. This text file was used to generate the grid of the numerical model in EFDC which the grids were consisted of 78 rows and 78 columns with 100 m wide on each side and the number of the active cells was 2040.

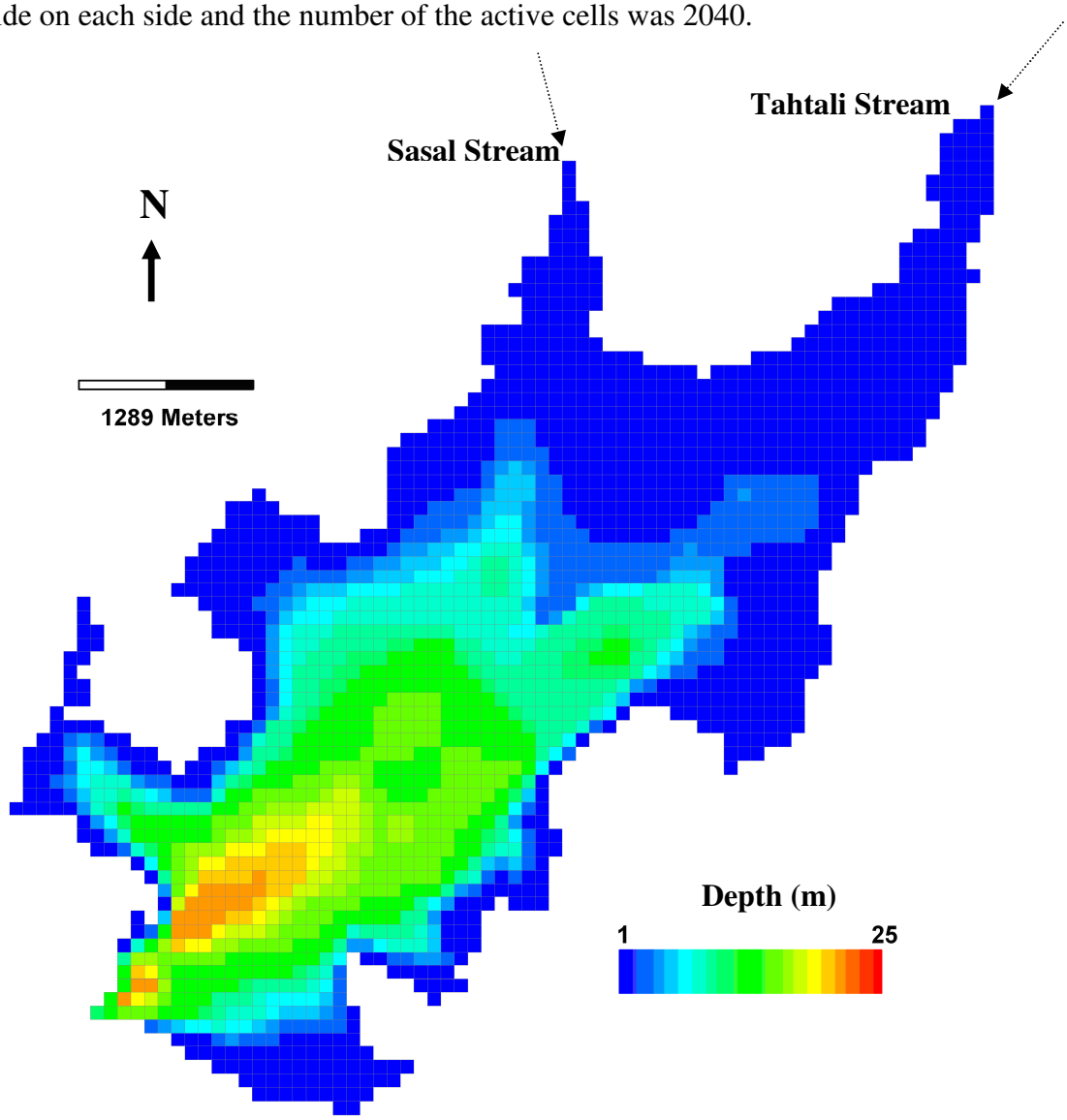

Figure 4.1 Bathymetric map of Lake Tahtali derived from topographic maps in 1995 showing two major streams. The length of numerical model grid cells is 100 m in –x and –y directions

The continuity equation (Equation 4.1); equations of motion (Equation 4.2; Equation 4.3); the hydrostatic assumption (Equation 4.4); shear stress equation (Equation 4.5); and heat transport (Equation 4.6) equations solved in the model are obtained in the following forms:

$$\frac{\partial H}{\partial t}+\frac{\partial Hu}{\partial x}+\frac{\partial Hv}{\partial y}+\frac{\partial w}{\partial \sigma}=Q_H \tag{4.1}$$

where x, y are horizontal Cartesian coordinates; σ is the vertical stretch coordinate; t is time; H is the water column depth; u, v, w are the velocities in x, y and z directions; Q_H is the volumetric source-sink term including rainfall, evaporation, infiltration, lateral inflows having negligible momentum fluxes, and lateral outflows.

$$\begin{aligned}&\frac{\partial (Hu)}{\partial t}+\frac{\partial (Huu)}{\partial x}+\frac{\partial (Huv)}{\partial y}+\frac{\partial (uw)}{\partial \sigma}-fHv\\&=-H\frac{\partial (p+p_{atm}+\Phi)}{\partial x}+\left(\frac{\partial z_b}{\partial x}+\sigma\frac{\partial H}{\partial x}\right)\frac{\partial p}{\partial \sigma}+\frac{\partial}{\partial \sigma}\left(\frac{A_v}{H}\frac{\partial u}{\partial \sigma}\right)\end{aligned} \tag{4.2}$$

$$\begin{aligned}&\frac{\partial (Hv)}{\partial t}+\frac{\partial (Huv)}{\partial x}+\frac{\partial (Hvv)}{\partial y}+\frac{\partial (vw)}{\partial \sigma}+fHu\\&=-H\frac{\partial (p+p_{atm}+\Phi)}{\partial y}+\left(\frac{\partial z_b}{\partial y}+\sigma\frac{\partial H}{\partial y}\right)\frac{\partial p}{\partial \sigma}+\frac{\partial}{\partial \sigma}\left(\frac{A_v}{H}\frac{\partial v}{\partial \sigma}\right)\end{aligned} \tag{4.3}$$

$$\frac{\partial p}{\partial \sigma}=-gH\frac{(\rho_w-\rho_0)}{\rho_0}=-gHb \tag{4.4}$$

$$(\tau_{xz},\tau_{yz})=\frac{A_v}{H}\frac{\partial}{\partial \sigma}(u,v) \tag{4.5}$$

where; f is the Coriolis acceleration; p is the excess water column hydrostatic pressure; p_{atm} is the kinematic atmospheric pressure; $\Phi = gz_s$ is the free surface potential; z_s is the free surface vertical coordinate; z_b is the bottom vertical coordinate; A_v is the turbulent momentum diffusion coefficient; g is the gravitational acceleration;

ρ_w is the actual water density; ρ_0 is the reference water density; b is buoyancy; and τ_{xz}, τ_{yz} are vertical shear stresses in x and y directions. Effects of earth rotation, pressure gradients, advection and horizontal mixing, and inner sources or sinks of buoyancy are neglected in the hydrostatic assumption in Equation 4.4.

$$\frac{\partial(HT)}{\partial T}+\frac{\partial(HuT)}{\partial x}+\frac{\partial(HvT)}{\partial y}+\frac{\partial(w)}{\partial\sigma}=\frac{\partial}{\partial\sigma}\left(\frac{A_b}{H}\frac{\partial T}{\partial\sigma}\right)+HR_T \tag{4.6}$$

where; T is temperature; A_b is vertical turbulent mass diffusion coefficient and R_T represents heating due to solar radiation.

The shear stresses at the lake bed $(\sigma=0)$, and water surface $(\sigma=1)$ are expressed along the model boundary as:

$$(\tau_{xz},\tau_{yz})=(\tau_{bx},\tau_{by})=C_b\sqrt{u_{bl}^2+v_{bl}^2}\,(u_{bl},v_{bl}) \tag{4.7}$$

$$(\tau_{xz},\tau_{yz})=(\tau_{sx},\tau_{sy})=C_s\sqrt{U_w^2+V_w^2}\,(U_w,V_w) \tag{4.8}$$

$$C_b=\left(\frac{\kappa}{\ln\left(\frac{\Delta_{bl}}{2\sigma_0}\right)}\right)^2 \quad ; \quad C_s=0.001\frac{\rho_a}{\rho_w}\left(0.8+0.065\sqrt{U_w^2+V_w^2}\right) \tag{4.9); (4.10}$$

The water surface and bed boundary conditions for heat transport are:

For water surface;
$$-\frac{A_b}{H}\frac{\partial T}{\partial\sigma}=\frac{(J_b+J_c+J_e)}{\rho_w C_{pw}} \tag{4.11}$$

For bed;
$$\frac{\partial(H_bT_b)}{\partial t}=\frac{I_b}{\rho_b C_{pb}}-C_{hb}\frac{\rho_w C_{pw}}{\rho_b C_{pb}}\sqrt{(u_{bl}^2+v_{bl}^2)}(T_b-T_{bl}) \tag{4.12}$$

Short wave solar radiation at the bed is defined as:

$$\frac{I_b}{I_s}=re^{-\beta_f H}+(1-r)e^{-\beta_s H} \tag{4.13}$$

where; τ_{bx} and τ_{by} = shear stresses at $\sigma = 0$; τ_{sx} and τ_{sy} = shear stresses at $\sigma = 1$; C_b = bottom drag coefficient (Equation 4.9); κ = von Karman constant; Δ_{bl} = dimensionless thickness of the bottom layer; $\sigma_0 = \frac{z_0}{H}$ dimensionless roughness height; u_{bl} and v_{bl} = velocity components in the hydrodynamic model's bottom layer; C_s = wind stress coefficient (Equation 4.10); ρ_a = air density; U_w and V_w = wind velocity components at 10 m above the water surface; J_b = net long-wave back radiation; J_c = convective heat transfer; J_e = evaporative heat transfer; c_{pw} = specific heat of water; H_b = active thermal thickness of the bed; T_b = bed temperature; I_b = short-wave solar radiation at the bed; ρ_b = bed density; C_{pb} = specific heat of the water-solid bed mixture; C_{hb} = dimensionless convective heat exchange coefficient; T_{bl} = bottom layer water temperature; I_s = solar radiation at the water surface; r = distribution factor; and β_f ; β_s = fast and slow-scale attenuation coefficients.

The transport of dynamically active constituents such as salinity, temperature, and suspended sediment is coupled with the momentum equations through an equation of state and the hydrostatic condition. The solution of hydrodynamic and transport equations requires specification of the vertical turbulent viscosity and diffusivity, horizontal and vertical boundary conditions, and the source and sink terms. EFDC uses turbulence closure scheme to calculate vertical, turbulent momentum diffusion (A_v), and mass diffusion (A_b) coefficients. This model was developed by Mellor and Yamada (1982) and modified by Galperin et al. (1988) and Blumberg et al. (1992). The model relates A_v and A_b to vertical turbulence intensity (q), turbulence length scale (l), and the Richardson number (Ri_q) by

$$A_v = \phi_v ql = 0.4 \frac{\left(1 + 8Ri_q\right)ql}{\left(1 + 36Ri_q\right)\left(1 + 6Ri_q\right)} \tag{4.14}$$

$$A_b = \phi_b ql = \frac{0.5ql}{\left(1 + 36Ri_q\right)} \tag{4.15}$$

$$Ri_q = \frac{gH \dfrac{\partial b}{\partial \sigma}}{q^2}\left(\frac{l^2}{H^2}\right) \tag{4.16}$$

where the stability functions Q_v and Q_b (Galperin, et al. 1988) account for reduced and enhanced vertical mixing in stable and unstable, vertically density stratified environments, respectively.

EFDC can simulate transport of cohesive and non-cohesive sediments as bed load or suspended load. Transport of sediments begins when the bed stress exceeds the critical stress (Shields stress). Bed velocity should be more than the critical shear velocity to start motion. Sediment is transported as suspended load when the bed shear velocity exceeds the settling velocity of sediment. EFDC uses the anti-diffusive MPDATA scheme (Smolarkiewicz, et al. 1986) for the advective terms in the transport equation (4.17) (Tetra Tech 1999).

$$\partial_t\left(m_x m_y H S_j\right)+\partial_x\left(m_y H u S_j\right)+\partial_y\left(m_x H_v S_j\right)+\partial_z\left(m_x m_y w S_j\right)$$
$$-\partial_z\left(m_x m_y w_{sj} S_j\right)=\partial_z\left(m_x m_y \frac{K_v}{H}\partial_z S_j\right)+Q_{sj}^E+Q_{sj}^I \tag{4.17}$$

where; S_j = concentration of the j_{th} sediment class; Q_{sj}^E, Q_{sj}^I = external and internal source-sink terms. The external source-sink term includes point and non-point source loads; and the internal source-sink term includes reactive decay of organic sediments or the exchange of mass between sediment classes, if floc formation and destruction were simulated.

4.1.1. Data Input Files

As input data, EFDC requires the geometry of the lake; atmospheric conditions; discharge; water temperatures; and withdrawal rate. The main input files in the numerical model are;

EFDC.INP: Master input file. There are 90 different card images which are used for defining the lake boundary conditions such as geometry of the lake, transport options, time related parameters, layer thickness, inflow, outflow, withdrawal, bed mechanical properties, and controls for 3D output.

ASER.INP: Atmospheric forcing file including rain, evaporation, solar radiation, cloud cover, temperature, and pressure. Also, the most important calibration parameters such as the penetration of solar radiation are specified in this file.

CELL.INP: Geometric characteristics of the lake are generated in this file. The model domain was formed using the coordinates of the basin in text format extracted from the digitized maps in ArcMap. The wet and dry cells can be specified and these cells are numbered due to wetting and drying conditions of the lake model. The number of rows and columns belong to the numerical model are specified in this input file.

DXDY.INP: Length of active I, J cells in –x and –y directions are in this file. The depths of the cells and the roughness values are also in this input file. In this study, depth values were calculated from the contour lines in the digitized maps using ArcMap and Surfer programmes.

LXLY.INP: Coordinates of I, J cells are specified in this file, and the wind force can be activated using this file.

QSER.INP: Time series input file for the discharges of inflow and outflows.

RESTART.INP: Input file to read initial conditions belonging to the previous model run.

SDSER.INP: Time series input file to specify the concentration of sediments coming with inflows.

TEMP.INP: Initial temperatures of the water column in each grid cell are defined in this input file.

WSER.INP: Time series input file to specify the magnitude and the direction of wind.

4.1.2. Sensitivity Tests of the Hydrodynamic Model Parameters

Sensitivity tests are needed to understand the effects of individual parameters on the model results. The sensitivity tests of input parameters such as wind, solar radiation attenuation coefficient, evaporation transfer coefficient, convective transfer coefficient, heat transfer coefficient, buoyancy influence coefficient, and the sensitivity tests of

parameters related to sediment transport; settling velocity, sediment type and thickness were performed in this study.

4.1.2.1. Effect of Wind on Water Temperature Time Series

Sensitivity of parameters affecting the hydrodynamics indicated that wind was the major controlling factor on circulation of lakes. Numerical model results of four days showed that enhanced wind force (two times stronger) caused increasing of surface water velocities (approximately 100% increase) in the whole lake (Figure 4.2). Velocities were calculated by averaging the velocity results in each grid cell.

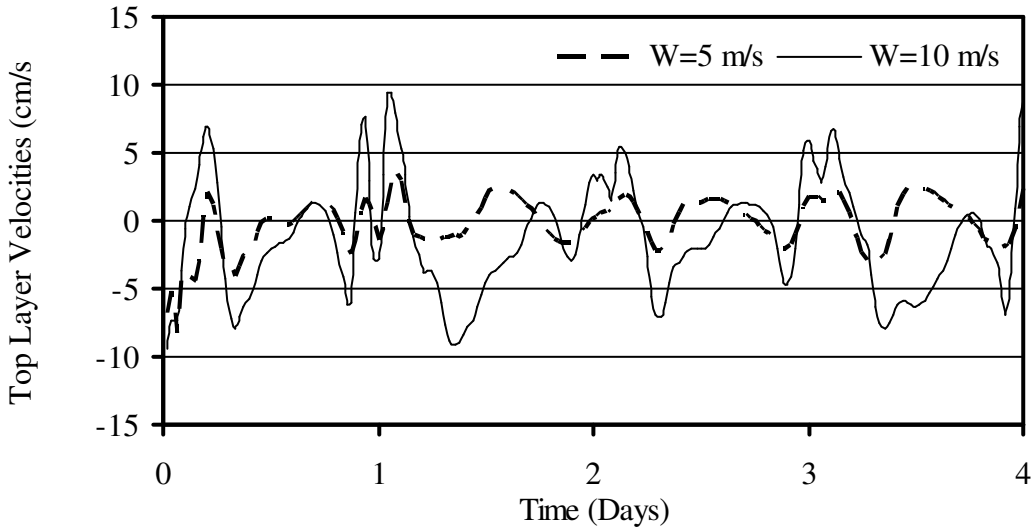

Figure 4.2. Comparison of surface velocities using different wind data during the model runs

Measured temperature profiles in August 2006 in metalimnion were further compared to the numerical model results. The comparisons indicated that water temperatures were highly affected by the cooling and warming of air temperatures. One of the reasons that thought to be a factor was the effect of internal seiches effective in epilimnion and metalimnion with a period of approximately one day due to the cessation of high winds picking up mostly in the afternoon. The measured wind data used in wind time series input file (wser.inp) were set to zero and the resulting temperatures were plotted. As can be seen in the figure (Figure 4.3) the fluctuations of temperature values at the stratified layer could not be observed. Due to the comparisons between the models which measured wind data in August, 2006 were used and the

model which there were no wind forcing, it was observed that wind was a major factor in controlling the water temperatures in metalimnion. The internal wave period with a period of one day was not observed when the measured wind data were not active in the numerical model.

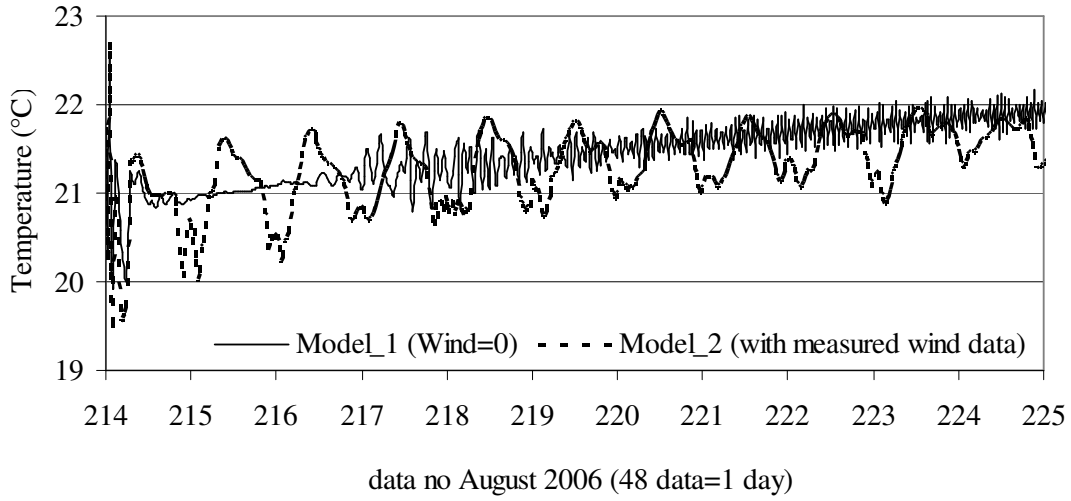

Figure 4.3. Comparison of modeled water temperatures at 11 m below the water surface corresponding to the stationary measurement point. Wind=0 during the first run; measured wind data in August, 2006 were used in the second run

4.1.2.2. Effect of Stratification on Hydrodynamics

Temperature is the major controlling factor for the presence of stratification in lakes since it affects the hydrodynamics of lakes by forming different density gradients in vertical. Large lakes or reservoirs are stagnant and flow velocity is too low when compared to rivers, therefore, they are usually exposed to stratification. In stratified lakes, metalimnion, the layer between the warmer upper layer (epilimnion) and the colder bottom layer (hypolimnion), behaves as a barrier between the top and the bottom layer and inhibits mixing in the lake. As a result, some useful compounds such as dissolved oxygen can not be transported through the water column.

The effect of stratification on velocity profiles was investigated by numerical modeling (Figure 4.4). In model runs, the magnitude and the direction of wind was constant (10 m/s to South). Seven vertical layers were used during the simulations which the thickness of the layers were tabulated in Table 4.1. A constant value was used as an initial temperature in the unstratified model whereas measured temperature values

were used for the simulation of stratified conditions. By looking at the results, flow velocities decreased and changed direction till the thermocline depth (at 10 m) and increased after that point. In contrast, there were no significant change in velocities under unstratified conditions till the thermocline point and after that point, velocities changed direction.

Table 4.1. The dimensionless layer thickness of the simulated layers. The first layer number represents the bottom layer

Layer Number	1	2	3	4	5	6	7
Dimensionless Layer Thickness	0.083	0.25	0.125	0.125	0.167	0.167	0.083

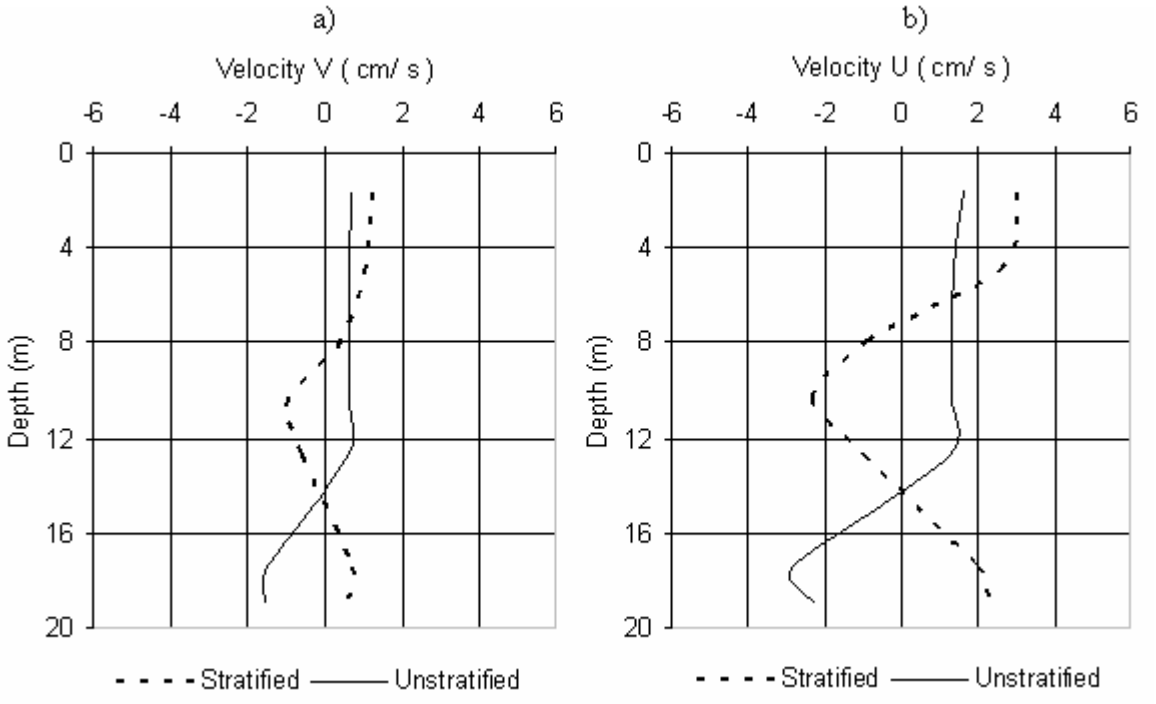

Figure 4.4. Simulation of North (a) and East (b) velocities under stratified and unstratified conditions on 31.08.2006 at a cell

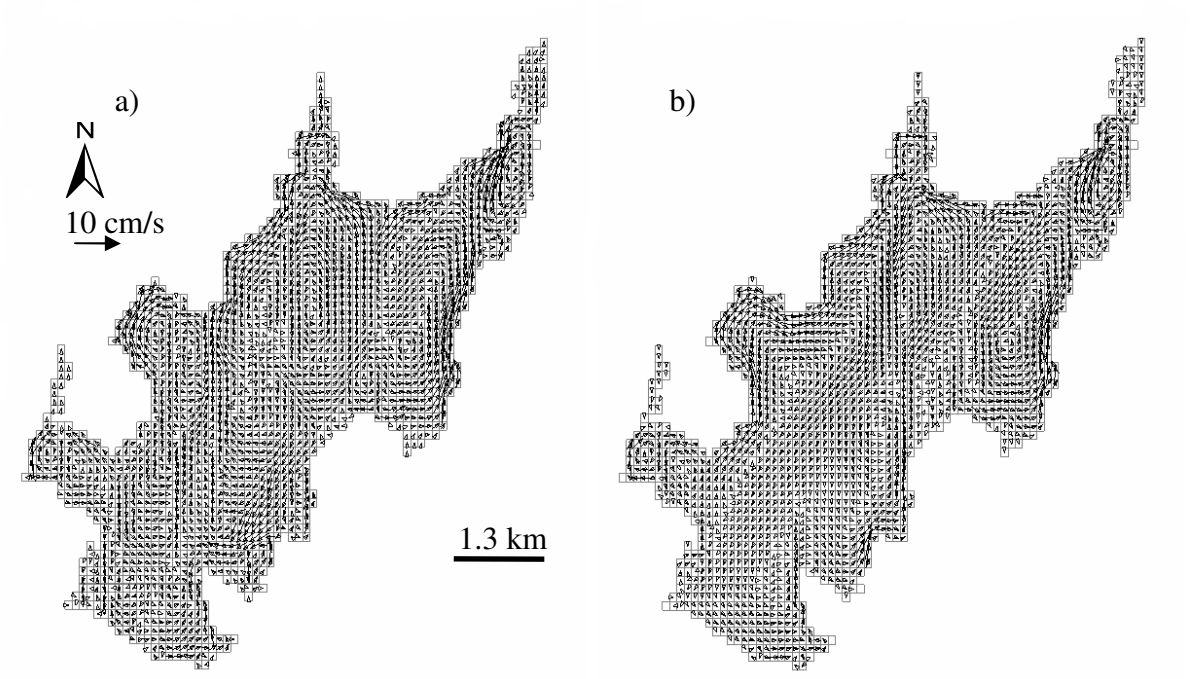

Figure 4.5. Velocity distributions in Lake Tahtali corresponding to the mid-layer in the water column. a) Stratified conditions b) Unstratified conditions. Wind was assumed constant with a speed of 10 m/s direction to South during the simulations

The distribution of flow velocities in the mid-layer of the whole lake corresponding to the stratified region at 10 m depth was also investigated to understand the sensitivity of numerical model to stratified and unstratified conditions (Figure 4.5). 6 days numerical model run results indicated that circulation patterns of stratified and unstratified conditions were significantly different. More circulation was observed under stratified conditions.

Sensitivity of the water temperatures under stratified and unstratified conditions was also investigated. As plotted in Figure 4.6, water temperatures in the stratified mid-layer followed a uniform structure and did not change significantly. However, water temperatures of the mid-layer under stratified conditions changed due to the cooling and warming air temperatures indicating that the penetration of solar radiation was more effective when the lake was stratified.

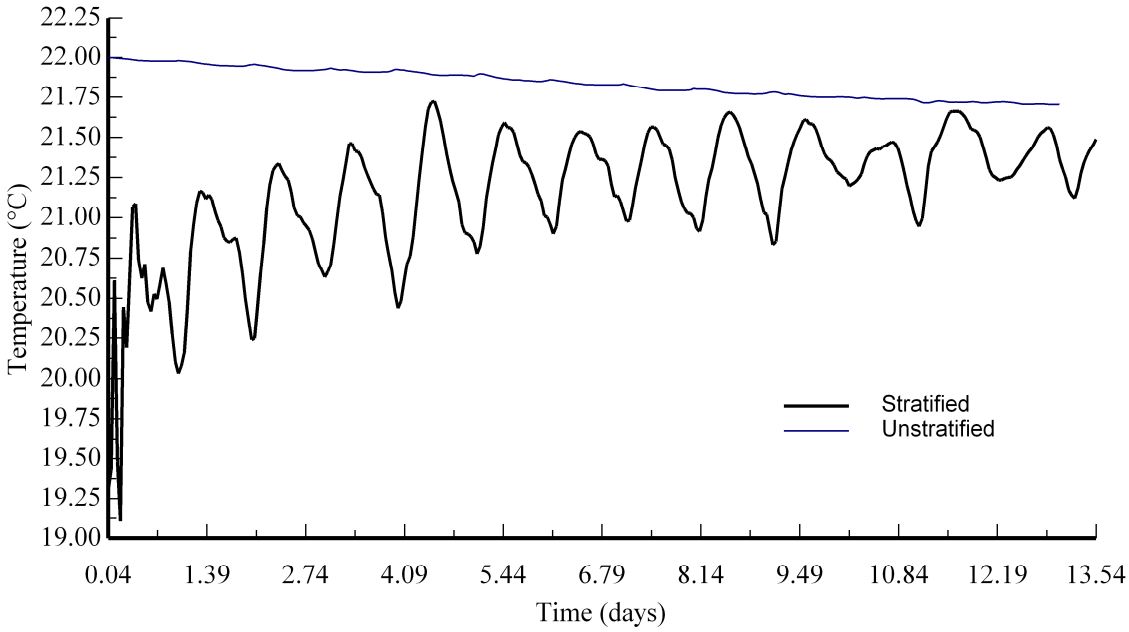

Figure 4.6. Simulation results of water temperature profiles under stratified and unstratified conditions corresponding to the mid-layer at 10 m below the water surface

4.1.2.3. Calibration Parameters

Since water temperature is also significant for lake hydrodynamics, the sensitivity test of the calibration parameters should be done to understand their effects on water temperatures. The parameters subjected to sensitivity test were tabulated in Table 4.2.

The values belonging to these parameters used in the numerical model were systematically altered with different values to understand how they affected water temperatures and the new water temperature results were compared to the current numerical model results. Results of this sensitivity test indicated that the most important parameters affecting the water temperature results were the ones which are tabulated below in Table 4.2.

Table 4.2. EFDC model parameters used for calibration

EFDC Model Parameter		Values Compared	
REVC	Evaporative transfer coefficient	-1.5	2.5
FSWRATF	Slow scale solar radiation attenuation coefficient	1	2.5
TBEDIT	Initial bed temperature	18	0
HTBED1	Convective transfer coefficient between bed and bottom water layer (m/s)	0	0.1
HTBED2	Heat transfer coefficient between bed and bottom water layer (No dim)	0	0.003
BSC	buoyancy influence coefficient 0 to 1, BSC=1; for real physics	1	0.5

After the model was run for 15 days with the measured weather data and the flow conditions in September, simulated water temperature results indicated that evaporative transfer coefficient (REVC) affected the water temperatures by causing a decrease between 1.5% and 2% in vertical (Figure 4.7). Slow scale solar radiation attenuation coefficient (FSWRATF) decreased water temperatures between 1.3% and 1.9% in vertical (Figure 4.8). Initial bed temperature (TBEDIT) affected the water temperatures and decreased between 1% and 2% vertically. The temperature difference at the bottom was more than the other layers (20%) which can be seen in Figure 4.9. Sensitivity test done for convective transfer coefficient between bed and bottom water layer (HTBED1) revealed that water temperatures were seriously affected by altering this parameter (decreased between 20% and 46% in vertical). The difference reached its maximum at the bottom layer (Figure 4.10). Similarly, as plotted in Figure 4.11, heat transfer coefficient between bed and bottom water layer (HTBED2) affected the water temperatures by decreasing them between 2.5% and 4% in vertical, and the difference at the bottom was again very high (44%). Finally, buoyancy influence coefficient (BSC) caused decreasing of the water temperatures between 1% and 2% in vertical, and the temperature difference at the bottom was 44% (Figure 4.12).

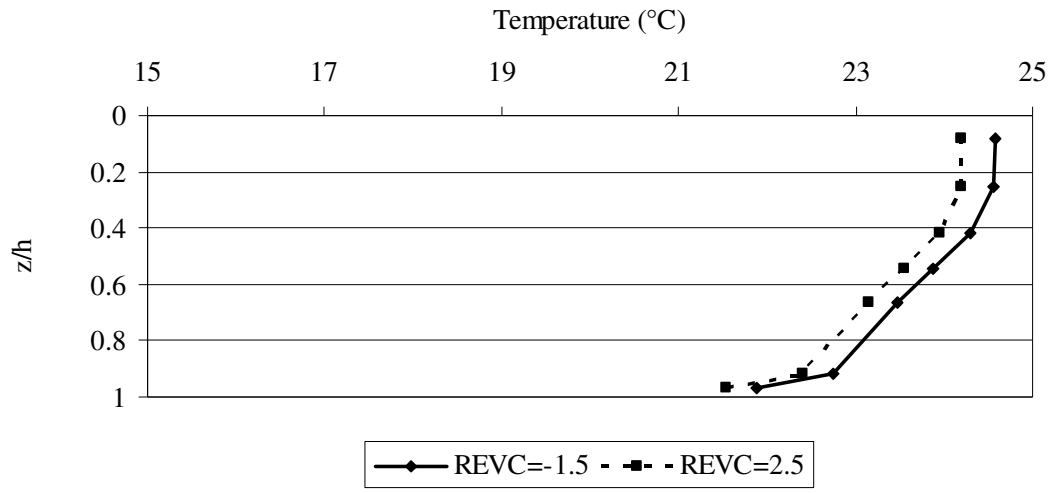

Figure 4.7. Effect of the parameter REVC (evaporative transfer coefficient) on water temperature. z/h is the dimensionless depth and represents surface when equal to zero. The temperatures are the average water temperatures of all grid cells

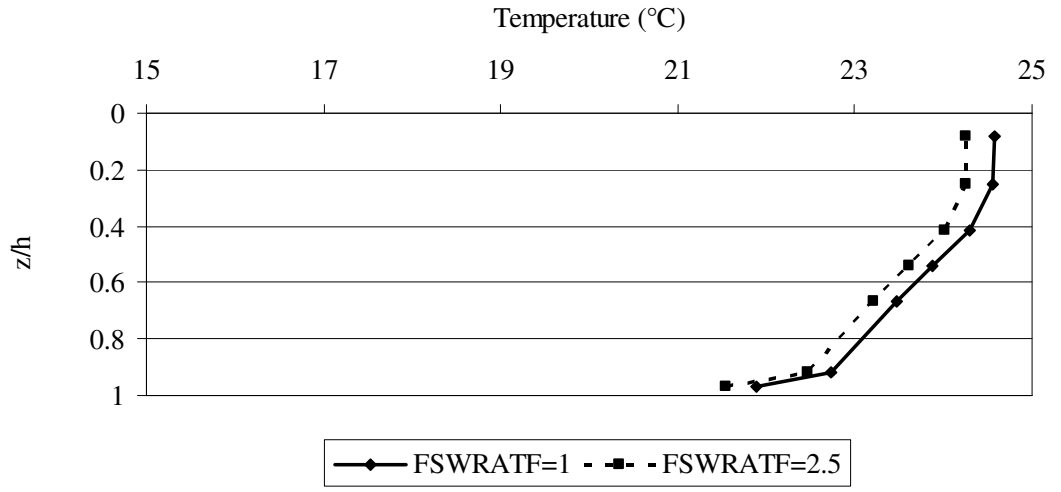

Figure 4.8. Effect of the parameter FSWRATF (slow scale solar radiation attenuation coefficient) on water temperature. z/h is the dimensionless depth and represents surface when equal to zero. The temperatures are the average water temperatures of all grid cells

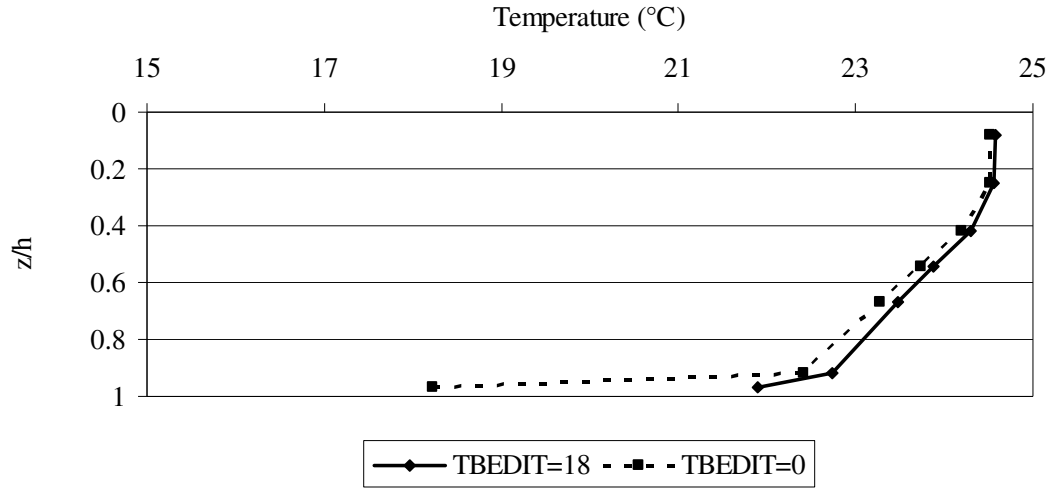

Figure 4.9. Effect of the parameter TBEDIT (initial bed temperature) on water temperature. z/h is the dimensionless depth and represents surface when equal to zero. The temperatures are the average water temperatures of all grid cells

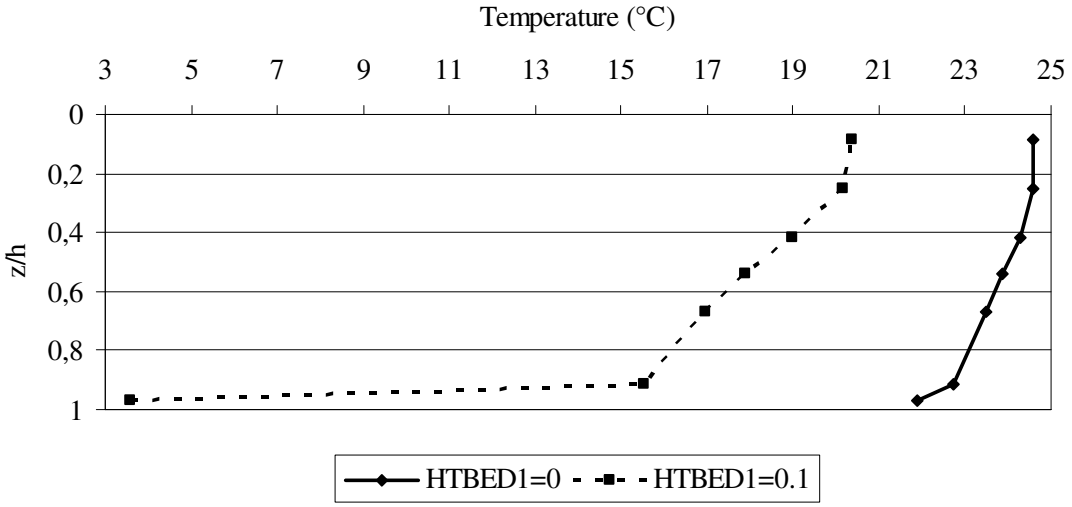

Figure 4.10. Effect of the parameter HTBED1 (convective transfer coefficient between bed and bottom water layer) on water temperature. z/h is the dimensionless depth and represents surface when equal to zero. The temperatures are the average water temperatures of all grid cells

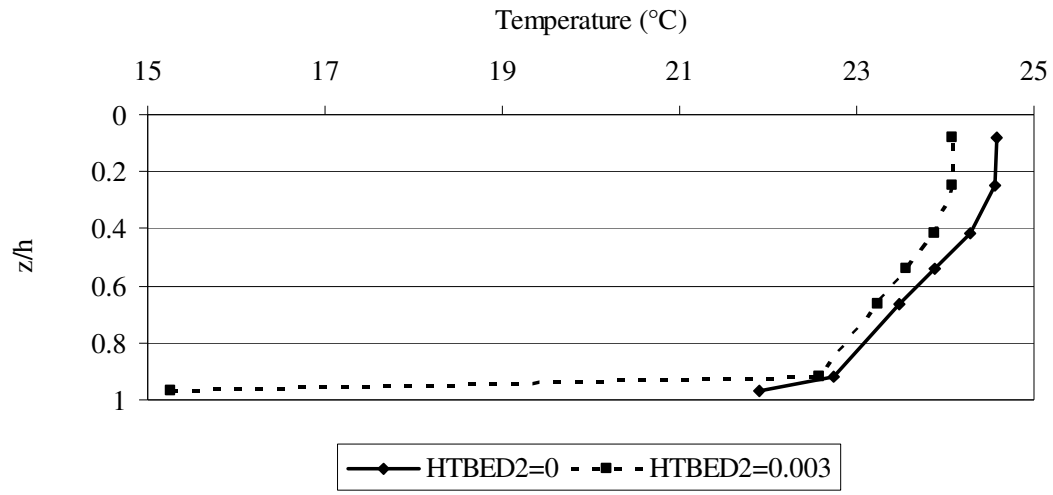

Figure 4.11. Effect of the parameter HTBED2 (heat transfer coefficient between bed and bottom water layer) on water temperature. z/h is the dimensionless depth and represents surface when equal to zero. The temperatures are the average water temperatures of each cell

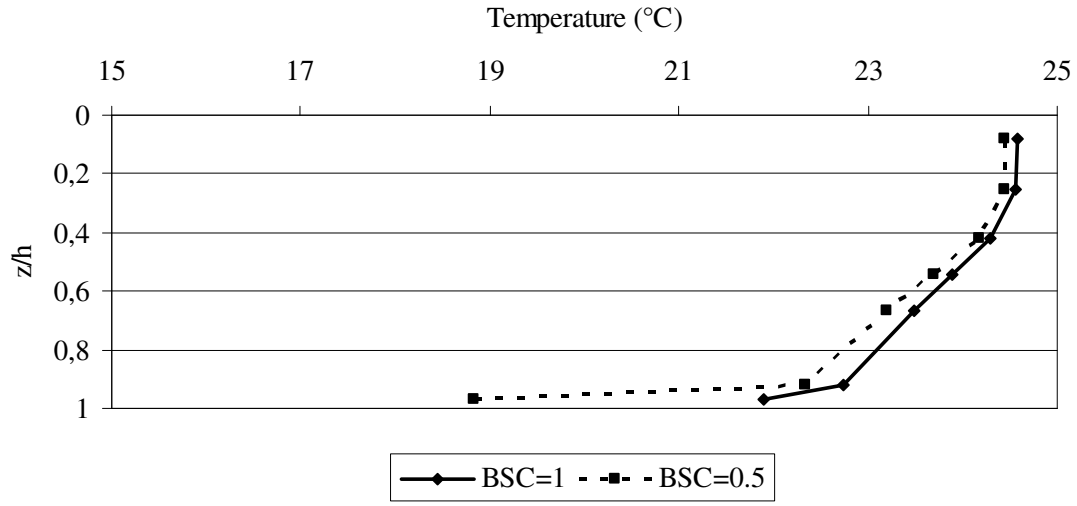

Figure 4.12. Effect of the parameter BSC (buoyancy influence coefficient) on water temperature. z/h is the dimensionless depth and represents surface when equal to zero. The temperatures are the average water temperatures of all grid cells

As seen from the results, water temperatures were mostly affected convective (HTBED1), and heat (HTBED2) transfer coefficients between bed and bottom water layer). The bottom temperatures were affected more when compared to the other layers.

An important parameter affecting simulated temperature values was solar radiation which the penetration of solar radiation through the water column is defined in equation (4.18) as;

$$I_z = SR * 0.5 * \exp[-nz] \tag{4.18}$$

where; I_z is the downward solar irradiance; SR is the short wave radiation; n is the extinction coefficient. It was observed that when smaller value of n is used the solar radiation penetrated further in the water column. A value of 0.5 was used as the extinction coefficient for Tahtali Reservoir model allowing the penetration of solar radiation until thermocline.

4.1.2.4. Sensitivity Test for Sediment Transport

EFDC can simulate the transport of cohesive and non-cohesive sediment transport. The variation of numerical model output due to different factors which have effects on sediment transport were investigated through sensitivity analysis. For this purpose, several variables including sediment concentration, settling velocity, discharge and sediment class were altered as part of the sensitivity analysis of these parameters. During these simulations, meteorological data were obtained from the weather station set up in the basin, measured water temperatures in the area were utilized, sediment thickness was set to 0.944 m, and velocities were set to zero initially in the model. Parameters and the boundary conditions used in the model were used as described in Chapter 9.

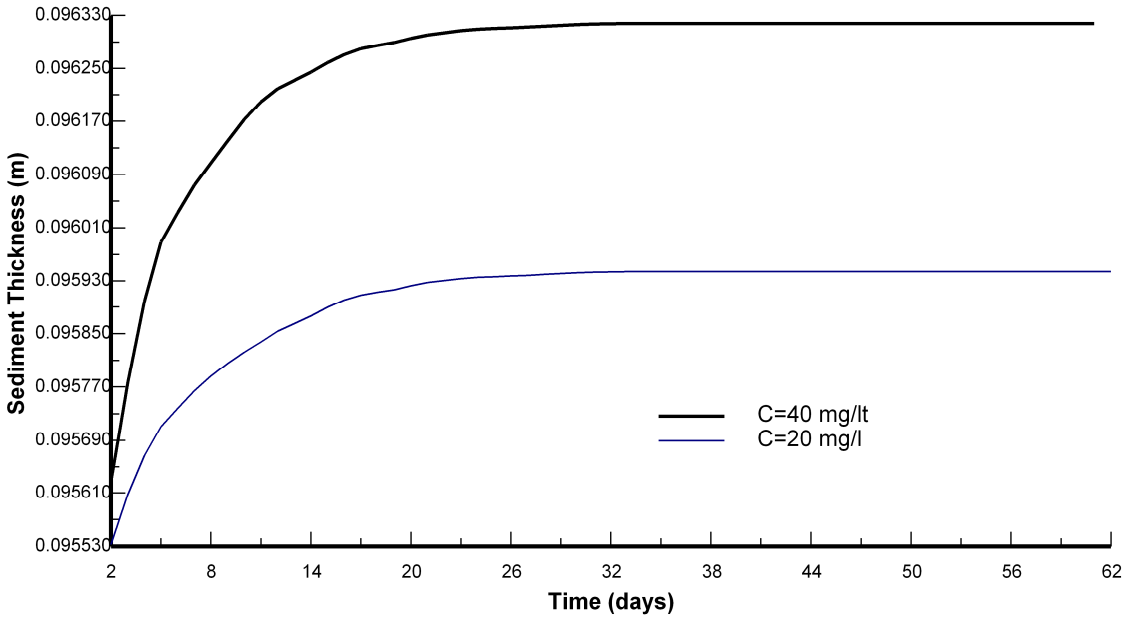

Figure 4.13. Sediment thickness variations of two different numerical model runs with different suspended sediment concentrations

In order to investigate the sensitivity of model to sediment concentrations, the model was run using two different initial cohesive sediment concentration in water column. The concentration of cohesive sediment in the water column was 20 mg/liter in the first simulation whereas it was used as 40 mg/liter in the second one. For these two simulations, sediment bed thickness values near the intake structure were compared and observed that the average annual sediment thickness was 0.30 cm more in the model that water column sediment concentrations were 40 mg/liter. This value was calculated by extrapolating the average sediment thickness of all grid cells utilizing 60 days model run results. Figure 4.13 shows the sediment thickness variation in time for different suspended sediment concentrations near the intake structure.

The effect of settling velocity parameter on sediment deposition in the lake was investigated. The value of settling velocity in EFDC main input file (EFDC.inp) was used ten times bigger than the current model. It was used 0.0005 m/s instead of 0.00005 m/s. Based on the numerical model results, it was concluded that the sediment thickness difference between two models were almost the same. Sediment thickness was calculated as 0.0960 m in the first model run whereas it was calculated as 0.0961 in the second run after 60 days of simulation.

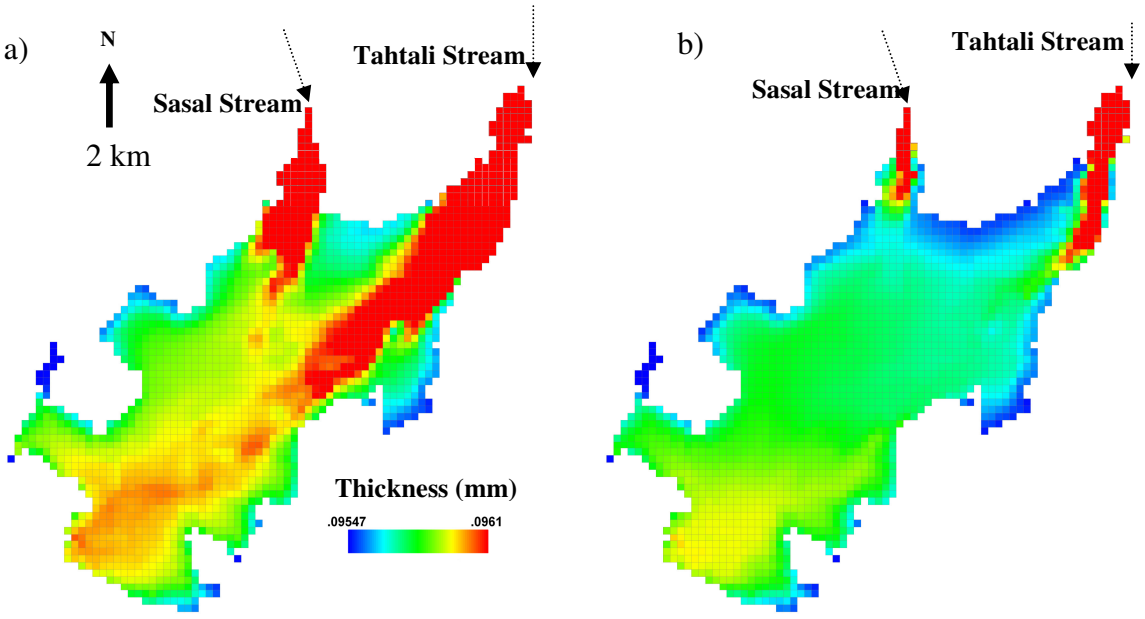

Figure 4.14. Numerical model grids of Lake Tahtali showing deposited sediment thickness in the lake. a) flood condition b) with low inflows

Increasing the inflows affected the rate of sediment transport at points where the streams entered the reservoir (Figure 4.14). As we diverge from the thalwegs, sediment thickness did not change significantly in the other parts of the lake. These two simulations were an indicator for the sensitivity of the numerical model to inflow discharges. Flood condition was needed to carry sediments to long distances, because sediments reached to the water intake structure only during the flood condition.

Sediment class was found to strongly influence results. Sediment class in the numerical model was selected in two different forms. The first simulation was carried out assuming the sediment class was silt (Figure 4.15a). The second simulation was implemented in order to investigate the deposition of sand in the lake (Figure 4.15b). As illustrated below, silt was deposited more than sand in the lake. By averaging the sediment bed thickness values of all grid cells, it was observed that the average annual sediment thickness was 0.24 cm more when the sediment type was silt. Silt was carried away faster than sand due to the specific gravities defined in EFDC master input file. The calculation was based on the extrapolation of average sediment thickness of all grid cells utilizing 60 days of model runs.

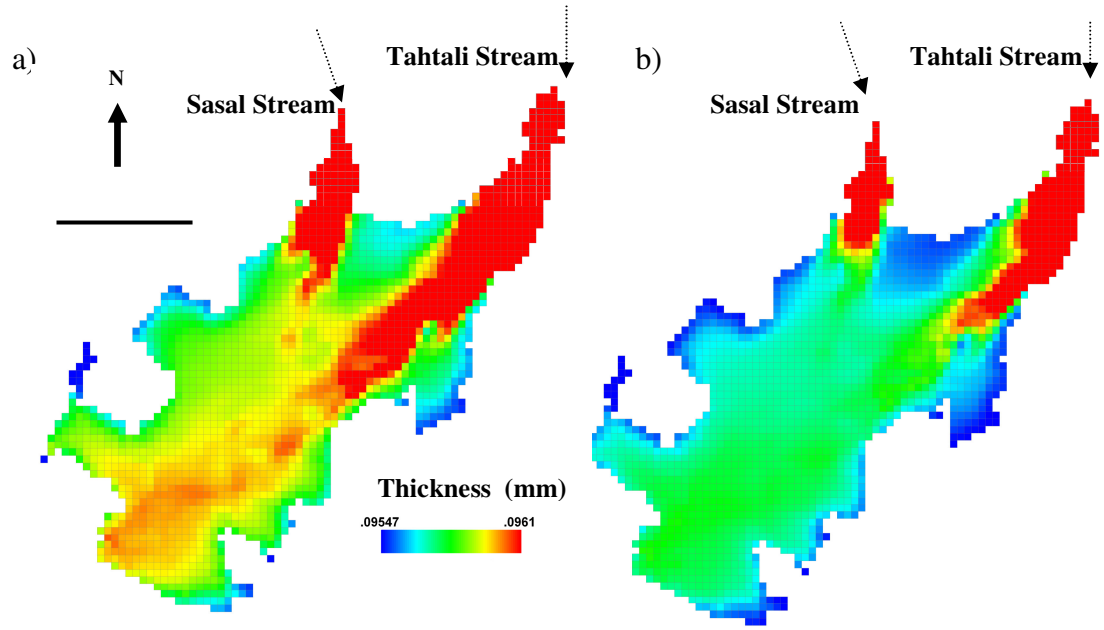

Figure 4.15. Numerical model grids of Lake Tahtali showing deposited sediment thickness in the lake. a) Deposition of silt b) Deposition of sand

CHAPTER 5

MODELING OF HYDRODYNAMICS IN LAKE TAHTALI

This chapter presents numerical modeling part of the study where input data comprising lake geometry, meteorological data, inflow discharge, withdrawal discharge, and the water temperatures measured in the area were used to model hydrodynamics and sediment transport in the lake. EFDC (Environmental Fluid Dynamics Code) was used for this purpose which can simulate transport and flow processes in all three dimensions.

Lake Tahtali is an example of a stratified lake which is vertically mixed during wet (September to November) season, and thermally stratified in dry (July to August) season. Stratification depends on many factors such as the geometry of the lake, climate, inflows and outflows. The residence time of the reservoirs are smaller when compared to other natural sources since reservoirs are stagnant and have low flow velocities. In this chapter, the effect of stratification on hydrodynamics was investigated due to the fact that stratification deteriorates water quality of Lake Tahtali.

Temperature profiles of the water column in Tahtali Reservoir were investigated through numerical modeling and monthly field observations to analyze the structure of stratification. Figure 5.1 depicts the measured temperature profiles of the water column in August, 2006 that was used initially for the numerical model simulations suggesting the dense stratification in the lake. The stratification started at 10 m, ended at approximately 14 m depth in August. The temperature difference between the surface and the bottom layer was 12°C. The temperature profile reached a uniform structure in November and the lake was mixed at a temperature of 15°C

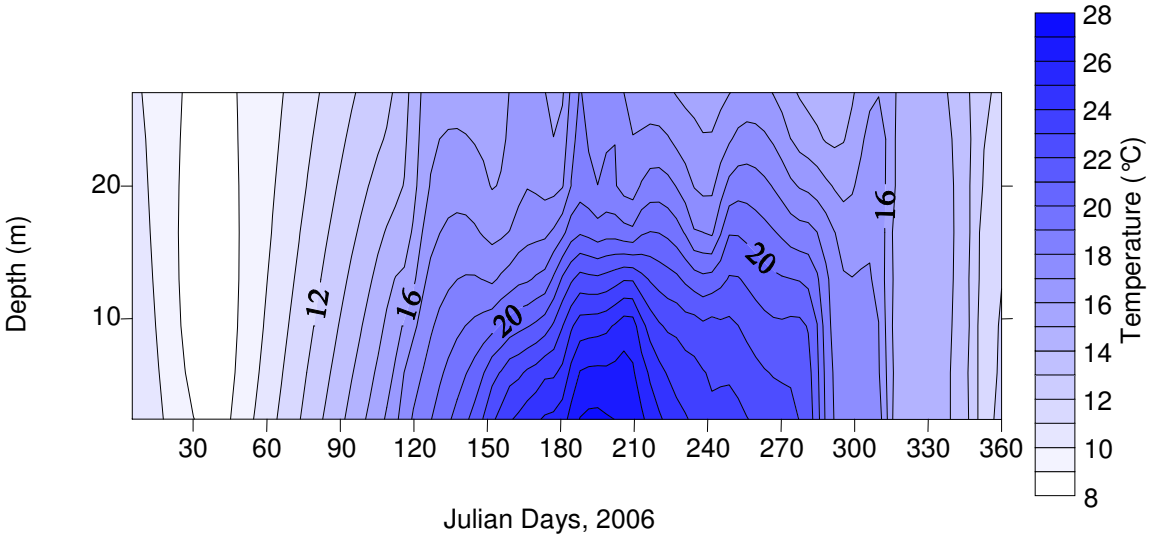

Figure 5.1. Observed water temperature profiles in Lake Tahtali during 2006

5.1 Lake Number

The degree of stratification in Tahtali Reservoir was assessed through non-dimensional parameter analysis. Lake Number, L_N (Imberger 1998), an indicator for the degree of stability and mixing in the lake, was used for this analysis. L_N was calculated for the lake using the measured meteorological data and water temperatures relating with the conditions in August, October, and November 2006 using the Equation (5.1). A typical cross section of a stratified lake was illustrated in Figure 5.2 (Elci 2004).

$$L_N = [S_t(H - h_T)] / \left| u_*^{\,2} A_s^{\,3/2} (H - h_v) \right| \tag{5.1}$$

where; S_t is stability (Equation (5.2)); u_* is the water shear velocity due to the wind (Equation (5.3));

$$S_t = \frac{1}{2} g' [[(A_1 A_2 h_1 h_2)(h_1 + h_2)] / [(A_1 h_1) + (A_2 h_2)]] \tag{5.2}$$

$$u_* = \left[0.0013 \left(\frac{\rho_a}{\rho_w} \right) U_{(10)}^2 \right]^{1/2} \tag{5.3}$$

where; g' is the reduced gravity (Equation (5.4));

$$g' = \left(\frac{\Delta\rho}{\rho'} \right) g \tag{5.4}$$

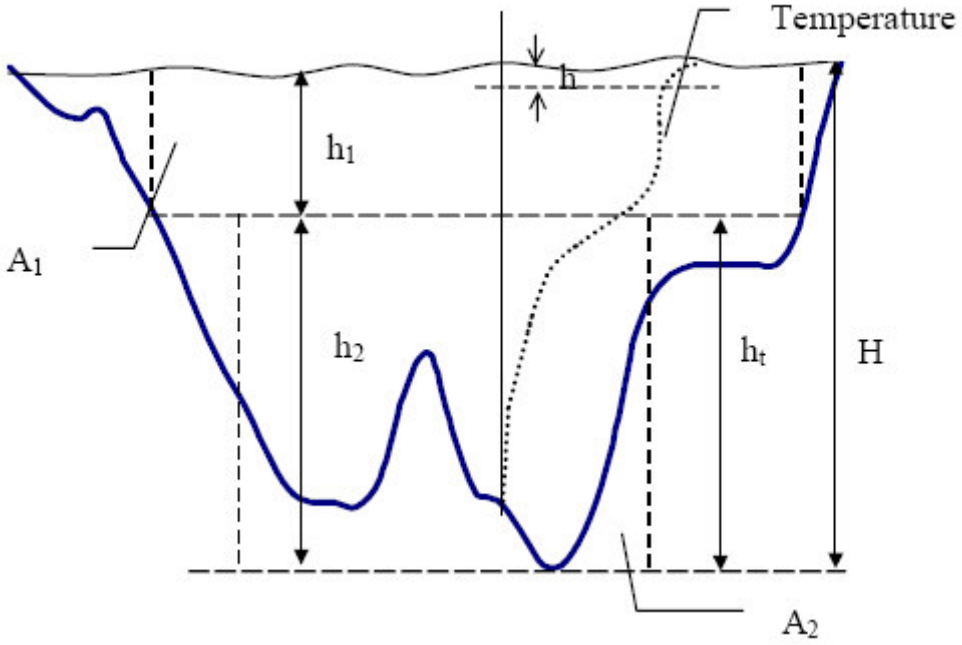

Figure 5.2. A typical cross section of a lake utilized for the calculation of L_N where; H is the total depth of the lake; h_T is the height from the bottom of the lake to the thermocline; A_s is the surface area of the lake; h_v is the height from the bed to the center of volume of the lake; A_1, h_1 is the area and the thickness of the upper layer; A_2, h_2 is the area and the thickness of the bottom layer; ρ_a is the density of air; ρ_w is the density of water; $U_{(10)}$ is the wind speed at 10 m above the water surface; $\Delta\rho$ is the density difference between the hypolimnion and the epilimnion; ρ' is the average density of the lake water; g is the gravity

After solving the Equation (5.1), L_N was calculated for August, October, and November 2006. Since the critical value for stratification was found to be 3, the wind speed corresponding to this value was calculated 3 m/s for Tahtali Reservoir. In August, 18% of the time, L_N was smaller than the critical value indicating dense stratification in the lake. However, in October, this value increased to 33% and finally reached a value of 100% in November indicating that there was no more stratification in the lake. In Lake Toolik, Alaska/USA, the lake was stable with 1 m/s wind speed as it was in Tahtali Reservoir. However, wind speed required for upwelling was 7 m/s for Lake Toolik (MacIntyre et al. 2006). A similar study on Lake Tahoe, the critical wind speed for upwelling was estimated 4 m/s (Schladow and Thompson 2000). The critical value of L_N is reached in Lake Hartwell when the wind speed was 18 m/s, suggesting stronger stratification when compared to other lakes (Elci, et al. 2000).

5.2. Hydrodynamic Model Set Up

The hydrodynamics of Lake Tahtali, effect of climate change, effect of withdrawal, and sediment deposition were simulated due to the variations in heat flux, wind forcing, inflows and outflows using EFDC. Lake Tahtali hydrodynamic model grid contains 6084 cells, 2041 of which were active horizontal curvilinear grid cells with seven vertical layers (Figure 4.1). The dimensionless vertical layer thicknesses used in simulations were tabulated previously in Table 4.1. The horizontal discretization of each computational cell (D_x, D_y) was 100 m on a side. The typical initial average water depth in each grid ranged from 1 m in the shallow region to 27 m in the deepest region. Time step used for the model was 10 seconds to insure numerical stability. The inflows were specified in the model using discharge data measured in Derebogazi where Tahtali and Sasal Streams merge. The withdrawal data were provided by IZSU (Izmir Water and Sewage Administration). The meteorological data were acquired from the meteorological station settled at southwest location of Lake Tahtali (Figure 5.3). The variation of air temperature, solar radiation and wind is illustrated in Figure 5.4 and Figure 5.5. All the velocities at the boundary were set to zero. Initial water temperatures were specified due to the measured values in the lake.

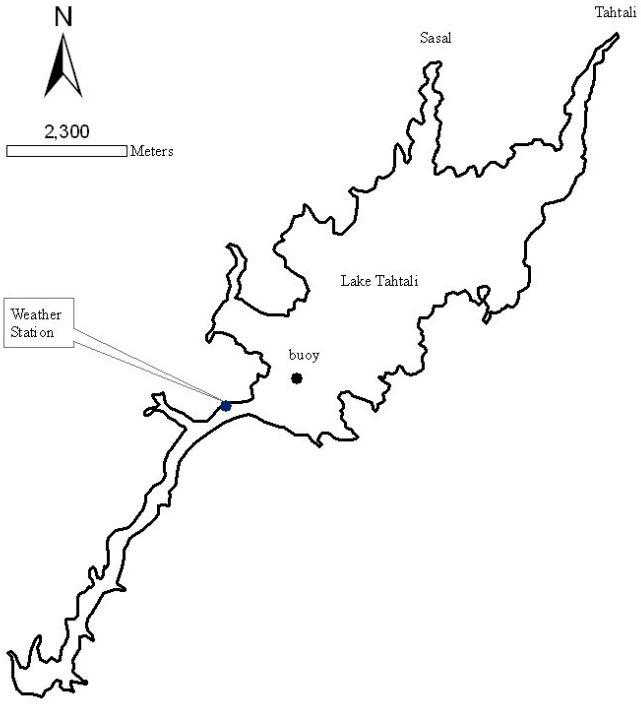

Figure 5.3. Lake Tahtali showing the meteorological station and the stationary measurement point at the buoy located at Southwest location of the lake

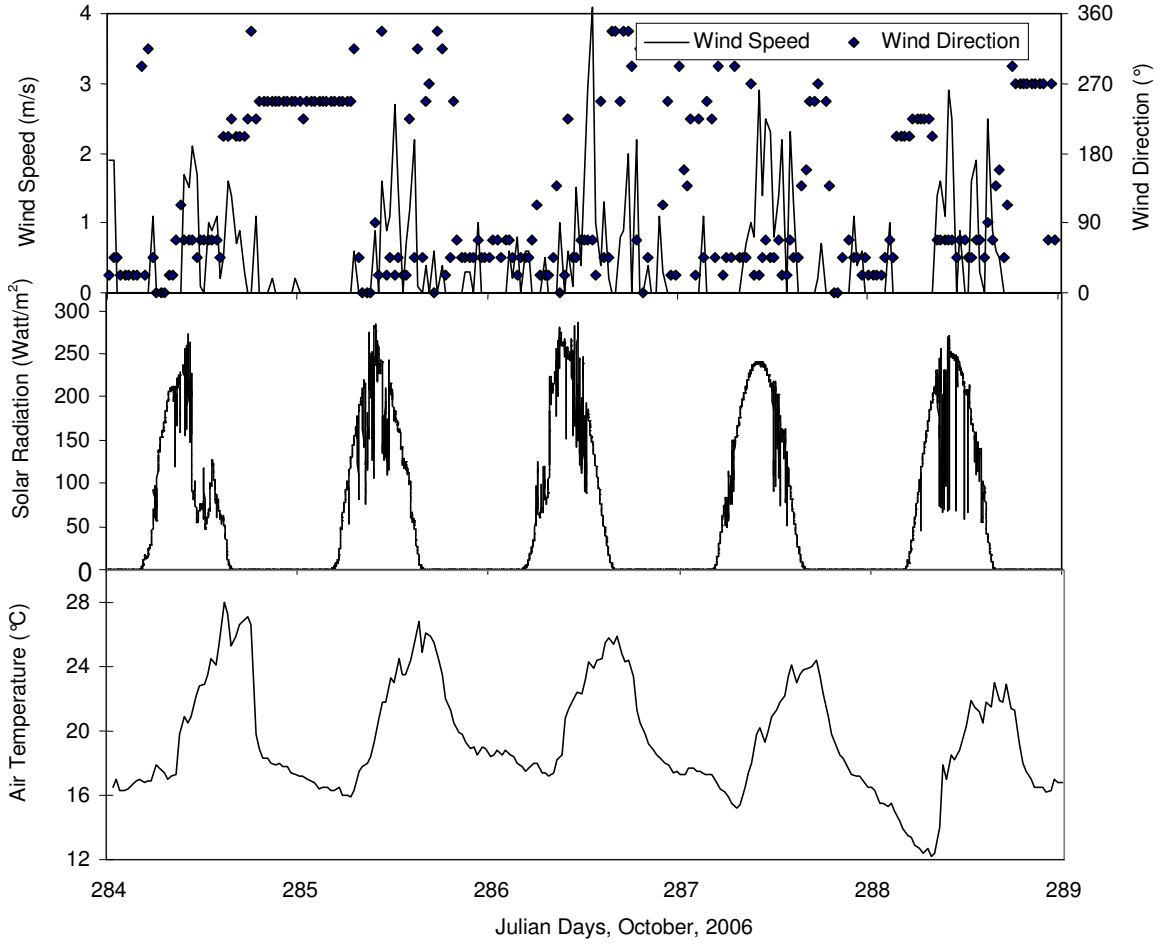

Figure 5.4. Time series of wind, solar radiation and air temperature data collected at the meteorological station in October, 2006

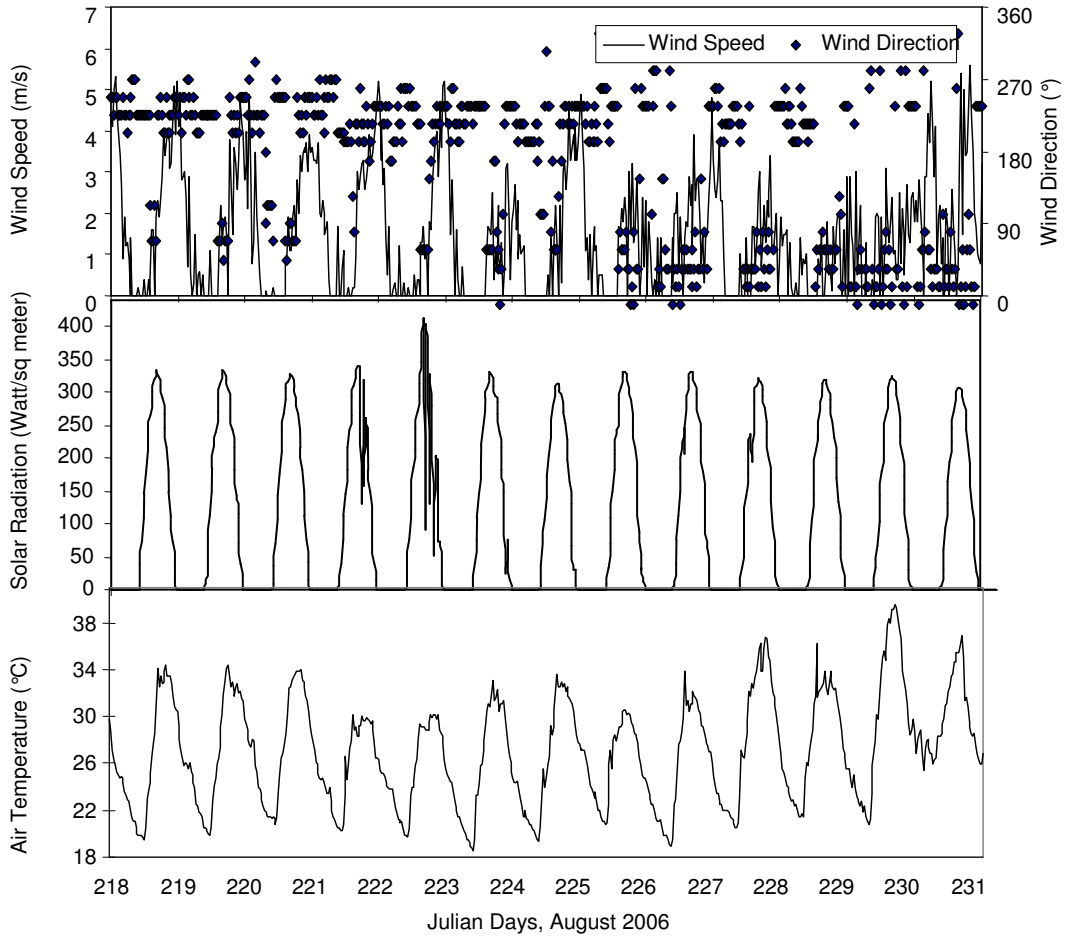

Figure 5.5. Time series of wind, solar radiation and air temperature data collected at the meteorological station in August, 2006

When the velocity vectors in vertical were simulated utilizing field data of August and October specified above, model results indicated that stratification affected the water velocities through the water column and reached higher values in October when stratification was observed less when compared to dense stratification in August (Figure 5.6). The numerical model results of vertical temperature gradient changed direction due to the thermocline point.

Water temperature results (Figure 5.7) at two different grid cells (one of them corresponding to the buoy and the other is near the water intake structure) were an indicator for the effect of withdrawal on hydrodynamic structure by reducing the stratification through the water column near the water intake structure which the topic was discussed further.

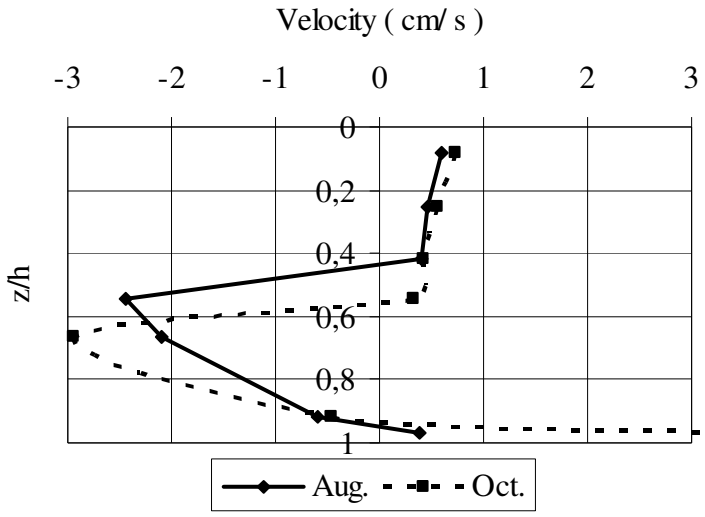

Figure 5.6. Simulated velocity vectors with measured data in August and October, 2006 corresponding to the stationary measurement point in Lake Tahtali. z/h is the dimensionless depth and represents surface when equal to zero

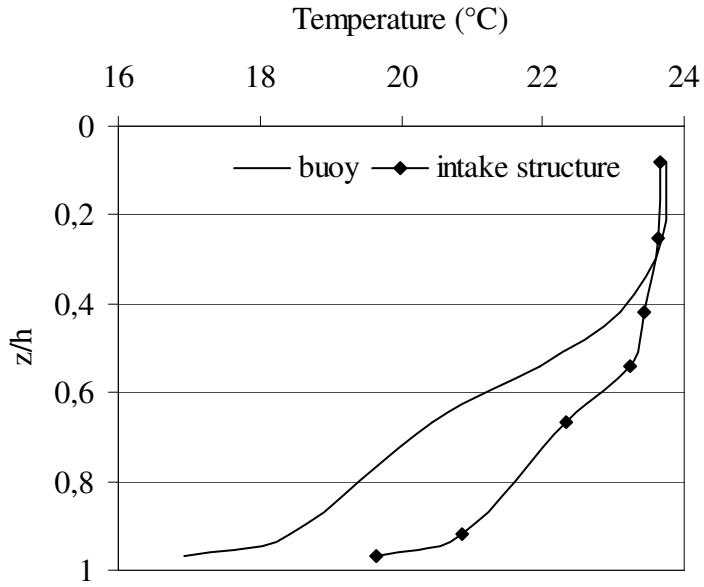

Figure 5.7. Simulated temperature profiles at the stationary measurement point and near water intake structure in Lake Tahtali with measured data specified above after a 13 days of simulation initially stratified in August. z/h is the dimensionless depth and represents surface when equal to zero

Comparison of velocity distributions at three different layers (top, bottom, and mid-layer) of different months (October and August) indicated that the circulation patterns were significantly different for these cases. When velocities were plotted

utilizing measured data in August and October (Figure 5.8 and Figure 5.9), differences were observed in both direction and magnitudes of velocity vectors. The model results produced velocity vectors indicating more circulation in October.

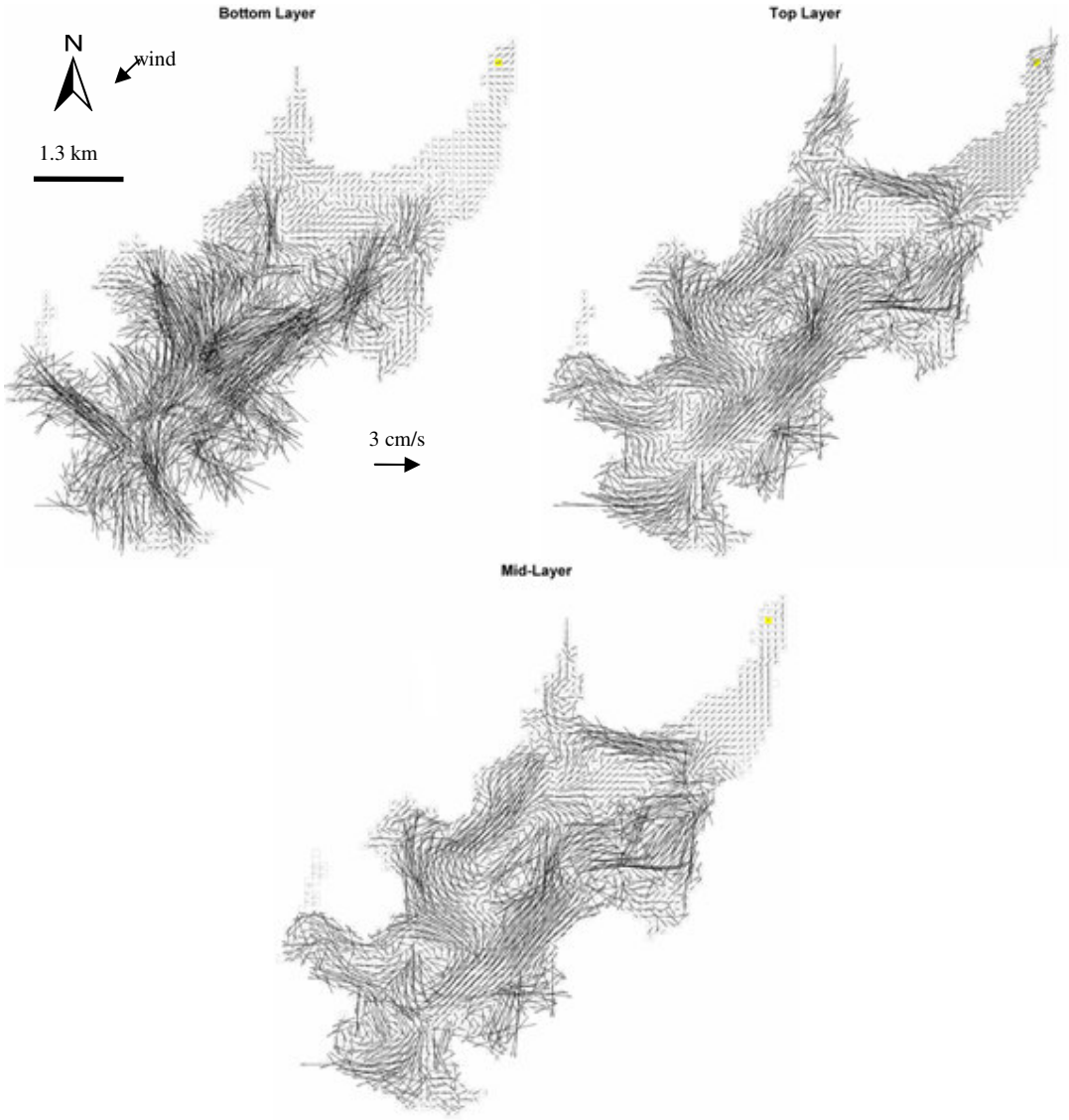

Figure 5.8. Velocity distributions at the bottom, top and the mid-layers in Lake Tahtali after 5 days of simulation initially stratified in October

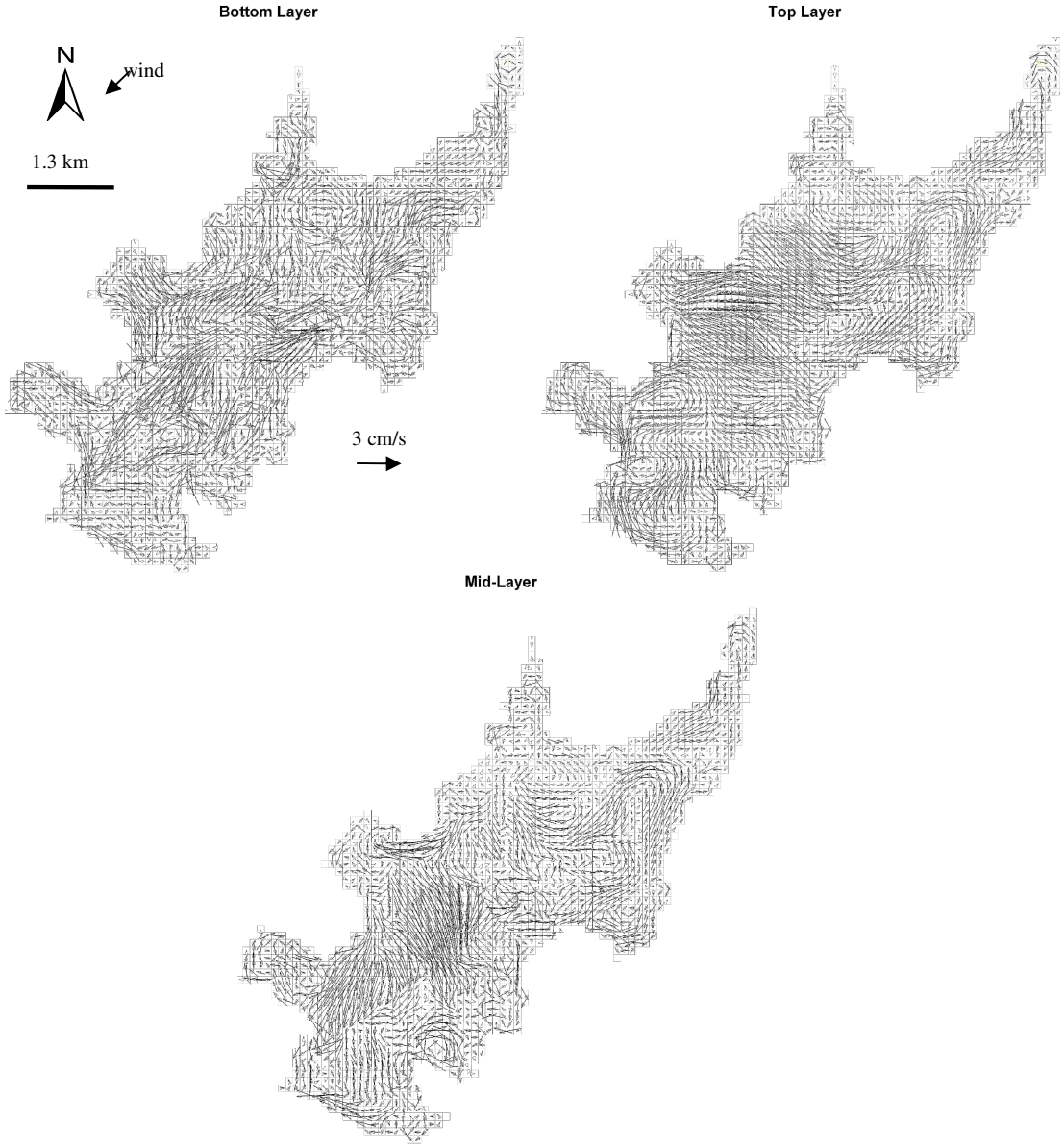

Figure 5.9. Velocity distributions at the bottom, top and the mid-layers in Lake Tahtali after 13 days of simulation initially stratified in August

CHAPTER 6

FIELD OBSERVATIONS IN LAKE TAHTALI AND COMPARISONS TO MODEL RESULTS

Continuous monitoring of environmental data provides reliable information about study site. Collected field data including meteorological data, flow, and water temperature can be used in the prediction of natural events and to minimize the effects of these events. Monitoring of environmental data has a great deal of importance for numerical modeling studies, since reliable field data means verification of the numerical model and prediction of processes accurately.

EFDC numerical model requires input files which provide information about the geometry of the lake, inflows, outflows, and the meteorological data. The meteorological data including atmospheric pressure, air temperatures, wind speed, wind direction, humidity, solar radiation, evaporation and rain were collected at the weather station. The temperature profile of the water column was measured by a hand-held instrument (water quality meter). The discharge of the inflows was measured by Acoustic Doppler velocimeter. The velocity profile of the water column was measured by Acoustic Doppler current profiler which were later used to make a comparison with the model flow velocity results. Sampling in the lake was performed between July-2006 and September-2007.

This chapter describes the field measurements conducted within the lake, the instrumentation used in data collection and comparison of collected data to numerical model results.

6.1 Instrumentation and Field Measurements

6.1.1 Velocity Data

Velocity measurements of the water column were made using a 1.5-MHz Acoustic Doppler Current Profiler (ADCP) instrument developed by Sontek/YSI

designed for measuring real time current profiles in water systems**.** ADCP used in this study has three transducer heads with different orientations (Figure 6.1). The transducers generate a narrow beam of sound. The reflections from the particles existing in the water column are used to calculate the relative velocity between the instrument and the scatterers in water. Bottom track option is available in ADCP and the distance from the transducer heads to the bottom can be detected.

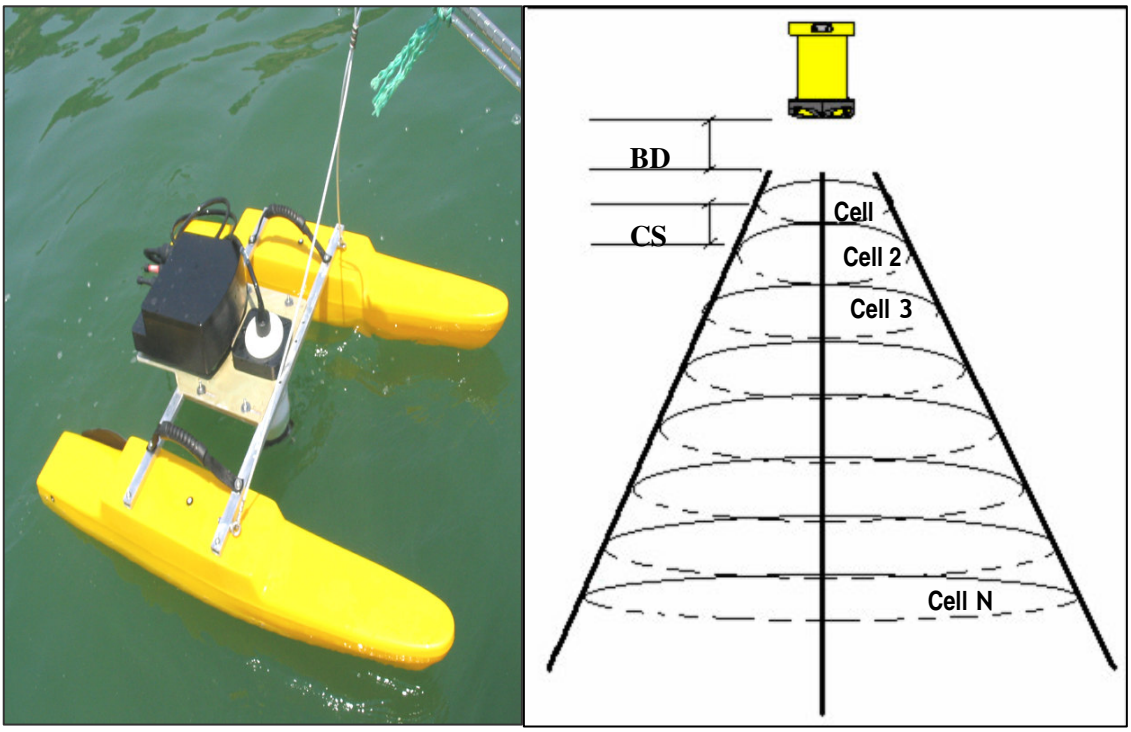

Figure 6.1. ADCP RiverCat Catamaran System with fiberglass pontoons, and parameters used to determine ADCP down-looking profiling range where BD is the blanking distance (0.4 m), and CS is the cell size (1 m)

The velocity vectors were measured at one location when the boat (Figure 6.2) was anchored at a depth of 19 m (buoy). The current deployment parameters were set to appropriate values before the data collection**.** The averaging interval was set equal to profiling range (30 seconds) for continuous deployments in order to reduce the power consumption. A 1.5-MHz ADCP can operate to a profiling range (depth) of about 25 m with a minimum resolution (cell size) of 0.25 m. Cell size used during the measurements was 1 m. The blanking distance (0.4 m for Tahtali) of the instrument was utilized to blank out the bad data close to the transducer. Averaging the data is important to reduce possible errors due to ADCP signal to noise ratio, frequency, depth

cell size, number of pings averaged, and beam geometry. External factors such as temperature, mean current speed, turbulence, density gradients and ADCP motion can also influence error. In Figure 6.3, measured velocity profiles of the water column using ADCP was compared for two different field trips. Figure 6.4 shows a sample transect record in Lake Tahtali by ADCP when the bottom track option was available. Wind speed ranged between 1-5 m/s during the measurements. One rule of thumb for wind-driven currents in open water is that; magnitude of mean currents is 3% of wind speed. This simple rule of thumb gives roughly 15 cm/s in agreement with the measurements. Some of the measured velocity data reached too high values during the first field trip. One of the reasons for these velocity errors was the excessive speed of the boat. The ratio of boat speed to ADCP speed should be less or equal to zero. The second field trip was implemented after slowing down with the boat (boat speed was approximately 3 m/s).

Figure 6.2. Boat used for field measurements in Lake Tahtali

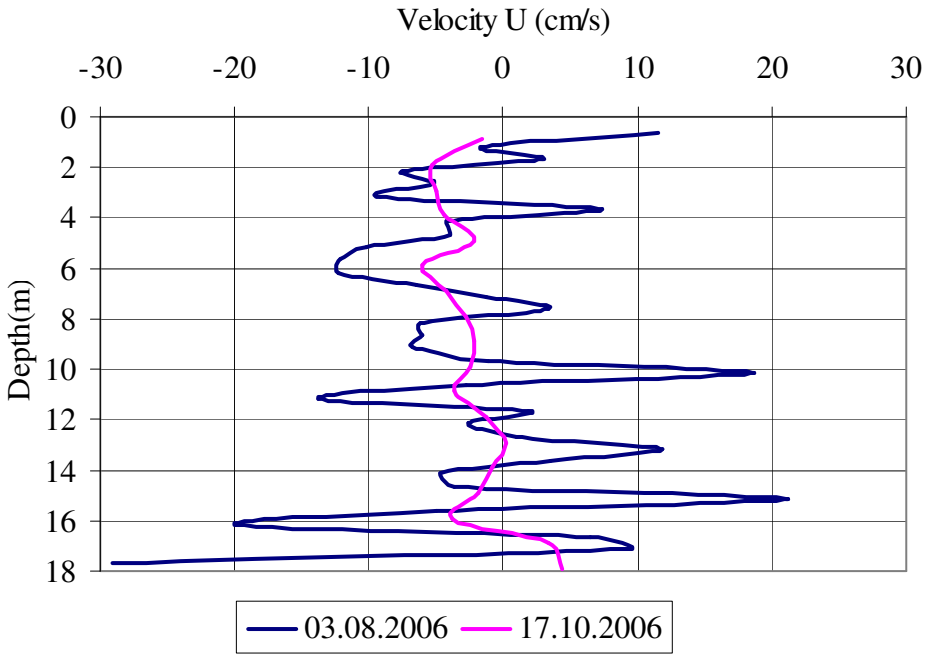

Figure 6.3. Velocity profile of the water column measured at the stationary point (buoy) by ADCP in August and October. Speed of boat was corrected during the second measurement day (October)

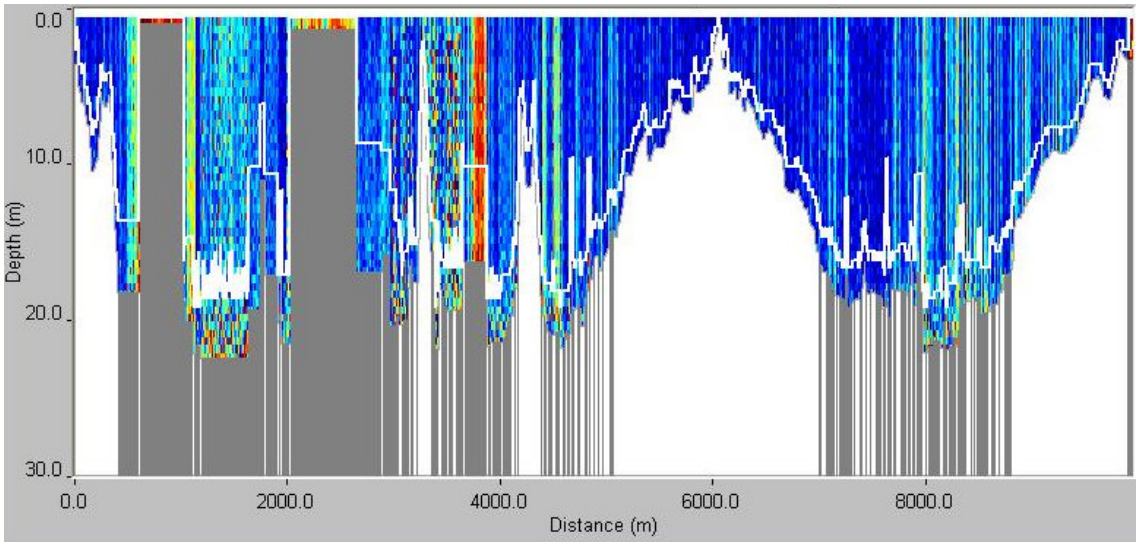

Figure 6.4. Transect depth measurement in Lake Tahtali recorded by ADCP

6.1.2 Temperature and Water Quality Data

The temperature profiles of the water column were measured by WQC-24 water quality meter designed by DKK-TOA. The instrument is capable of measuring water quality parameters (pH, conductivity, salinity, dissolved oxygen, turbidity, temperature),

and a depth sensor is attached (Figure 6.5). The vertical temperature profile of the water column in the lake was measured at monthly intervals at stationary measurement location. The instrument was left at the buoy at the end of each field trip until the next field trip (one month later) fixed at approximately 10 m depth corresponding to the stratified region in the water column. There was 1800 data storage capacity of water quality meter instrument. Data were recorded every 30 minutes in Lake Tahtali, corresponding to 35 days of data storage. Measured values were used for defining the initial conditions related to water temperatures in the numerical model. Figure 6.6 shows the measured temperature and turbidity values during the field trips between 27.7.2006 and 15.6.2007

Figure 6.5. Water quality meter for measuring temperature profiles of the water column

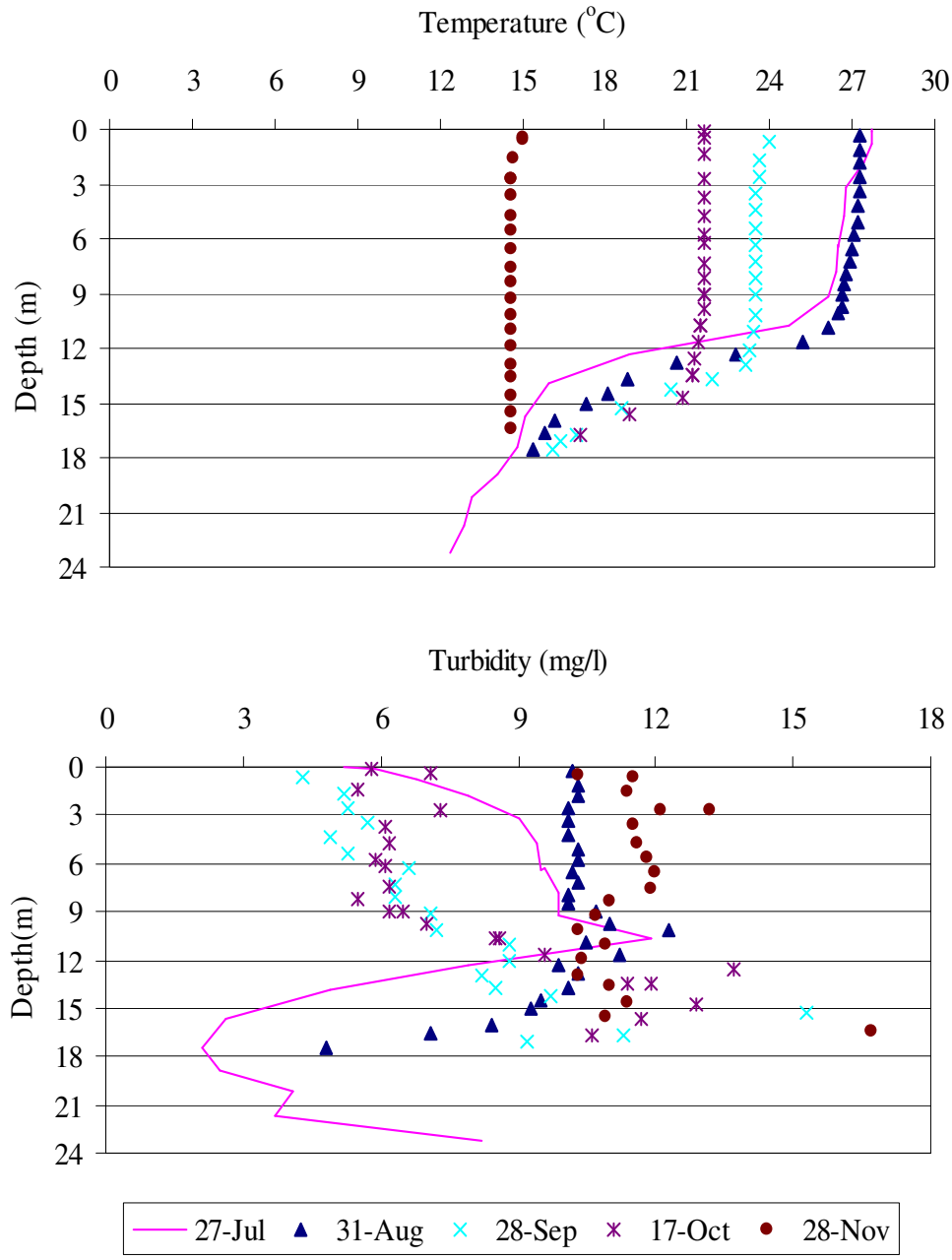

Figure 6.6. Graphs showing the temperature and turbidity measurements with respect to depth by water quality meter in Lake Tahtali between 27.07.2006 and 15.06.2007

6.1.3 Wind Data

The meteorological data were acquired from the weather station designed by TFA (Master Touch) installed at the Southwest location of Lake Tahtali (Figure 6.7). Data collected at this weather station included air pressure, air temperature, humidity,

solar radiation, wind speed, wind direction, rain and evaporation values (Figure 5.4 and Figure 5.5).

Figure 6.7. Meteorological station set up at Southwest location of the lake to record the meteorological data required as an input to the numerical model

6.2. Comparison of Field Measurements with Numerical Model Results

Input data to the numerical model consisted of wind speed, wind direction, air temperature, water temperature, solar radiation, evaporation, inflows and outflows. The initial conditions of the model were defined due to measurements implemented in the area, and the bathymetry of the model was also adapted to the current conditions at the time of the comparison.

6.2.1 Simulation of Velocities

Flow velocities in the water column after a 4 days simulation were compared with field observations (Figure 6.8). An average measured wind data of 3 m/s was used as an input during the simulations for the initial water temperature given in Figure 5.1 and meteorological data recorded in July-2006 at the weather station. Discharges of the rivers were 0.04 and 0.16 m^3/s as measured in Sasal and Tahtali rivers respectively. The

water velocity data were measured at 1 meter intervals in the water column using ADCP. The velocity error ranged between 0.05 - 4.2 cm/s in the water column. These values are comparable with other reported values. Rueda et al. (2003) reported errors of 2 - 5 cm/s for Clear Lake. Elci and Work (2004) compared the measured and the modeled velocities in Lake Hartwell and observed velocity errors ranging from 3.6 to 6 cm/s. In another study, Jin et al. (2000) reported velocity errors ranging between 1.52 and 4.76 cm/s for Lake Okeechobee.

The results of the comparisons indicated that numerical model predicted the measured velocities except for the North top surface velocities. The reasons for the discrepancy between the top surface velocities of the modeled and the measured were further investigated.

First, the effects of inflows and outflows on velocity profiles were investigated through a sensitivity analysis. The model was run without inflows coming into the lake, and the simulated velocities were compared with those obtained when inflows were considered. The same sensitivity test was repeated for outflow. As a result, the velocity differences were observed 4% in both cases. The effect of inflows and outflows on the velocity profiles of Lake Tahtali was found insignificant.

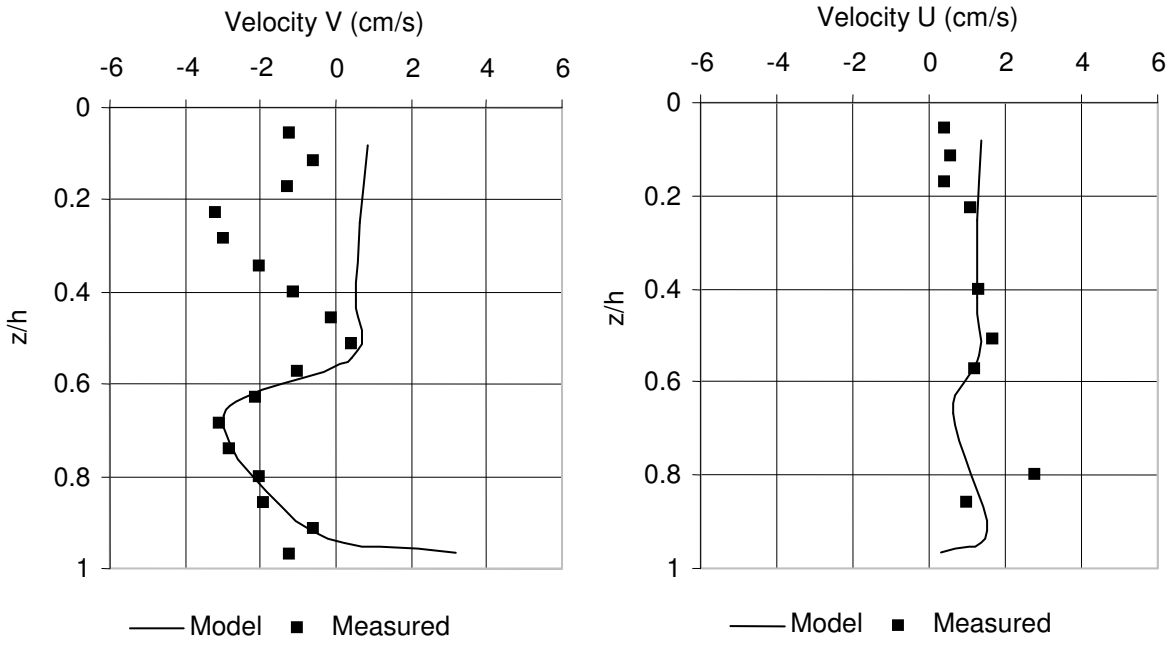

Figure 6.8. Comparison of measured North (V) and East (U) velocities on 28.09.2006 with the simulated velocities recorded at the buoy. z/h is the dimensionless depth and represents surface when equal to zero

Sensitivity analysis conducted to test the effect of different parameters on velocities and temperature profiles indicated that water velocities were strongly dominated by the wind data and correct measurement of wind stress on the lake surface is necessary for accurate prediction of velocities in the water column.

Due to discrepancies between the modeled and observed velocities, the reason for differences between two were investigated. The wind data measured by a hand-held instrument on the lake surface (Elevation=60 m above the sea level) were compared to the data collected at the weather station (Elevation=80 m above the sea level) installed at the lake shore (Figure 6.9). The measured wind speed in the open water was higher than the wind data recorded at the weather station corresponding to the time used for the comparison of the numerical model and the measured velocity vectors. The weather station displayed 2.5 m/s wind speed while the speed at the lake surface (buoy) was 5 m/s at the same time, which would be expected due to larger fetches on the lake surface. So, each wind data used as an input for the model was modified to reflect the wind speed felt on the open water. Since the effect was investigated for the top surface east velocities, mean surface east velocity of the first model was 1.5 cm/s when compared to 3.5 cm/s in the model with enhanced wind forces. Numerical model results indicated that water velocities were strongly dominated by the wind data and correct measurement of wind stress on the lake surface would lead to better results in the comparisons of the measured and the modeled data.

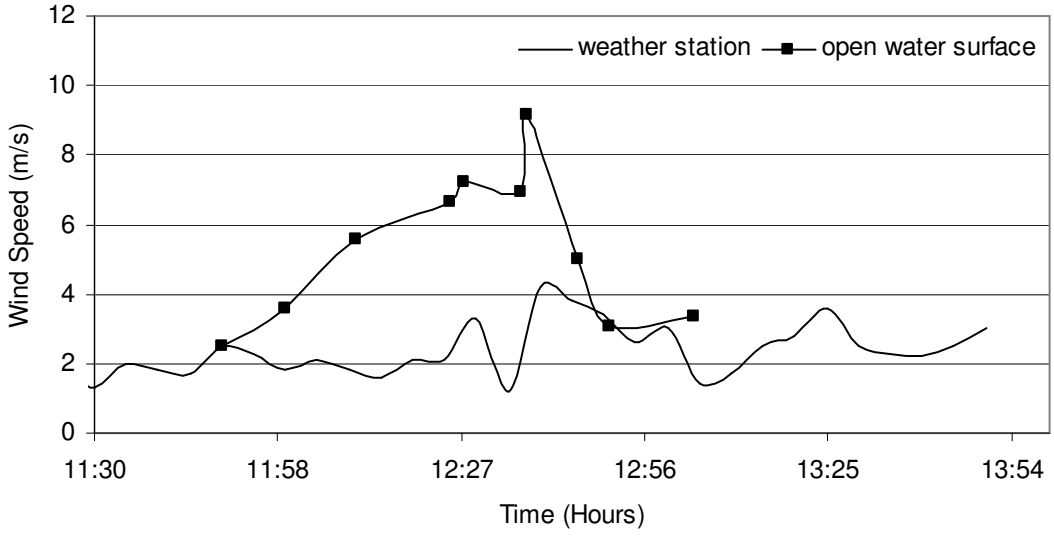

Figure 6.9. Comparison of wind speed between the data recorded at the meteorological station and at the buoy on 28.09.2006

6.2.2. Simulation of Temperature

The time series of temperature values were measured at 30 minutes intervals at 11 m depth below the water surface corresponding to the stratified region. Numerical simulations of temperature values were compared with field observations (Figure 6.10). The water temperatures were highly affected by the cooling and warming air temperatures in August but the water temperatures in October did not show the same character due to the daily variations of air temperature. The daily variations of the temperatures are also attributed to the internal seiches effective in epilimnion and metalimnion with a period of approximately one day due to the cessation of high winds picking up mostly in the afternoon. This value is close to the period of basin scale internal wave calculated using the equation (6.1) suggested by Spiegel and Imberger 1980.

$$T = 2L\sqrt{\frac{(g'*h_1*h_2)}{H}} \tag{6.1}$$

where, L is the length of the reservoir, H is the total depth, h_1 and h_2 are the heights of upper and lower layers.

For the comparisons of measured and simulated time series, root-mean-square error (RMSE) was calculated by Equation (6.2).

$$RMSE = \left[\sum_{n=1}^{N}\frac{(T_{est}-T_m)^2}{N}\right]^{1/2} \tag{6.2}$$

where; T_{est} is the modeled temperature profile; T_m is the measured temperature profile and N is the number of data points. RMSE in August was calculated 0.968 in degree Celsius whereas in October this value decreased to 0.571. These values are comparable with the other studies in literature. Jin et al. (2000) reported RMSE of 0.7 for Lake Okeechobee and Rueda et al. (2003) reported RMSE of 0.414 and 0.608 in two different stations in Clear Lake.

a)

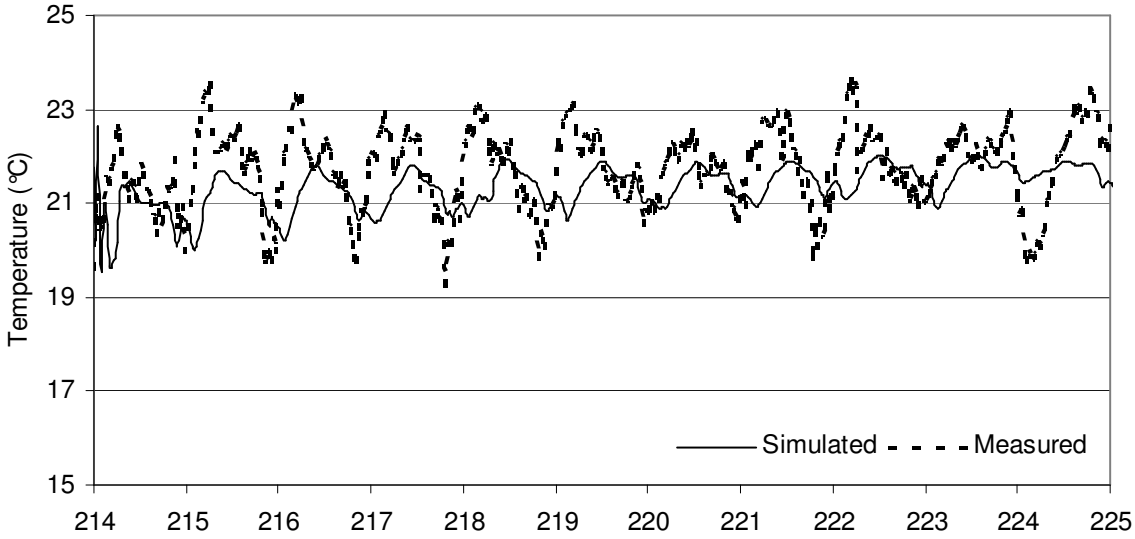

b)

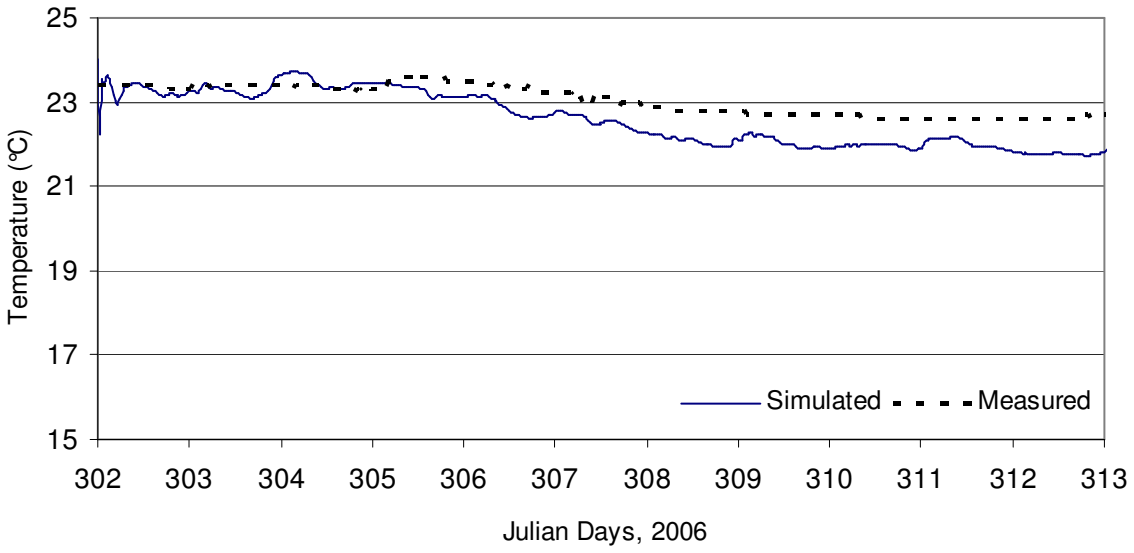

Figure 6.10. Comparison of measured and modeled water temperatures at 11 m below the water surface at the buoy. Graph (a) is the measurement for August, 2006; (b) is for November, 2006

CHAPTER 7

EFFECTS OF SELECTIVE WITHDRAWAL ON HYDRODYNAMICS

In water supply reservoirs, selective withdrawal is commonly implemented to control released water temperature for quality purposes. In this chapter, the effects of selective withdrawal on hydrodynamics of a stratified reservoir were investigated through numerical modeling and analytical analysis. A 3–D hydrodynamic model was applied where observations of water temperature time series recorded every 30 minutes at the thermocline and measured temperature profiles along the water column were used to validate the numerical model. The effect of selective withdrawal from four outlets located along the water intake structure of Tahtali Reservoir in Turkey on water temperatures was investigated and the effects on thermal stratification structure were discussed.

In stratified lakes, the density gradient is most pronounced at thermocline, but there is also a weak temperature gradient throughout the hypolimnion, where the outlet structures of a reservoir are normally located. If water is withdrawn from such an outlet at small discharges, the vertical density gradient may produce buoyancy forces sufficiently strong to prohibit extensive vertical motions so that the water withdrawn comes from a thin horizontal layer at the level of the intake. At somewhat larger discharges the withdrawal layer may intersect the thermocline and at very large discharges the effects of buoyancy may be completely overwhelmed and the flow returns to potential flow. (Fischer, et al. 1979). Following Ivey and Blake (1985), outflow dynamics at the outlets were investigated via transition number as defined in Equation (7.1):

$$S = \left(Q^2 N \upsilon^{-3}\right)^{1/15} \tag{7.1}$$

where; S is the transition number; Q is the total discharge; N is the buoyancy frequency; υ is the kinematic viscosity. If $S > 3$; the inertia-buoyancy regime governs the flow, forming a layer of constant thickness;

$$\delta = C_3 \left(QN^{-1}\right)^{1/3} \tag{7.2}$$

where; C_3 is the withdrawal coefficient and $C_3 = 1.42$ gave the best results for layer thickness δ in inertia-buoyancy regime. S was calculated as 15 suggesting the strong buoyancy forces and that the water withdrawn comes from a thin horizontal layer at the level of the intake.

Wood and Binney (1976) examined the drawdown of water from the upper layer into a line sink positioned in the lower layer, suggesting the use of Froude number to define the critical discharge at which the drawdown occurs. Two cases may be defined for the radial flow. First, the outlet is close to the bottom of the lake (Equation (7.3)) and second, the outlet may be very much closer to the thermocline (Equation (7.4)).

$$F_{3c} = \frac{Q_{3c}}{\left[\left(\frac{\Delta\rho + \alpha^2 \Delta^1 \rho}{\rho_0}\right) g d^5\right]^{1/2}} = 1.02 \qquad d \approx (H - h)) \tag{7.3}$$

$$F_{3c} = 2.04 \qquad d << (H - h) \tag{7.4}$$

where; $\Delta\rho$ is the density difference between the water at the surface and at the thermocline; α^2 is the density jump coefficient; $\Delta^1\rho$ is the density difference between the water at the offtake and that at the top of the hypolimnion; *d* is the distance between the center of the outlet and the layer interface. Wood (2001) summarized the existing theory for both line and point sink cases, showing that the ratio of discharges from a multiple-layered stratification is determined by the density difference between the layers, the location of a virtual control relative to the sink, and a total discharge at the valve.

In Tahtali Reservoir, there are four outlets located at different depths of the water intake structure (Figure 7.1). The elevations of the outlets are 50, 43, 36 and 29 m respectively from the sea level. The water intake structure is reinforced concrete with a diameter of 17 m and 35 m height. The water withdrawn from one of these valves is pumped to the water treatment plant through two steel pipes with a diameter of 1.6 m. The critical discharge was calculated for three different outlets. The 43 m outlet level is very much closer (1.2 m) to the thermocline point so by using the equation (7.4), the critical discharge for the outlet at 43 m was calculated 0.15 m^3/s. For the other two outlets 36 m and 29 m, the critical discharges were calculated 21 m^3/s and 36 m^3/s

respectively using the equation (7.3). According to this analysis, with outflow rate of $3m^3/s$, the drawdown can only be observed when water is withdrawn from the outlet located above the thermocline.

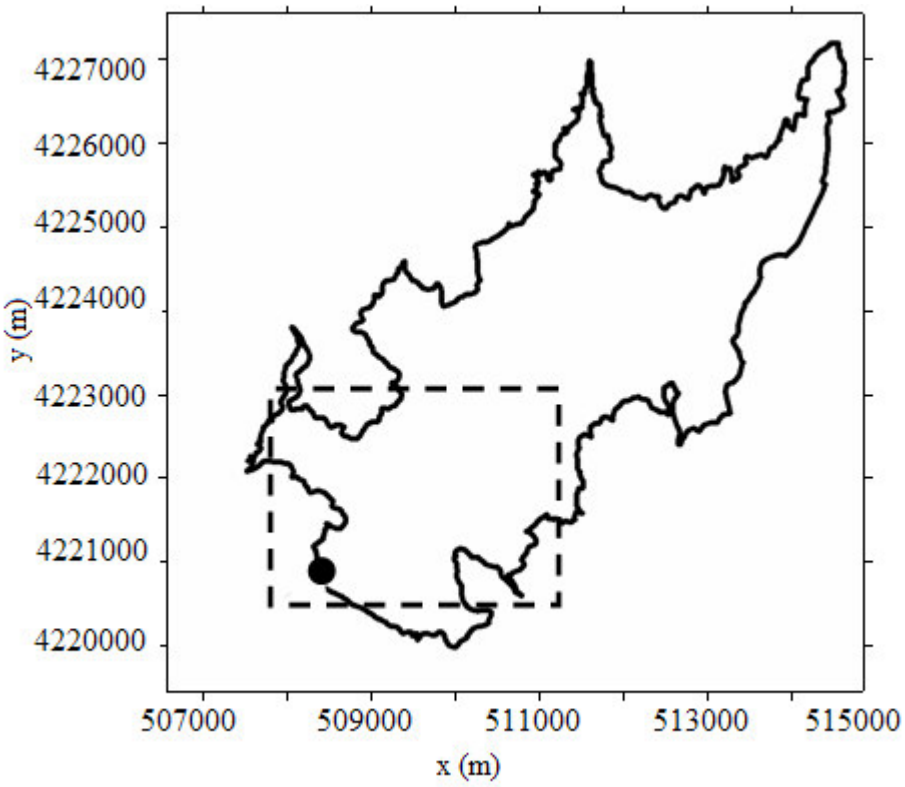

Figure 7.1. Map of Tahtali Reservoir. Dashed box shows the model domain in which withdrawal effects were investigated. Circle shows the location of water intake structure

7.1. Modeling Effects of Water Withdrawal from Different Outlets

The effect of selective withdrawal on stratification patterns of the lake was investigated using EFDC model. The outlet at 43 m elevation was within the stratified region in the water column. The model runs were implemented one by one for all selective withdrawal levels to understand which outlet level would encourage mixing in the water column. The temperature differences simulated by the model when water was withdrawn from different outlets are shown in Figure 7.2. When the water was withdrawn from the outlet located at 50 m from the sea level (Figure 7.2a), the water temperatures in the mid-layer became 0.5% colder. As the withdrawal was from lower

outlets (Figure 7.2b; 7.2c; 7.3d), water temperatures in the stratified layer increased 0.5% at 43 m and 36 m; 4% at 29 m indicating more mixing affecting the area within the radius of 2 km. When the temperature differences were plotted in vertical at a cell located 300 m away from the withdrawal point, water temperatures were decreased by 0.5% for the 50 m outlet. Withdrawing water from 43 m and 36 m outlets increased the temperatures by 0.65%. And when the outlet at 29 m was used, the temperature in hypolimnion increased up to 6% (Figure 7.3). 12 days simulations indicated that temperature increased and became warmer in the stratified layer when the water was withdrawn below thermocline depth.

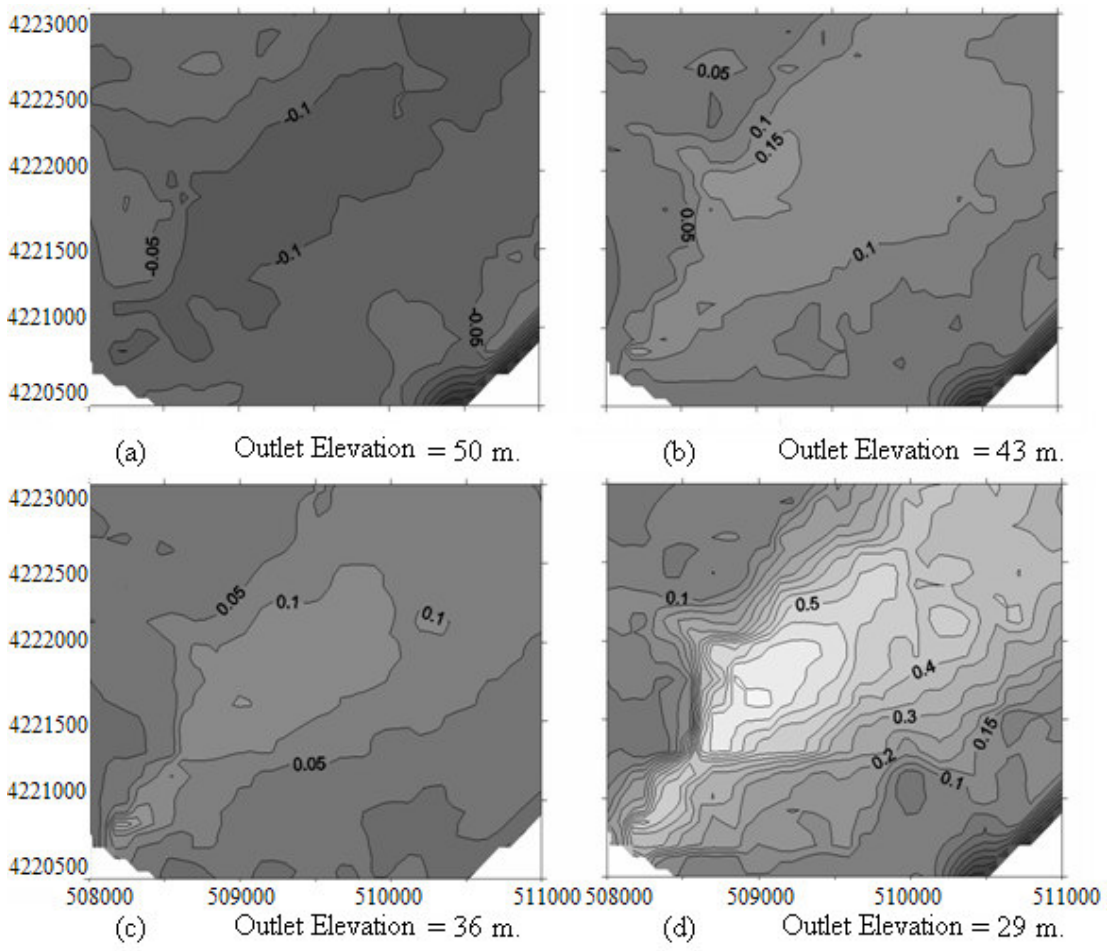

Figure 7.2. Distribution of water temperature differences between two models (before and after withdrawal) in the stratified layer (depth=11 m). The water level was 54 m (above the sea level) during the simulation period in August. The withdrawal point is located at x = 508000; y = 4220500. The color gets lighter as the temperature increases

In addition to the water temperature distribution, the effect of withdrawal on North velocities was compared in Figure 7.4. The upper withdrawal increased the velocities in epilimnion by 34%, whereas the lower withdrawal increased the velocities by 47% in hypolimnion validating the impact of withdrawal level. It is recommended to withdraw the water at the outlet located at 29 m to encourage mixing in the water column.

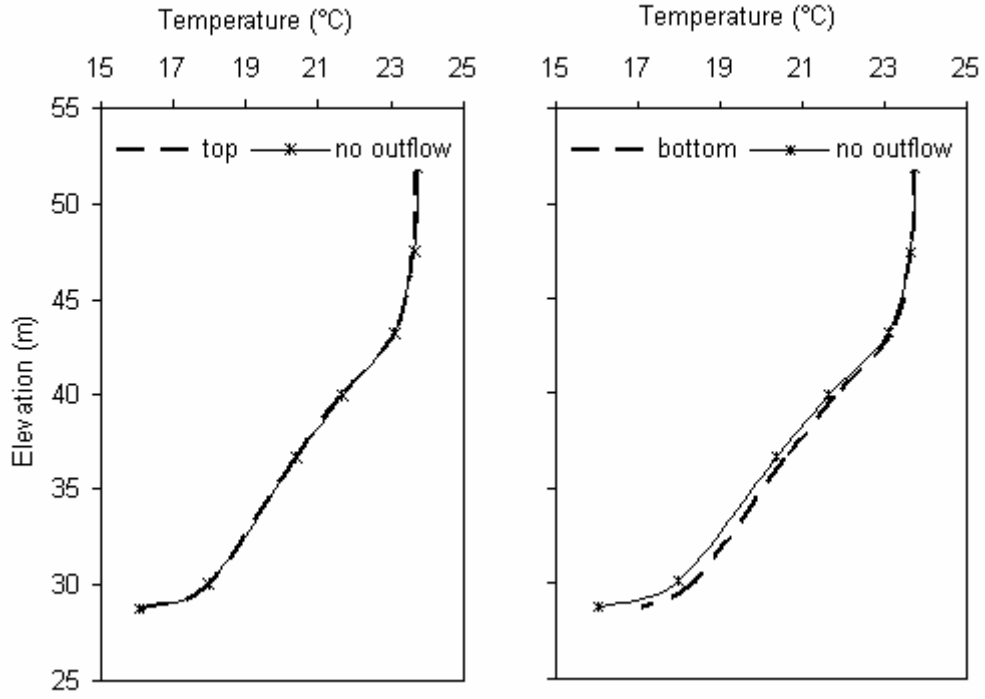

Figure 7.3. Comparison of the withdrawal effect on water temperatures of the top (Elevation= 50 m), and the bottom outlet (elevation= 29 m) with the model assumed that there was no outflow at the cell 300 m upstream of the withdrawal point

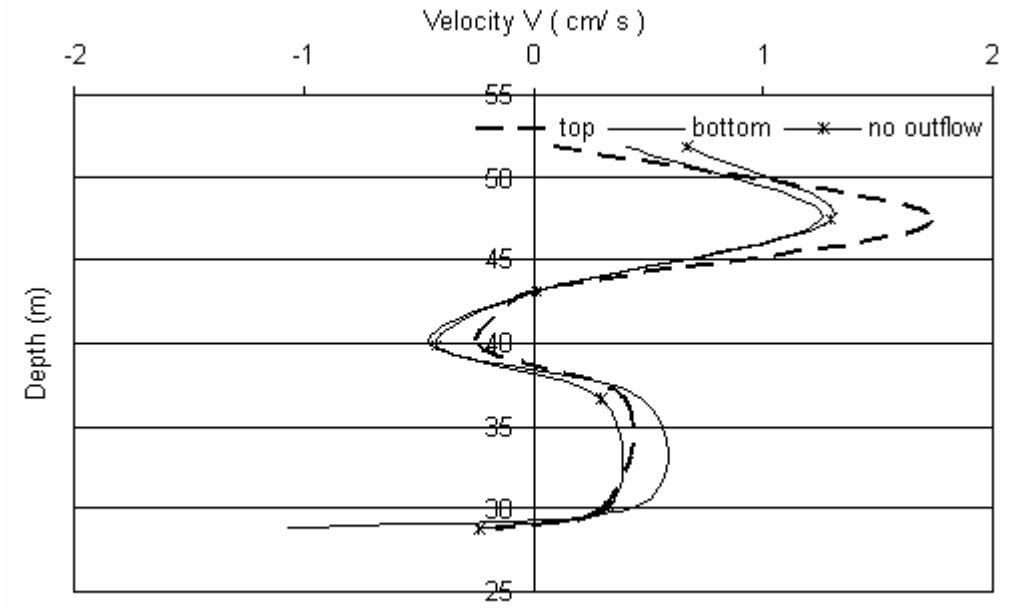

Figure 7.4. Comparison of the withdrawal effect on flow velocities at the top (Elevation= 50 m), and at the bottom outlet (elevation= 29 m) with the model that there was no outflow at the cell 300 m upstream of the withdrawal point

Among various water quality management techniques summarized in the literature for artificial destratification (Dortch 1997), it is recommended to use hydraulic destratification in Tahtali, using small diameter diffuser ports creating high velocity water jets. This type of treatment would mix hypolimnetic and epilimnetic water and would prevent anoxia. Hypolimnetic aerators can be used as a stirrer and a bubbler (Lindenschmidt and Hamblin 1997) to promote mixing between epilimnion and hypolimnion.

CHAPTER 8

EFFECTS OF CLIMATE CHANGE ON HYDRODYNAMICS

Climate change is one of the most severe problems people are facing in today's world. Sometimes referred to as "Global Warming", climate change refers to global changes in temperature, wind patterns, and precipitation in the Earth's climate system. According to scientists, these changes are the result of human activities. Increasing use of fossil fuels, and cutting down of forests causes increases in greenhouse gas amounts. The releases of greenhouse gases have shifted the natural balance of atmosphere by trapping the heat. As a result, the more heat means, the warmer the Earth becomes.

Changes in air temperatures and weather patterns have many effects on physical environment, health, and economy. Based on the change, climate may become warmer or colder. Amounts of rainfall or snowfall can decrease or increase. In recent years, these changes are happening faster; there has been drought in some regions in the world whereas floods and strong storms have been observed in other places. There has been an increase in sea levels because of melting of ice cabs. Species of animals and plants may become extinct because of the changes in climate.

The possible effects of climate change which became a big threat for today's world by affecting both the groundwater and surface water resources were investigated in this chapter. The hydrodynamic model (EFDC) was used to model the effects of climate change on stratification patterns.

8.1. Modeling of Climate Change in Gediz and Büyük Menderes River Basins

To investigate the possible effects of climate change, a study was carried out by Dokuz Eylul University - Water Resources Management Research and Application Center. The effects of climate change were investigated for Gediz and Buyuk Menderes River Basins near the city of Izmir (Sumer 2006). Each basin was analyzed by dividing

it into sub-basins to get more accurate model results. Gediz basin, the second largest in the Aegean region, has a total drainage area of about 18,000 km^2. The basin experiences drought from time to time because of environmental pollution. The second basin, Büyük Menderes, is the second longest river in the Aegean region. Büyük Menderes Delta is an important wetland with an area of 9,800 ha, and has a total drainage area of 24,976 km^2. The annual runoff is in the order of 3 km^3, which accounts for 1.6% of Turkey's potential (Ministry of Environment and Forestry 2007). These basins have been turned into extensive water resource systems including Lake Tahtali (Figure 8.1). The study was carried out using spatially averaged temperature and precipitation to evaluate climate change effects in Gediz and Büyük Menderes River Basins. MAGICC/SCENGEN climate model was used for creating two different scenarios (ASF model of A_2 and MESSAGE model of B_2 storylines) for three projection years of 2030, 2050 and 2100. The case was investigated annually and seasonal. The estimated changes in temperature and precipitation are shown in Table 8.1.

Figure 8.1. Map showing Gediz and Büyük Menderes River Basins
(Source: Sumer, 2006)

8.2. Modeling of Climate Change in Tahtali Basin

Simulation results carried out by Dokuz Eylül University- Water Resources Management Research and Application Center indicated that runoff changes would be 20%, 35%, and 50% less in years 2030, 2050, and 2100 respectively. This will cause

serious problems for water resources and many other things including agricultural and industrial cases.

Table 8.1. Generated changes in temperature under IPCC B_2-MES scenario (top) and IPCC A_2-ASF scenario (bottom) carried out by DEU-SUMER (2006). DJF: December, January, February; MAM: March, April, May; JJA: June, July, August; SON: September, October, December

Period	Baseline			2030		2050		2100	
	Observed	Modeled							
	Mean	Mean	Std.	Change	Ch. In Var.	Change	Ch. In Var.	Change	Ch. In Var.
	°C	°C	°C	°C	%	°C	%	°C	%
Annual	16.3	16.4	0.4	1.2	5.1	1.8	7.9	3.2	14.7
DJF	9.4	9.4	0.8	1.0	-2.5	1.5	-3.9	2.6	-7.2
MAM	14.4	14.4	0.6	1.1	2.7	1.7	4.1	2.9	7.7
JJA	23.4	23.5	0.6	1.6	3.8	2.4	5.9	4.1	10.9
SON	17.8	17.8	0.8	1.4	-2.0	2.0	-3.1	3.6	-5.7
Period	Baseline			2030		2050		2100	
	Observed	Modeled							
	Mean	Mean	Std.	Change	Ch. In Var.	Change	Ch. In Var.	Change	Ch. In Var.
	°C	°C	°C	°C	%	°C	%	°C	%
Annual	16.3	16.4	0.4	1.2	4.0	2.0	7.7	4.4	20.6
DJF	9.4	9.4	0.8	1.0	-2.0	1.6	-3.8	3.5	-10.1
MAM	14.4	14.4	0.6	1.2	2.1	1.9	4.0	4.1	10.8
JJA	23.4	23.5	0.6	1.5	3.0	2.5	5.7	5.5	15.3
SON	17.8	17.8	0.8	1.2	-1.6	2.0	-3.0	4.7	-8.0

The simulation results of Gediz and Büyük Menderes River Basins were used to investigate the effect of climate change in Lake Tahtali. Air temperatures in summer months were expected to be 3.8%; 5.9% and 10.9% more than today's temperatures in years 2030, 2050 and 2100 respectively in the first scenario shown in Table 8.1. The expected air temperatures belonging to year 2100 were used as an input to the numerical model of Lake Tahtali to investigate the effects on hydrodynamics. Climate change effect was investigated in the area where withdrawal effect was also investigated

(Chapter 7) and in the whole lake to investigate the effect on surface water temperatures.

The air temperatures of the model which August measured data of wind speed, atmospheric, and hydrologic conditions were used were enhanced due to the expected 10.9% increase in 2100. The thermocline was at 10 m depth below the water surface in August, 2006. Due to the climate change model results, the starting point of stratification increased up to approximately 9 m depth (Figure 8.2). The amount of dissolved oxygen between the water surface and the thermocline was 5 mg/liter in August measurements whereas it was 2 mg/liter in hypolimnion. Since the thermocline was at 9 m depth in climate change model, the volume of epilimnion was less when compared to 2006 meaning worse water quality in the lake. This 1 m difference between the thermocline depths of 2006 and 2100 caused deterioration of 20 million m^3 more water in the lake. Climate change model results showed that the volume of stratified region got bigger meaning less dissolved oxygen in lake water.

The effect was also investigated in horizontal in the whole model domain. Due to the model results, 10% increase in air temperatures resulted in 7% increase in surface water temperatures (Figure 8.3).

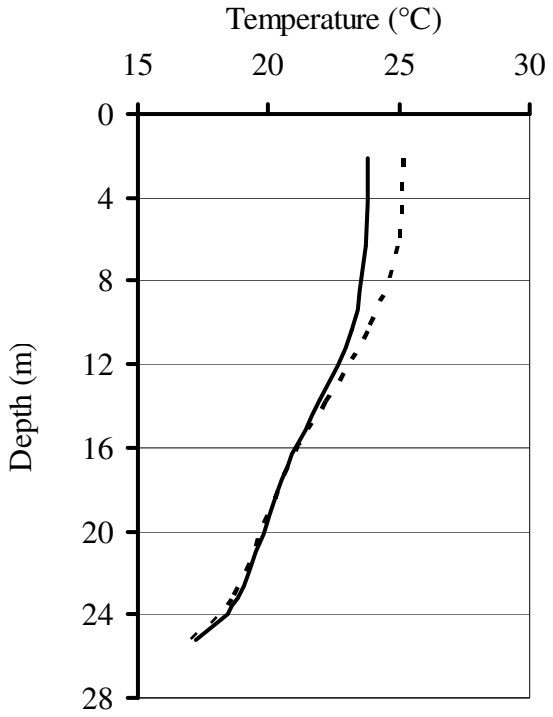

Figure 8.2. Comparison of stratification in years 2006 and 2100 using a vertical profile at the buoy

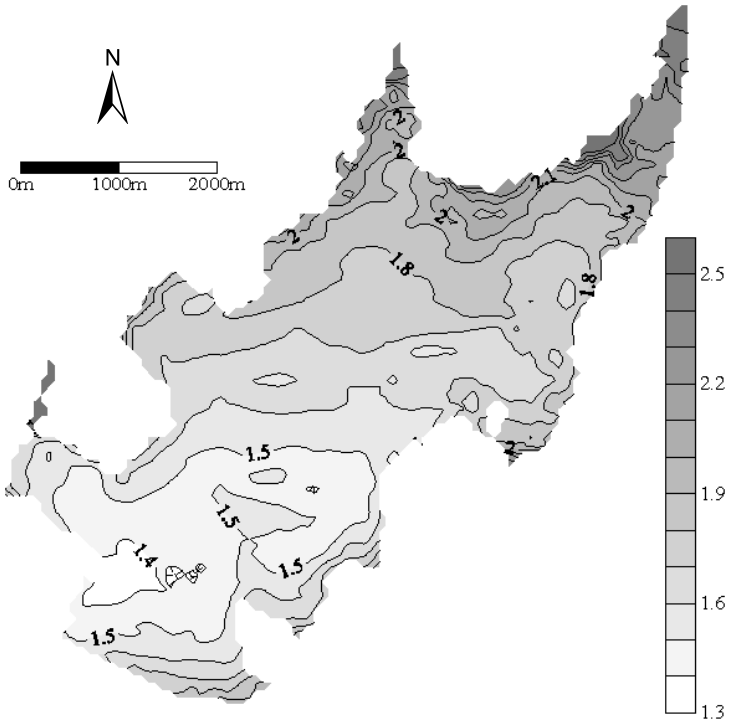

Figure 8.3. Surface water temperature differences in ^{0}C of August, 2006 and in the future (Source: Summer, 2100)

Table 8.2 shows the simulation results of runoff changes conducted by DEU-SUMER in Gediz and Buyuk Menderes river basins. The effect of decreasing runoff was investigated through numerical modeling. B_2 runoff change scenario results of year 2100 (-58%) were used to understand the effect on hydrodynamics. Current runoff data of Lake Tahtali numerical model previously ran with measured data of September 2006 (wind, air temperatures, water temperatures and inflow rates) was decreased by 58% and the case was analyzed.

Table 8.2. Runoff changes modeled by DEU-SUMER (2006) under climatic conditions belong to years 2030, 2050, and 2100 in Gediz and Buyuk Menderes River Basins

	2030		2050		2100	
	B_2 (%)	A_2 (%)	B_2 (%)	A_2 (%)	B_2 (%)	A_2 (%)
Gediz Basin	-23	-32	-35	-48	-58	-71
B. Menderes Basin	-10	-21	-20	-38	-45	-71

Precipitation is another important component of hydrological cycle and should be considered for the future climate change simulations. It is expected that the summer temperature increases and the winter rainfall decreases in the Mediterranean region (IPCC, 2001). In summer, not many changes expected in the amount of precipitation over Turkey. Harmancioglu and Ozkul (2008) investigated the effects of climate change on precipitation and temperature using GCMs considering two different emission scenarios (B2-MESSAGE and A2-ASF) over the test basin (Gediz and B. Menders River Basins). According to the simulation results, an increase of 1.2^{o}C in mean annual temperature and a decrease of 5% in mean annual precipitation were expected for the year 2030. For 2050, 2^{o}C of increase in mean annual temperature and 10% decrease in mean annual precipitation were simulated. The simulation result of around 10% decrease in 2050 for the precipitation was used as an input to the numerical model of Lake Tahtali to understand the effect of change in precipitation on hydrodynamics. The input data of September, 2006 were used in the simulations.

In addition to the climate change simulations (temperature, runoff, and precipitation) specified above, another model was run with the combined effects of these three. The effect was investigated for the average surface water temperatures in Table 8.3 corresponding to survey transects shown in Figure 8.4 in Lake Tahtali.

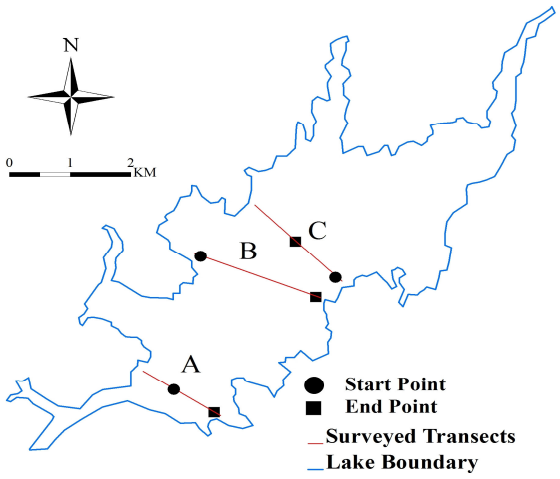

Figure 8.4. Survey transects in Lake Tahtali (Water elevation above the sea level= 46 m)

Table 8.3 Change in variation of average surface water temperatures of today (September, 2006) and in the future (2050, and 2100) for air temperature, runoff, precipitation, and combined effects of them in A, B, and C transects

	Variation in Surface Water Temp (^{o}C)		
	A (%)	B (%)	C (%)
Current Model	0.00	0.00	0.00
Increased Air Temperature (10%)	1.00	3.00	2.00
Decreased Runoff (-58%)	23.00	25.00	25.00
Decreased Precipitation (-10%)	0.00	2.00	1.00
Combined	23.00	26.00	25.00

As seen from the table (Table 8.3), decreased runoff caused a significant increase in surface water temperatures which the change of variation was approximately between 23% and 25%. The difference gets bigger in B, and C transects for the reason that these transects are closer to the inflow region. The other parameters; air temperature and precipitation caused an increase between 1% and 3% in surface water temperatures in A, B, and C transects. The variation in surface water temperatures with decreased runoff data were higher when compared to other two model runs since water temperatures are strongly affected by the temperature of coming inflows especially if there is a flood condition.

CHAPTER 9

MODELING OF SEDIMENT TRANSPORT AND DEPOSITION

Soil erosion causes the deterioration of ecology by having both on-site (with the loss of fertile soil) and off-site (by deposition of eroded sediments) effects. Transport of sediments with pollutants attached on them can cause disruption of ecosystems, reduces reservoir's lifetime and hydrodynamic potential of dams and can contribute to contamination of drinking water supplies. Reduction in storage capacity has impacts on the function of reservoir's usage purpose and results in notable costs on the economy of the region. In addition; sedimentation creates the scouring of the river channels which causes problems for water supply and navigation. Especially in large reservoirs, it plays very important role in a country's development of its economy and ecology. Estimating sediment deposition is important for project design and planning of monitoring of sediments and for better operation of dams (Graf 1984, Fan and Morris 1992). Heavy metals have affinity to attach to cohesive sediments and might behave as the major pollutant and carrier. When sediment particles carried into a reservoir, they not only cause silting up of reservoir but can also deteriorate water quality. (World Meteorological Organization 2003).

It is essential to predict effects of sedimentation and loss of storage capacity in advance for better operation of the reservoirs. Current research on reservoir sedimentation prediction is mainly based on numerical modeling of sediment transport methodologies (Hotchkiss and Parker 1991) and investigation of transport parameters in the laboratory (Guy, et al. 1966, Soni 1981).

Surveying and numerical modeling of reservoirs are required to determine sedimentation rates and to assess overall capacity of the reservoir. For surveying, manual sounding poles, sounding weights and echo sounders are commonly used. For reasons of economy, accuracy and expediency, sedimentation surveys were carried out in small reservoirs or cross small river reaches. More advanced instruments have been adopted as electronic distance measuring systems for large reservoirs. Sedimentation surveys are best reliable for the accurate positioning of measuring points where no

deposition or erosion takes place, the elevation of the bed surface should coincide with that measured in a previous survey. This is a good check of the accuracy and reliability of the sedimentation surveys. In addition to this detailed bathymetry map, thickness and long-term average accumulation rates of the lake can be determined by using echo sounder systems (Odhiambo and Boss 2004). Other studies in literature about surveys implemented using acoustic methods includes the technical details of scanning (Urick 1983), techniques used for sediment mapping (Higginbottom, et al. 1994), and the comparison of different echoes on sediment type (Collins and Gregory 1996).

In this chapter, sedimentation patterns within the main pool of Lake Tahtali were described. The transportation of the cohesive sediments carried by two rivers (Sasal and Tahtali) and the depositional zones were investigated using EFDC (Environmental Fluid Dynamics Code) numerical model and the results were compared to the calculated erosion results by USLE method.

9.1. Prediction of Erosion by USLE

Universal soil loss equation (USLE) predicts the long term average annual erosion rate on a field slope based on the rainfall regime, soil type, cropping system and the management practices. USLE is used only for sheet or rill erosion calculation in long term and does not account for the times that strong winds and heavy rains occur. In the study carried out by Odhiambo and Boss (2004), long term average accumulation rates were calculated to model sediment infilling and projected lifetimes in Lee Creek Reservoir and Lake Shepherd Springs in the Ozark Plateau of Northwestern Arkansas which USLE model suggested that rill erosion was a dominant process of sediment erosion and transport within in both watersheds. (Golson, et al. 2000) studied the accuracy of USLE Method by comparing the method with other applications like MUSLE (Modified USLE) and the Onstad –Foster Equation.

The average annual erosion rate was calculated for Tahtalı Basin using USLE method. This method states that;

$$A = RKLSCP \tag{9.1}$$

where; A is the average annual soil loss in $ton/ha/year$; R is the rainfall erosivity factor; K is the soil erodibility factor; L is the slope length factor in m; S is the slope

steepness factor; C is the cropping management factor; P is the supporting practice factor.

Rain erosivity factor is calculated due to 8-32 years of data collected at 96 different weather stations in Turkey (Dogan 2002). The average annual R value calculated for Izmir (R=166) is used to predict the soil erosion in Tahtalı Basin. The distribution of calculated R values per month for Izmir is given in Table 9.1. As expected, R values are higher in winter months.

Table 9.1. Distribution of rain erosivity factors (R) measured in Izmir- Menderes due to 20 years measured data

Months	Jan	Feb	March	April	May	June	July	August	Sep	Oct	Nov	Dec
R (ton-m/ha)	19.172	16.692	18.076	7.027	7.852	2.339	0.855	0.87	4.204	22.664	26.761	37.045

Soil erodibility factor (K) is the average soil loss in a particular soil land and changes due to the characteristics of soil. The infiltration rate of the soil type and the reflection of soil under different rain events are important to understand K factor. K value ranges between 0 and 1 where high K value means the more sensitive soil type to erosion. The soil erodibility map of Tahtalı Basin with respect to different soil types are shown in Figure 9.1 (Ministry of Agriculture and Rural Affairs 2006). K values for different soil types were assumed as;

- 0.15 for low or non erosive
- 0.28 for medium erosive
- 0.45 for high erosive
- 0.60 for very high erosive soils

As seen from the figure, high erosive soils are located close to the lake. In general, erosion is very low or non in alluvial soil types; low or medium in colluvial soil types and finally high in soils including silt and iron as an ingredient.

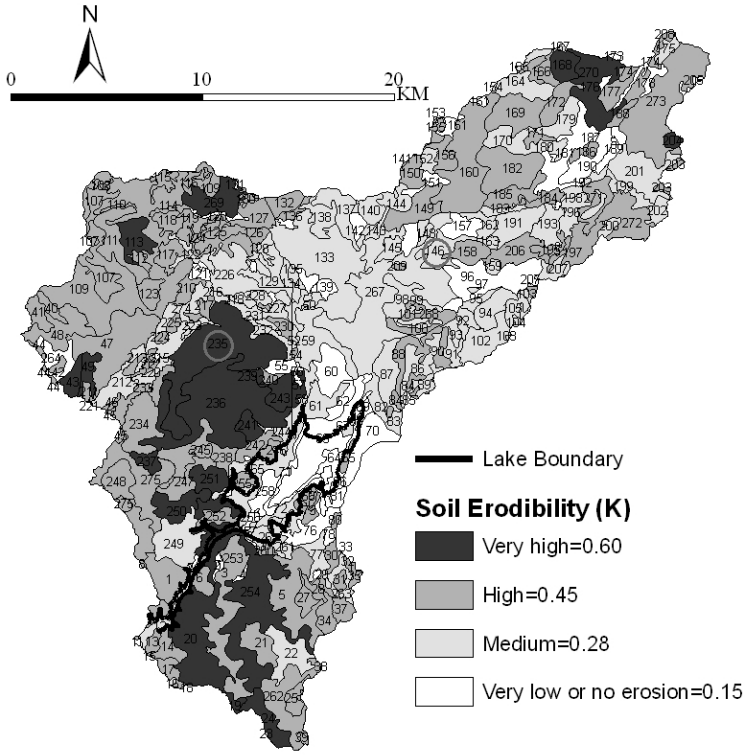

Figure 9.1. Chorophlet map of Tahtalı Basin showing erosion types of the polygon layers

Slope length is the horizontal distance between the starting and the ending point of a land slope. The more slope length means the more erosion in the area. Different equations are available for the calculation of slope length factor (L). In this study, the equation used for Tahtalı Basin is;

$$L = (I/22.1)^{0.5} \tag{9.2}$$

where; I is the slope length in (m).

Slope steepness factor is the effect of slope on soil erosion. If the slope of the land is high, more erosion occurs in the area. Slope steepness factor affects the rate of erosion more than the slope length. The average slope of Tahtali Basin is 15%.

The crop management factor makes use of the crop type in the calculation of USLE. It's important how the vegetal cover absorbs the energy of rain. The vegetal cover can reduce the drop size and provides mechanical protection by increasing the infiltration capacity of soil.

Figure 9.2 gives different land usages in Tahtalı Basin. As can be seen from the figure, Tahtali Basin is mainly covered with forests (35%) and heath bell (31%). Forest lands are low erosive whereas heath bell lands are considered high erosive. Erosion of

soils is highest in fallow lands where crop management factor is equal to 1 in these lands.

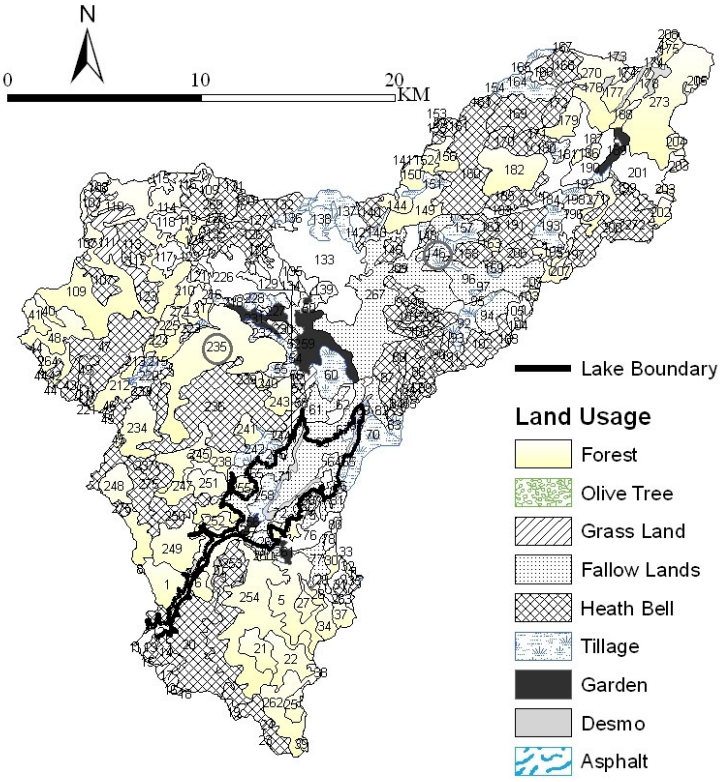

Figure 9.2. Chorophlet map of Tahtalı Basin showing the land usages

Soil erosion can be controlled and reduced by protective measures such as furrowing, soil replacement, and seeding of the land. The average practice factor for Menemen/ Izmir was found as 0.44 in average (ranging between 0.10-0.92). The annual soil erosion in each polygon shown in Figure 9.1 was calculated. For instance, for the polygon number 235 circled in the chorophlet map, the crop type is forest (C=0.001); erosion rate is high due to the vegetal cover (K=0.60); slope and the slope length of the polygon were calculated using the measured values available in attributes table of digitized maps of the basin (L=737 m; S=25%); the average annual R value calculated for Izmir (R=166) was used and the supporting practice factor for the reservoir area was taken as 0.44. As a result, the erosion rate of the soils in polygon number 235 (Figure 9.2) was found to be $0.265\, ton/ha/year$. Similarly, for the polygon number 146, this rate was calculated as $16.9\, ton/ha/year$. Comparison of two polygons indicated that

although the other characteristics of the polygons were the same, the crop type in polygon number 146 was tillage in which cropping management factor was very high (C=0.48) indicating more erosion would occur in the area (Table 9.2). Total sum of 245 polygon layers were considered in the whole basin of Tahtali. The steps summarized for two polygons (235 and 146) were repeated for each polygon and the total erosion rate occurred since 1995 was calculated $19x10^6 tons$ (Elci, et al. 2008).

Table 9.2. Calculation of erosion rate by USLE method for two polygon layers

object	Land Usage	A (t/ha/year)	R	K	L	S	C	P
146	Tillage	16.913	166	0.28	530	0.10	0.480	0.44
235	Forest	0.265	166	0.60	737	0.25	0.001	0.44

9.2. Modeling of Sediment Deposition

Data describing sediment concentration, sediment class, fall velocity and critical shear stresses were needed for the numerical model to simulate sediment transport. Due to the lack of TSS (total suspended solids) measurements in the reservoir's tributaries, an average sediment concentration value was used (500 mg/l) as an input to the numerical model utilizing the turbidity measurements implemented in the lake. Effect of atmospheric and hydrologic conditions (inflow, outflow, water temperatures and the weather patterns) on lake hydrodynamics varies with time and the deposition in the lake has occurred between the years 1995 and the end of 2007. Long term average seasonal data were used for runs implemented for two months to investigate sediment deposition in Lake Tahtali where data used for the first month represented flood condition in the lake. Flows corresponding to flood condition were determined due to the number of rain events occurred in December, 2006 recorded in the area by IZSU (Izmir Water and Sewage Administration). The initial geometric and the topographic conditions belong to year 1995 was used to construct bathymetric maps. For meteorological data, long term average (1954-2006) air temperature and the rain data measured at the weather station located in Menemen, Izmir were used which data were recorded by Menemen Research Institute of Soil and Water Resources. Long term average water temperatures in the lake and the tributaries measured by IZSU between 2001 and 2006 were utilized in the

numerical model. The other inflow data were used from the long term average discharges illustrated in Figure 3.2 measured by General Directorate of Water Resources. The withdrawal rate used was constant and 3 m^3/s. The soil granulometry of rivers given in Figure 3.3 was used to determine the sediment types that will be simulated in the model (d_{50}= 0.03 mm for Tahtali; d_{50}=0.02 mm for Sasal). Sediment types were specified due to these d_{50} values. Only cohesive sediments were simulated in the model since non-cohesive concentration was negligible when compared to cohesive sediments. Based on the conditions specified above, the sediment transport parameters to be used in the simulations were selected as summarized in Table 9.3.

Table 9.3. Sediment transport parameters used in EFDC numerical model

Model Parameter	Value
SEDO: constant initial cohesive sediment concentration in water column (mg/liter)	20
SEDBO: constant initial cohesive sediment in bed per unit area (gr/m^2)	$1.193x10^5$
SDEN: sediment specific volume (m^3/gr)	$4x10^{-7}$
SSG: sediment specific gravity	1.74
WSEDO: constant or reference sediment settling velocity (m/s)	$5x10^{-5}$
TAUD: boundary stress below which deposition takes place (m^2/s^2)	$2x10^{-4}$
TAUR: boundary stress above which deposition takes place (m^2/s^2)	0.013
WRSPO: reference surface erosion rate (g/m^2s)	0.01

At least, 7 days of model run was needed for sediments to settle 29 m (max depth) with the specified settling velocity (0.00005) which was calculated by the formula in equation (9.3);

$$w = \frac{4}{9}\frac{(\gamma_s - \gamma_w)}{\gamma_w} g \frac{d^2}{\nu} \tag{9.3}$$

where; w is the settling velocity of depositing sediment; γ_s is the specific weight of sediment; γ_w is the specific weight of water; g is the acceleration of gravity; d is the diameter of sediment; and ν is the kinematic viscosity of water. The model was run for

two months with the initial conditions described above. The computational grid size of the model was the same grid mentioned in Chapter 5. The sediment thickness results of the model run of 60 days were calculated for 12 years to make a comparison between the numerical model results and the measured deposition in the lake occurred since 1995.

The depositional zones in the lake after 60 days of simulation were shown in Figure 9.3. Deposition rates due to the suspended concentration in the lake did not change significantly but resulted in a uniform structure. On the other hand, deposition due to sediments carried by two rivers (Sasal and Tahtali) showed that the sediments deposited more in deeper areas. It was observed that sediments were carried to long distances only during the flood condition. When sedimentation results were calculated for 12 years, the thickness was calculated about 1 m at deepest regions close to the river entrances. Figure 8.4 shows the transects used for the investigation of sediment deposition by EFDC. The average sediment thickness of the deposited sediment after the simulations was estimated 3 cm in A, B, and C transects respectively (results extrapolated for 12 years).

Using the actual sediment loadings especially during the flood condition would lead to better results for the numerical model results. In addition to this, due to the lack of TSS (total suspended sediment) measurements in the reservoir's tributaries, utilizing a single measured concentration value would be a reason for the differences. Also, the model simulated the lake hydrodynamics for 60 days, but the calculated value by USLE was the result of the whole erosion in the basin which lasted 12 years beginning from 1995, and ending in 2007. Making an extrapolation of the model deposition results for such long time might give erroneous results for the prediction of sediment deposition.

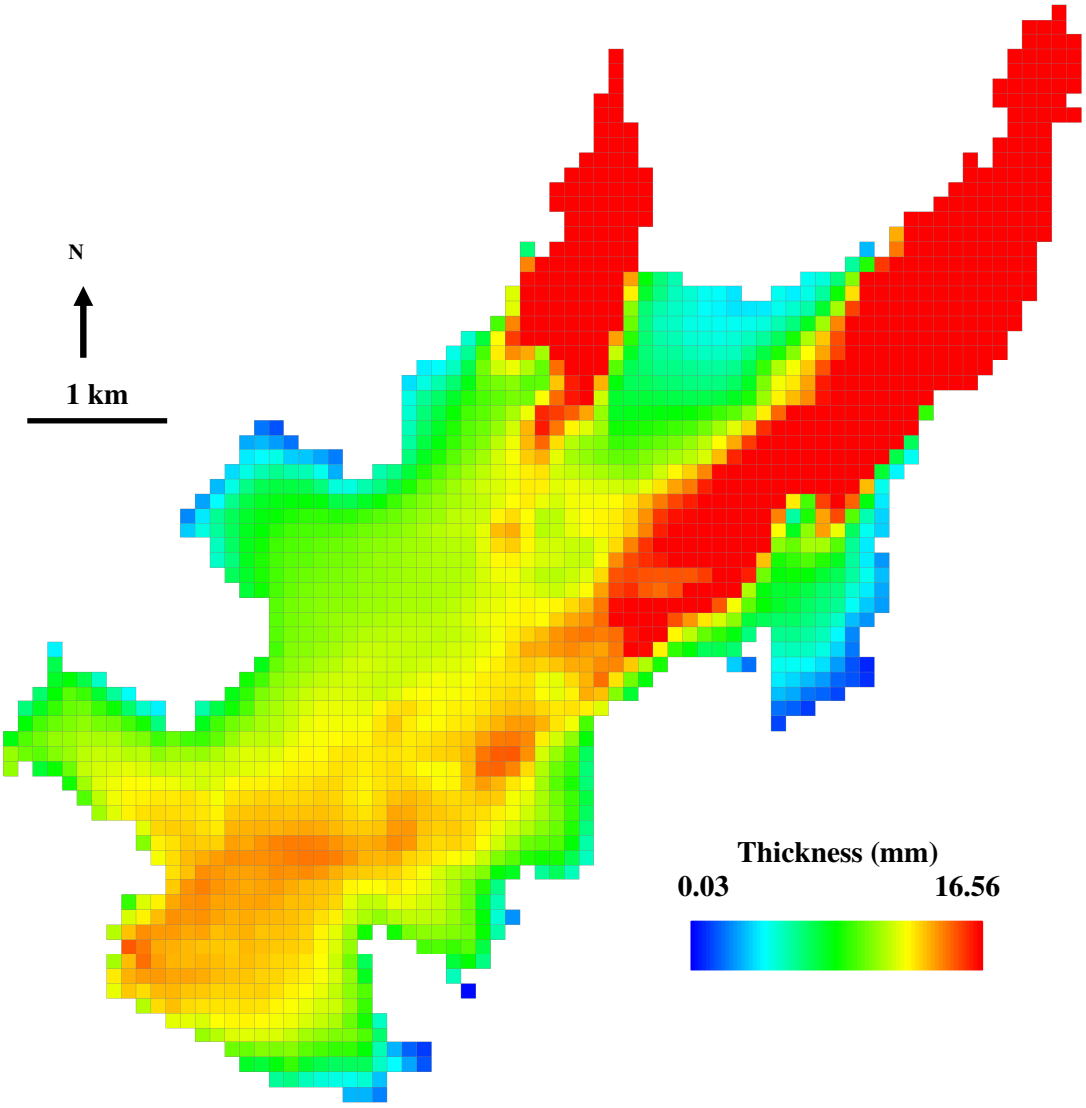

Figure 9.3. Depositional zones in Lake Tahtali after 60 days of run

CHAPTER 10

CONCLUSIONS

This study investigated the hydrodynamics of a thermally stratified reservoir where the focus was given on the effects of stratification on temperature and flow dynamics of reservoir. Within this study, effects of climate change, effect of selective withdrawal of water by intake structure and fate of sediments transported by the tributaries were also investigated. A 3-D numerical model was utilized for this study.

The numerical model was verified with the field observations. The model results were harmonious with the measurements conducted in Lake Tahtali. Depending on the comparisons of velocity measurements, it was concluded that the possible reason for the discrepancy of the model and the simulated velocities was mostly the underestimation of wind stress exerted on the lake surface due to the surrounding topography. Thus, the correct measurement/estimation of wind distribution over the lake surface is required for better numerical model results. Also, the comparisons between the model results and the measured data were performed using measurements at a single point. Collecting data at different stations would lead to better insight about the hydrodynamic structure of the lake.

The comparisons were also made for the measured and simulated time series of temperature data at the thermocline point. The numerical model results were in good agreement with the measurements. The discrepancies between measured and modeled values (RMSE: 0.97 (August) and 0.57 ºC (October)) can be attributed to hydrostatic assumption used in the numerical model. Hydrostatic assumption, in which vertical accelerations are neglected, introduces artificial numerical diffusion of the density

structure. Thus, the amplitudes of the internal waves observed in August were damped faster than the physical processes observed in the lake.

The existence of stratification in the lake was validated by both field measurements and nondimensional analysis to assess the degree of stratification. The effects of stratification on hydrodynamics of the lake were discussed using numerical model simulations. The results indicated that lake is strongly stratified, and the thermocline point behaved as a barrier under stratified conditions. It was observed that, the velocities decreased and changed direction till the thermocline depth and increased after that point. Winds bigger than 3m/s was the required limit for mixing in the lake.

The effect of withdrawal level on stratification patterns of the lake was also investigated through numerical modeling. The analysis was conducted using four different outlets located along the water intake structure of Tahtali Reservoir in Turkey and the effects of withdrawal on thermal stratification structure were discussed. Selective withdrawal of water in reservoirs is commonly used to control the quality of water released. Numerical analysis based on different outlets indicated that withdrawing water from bottom outlet would lead to water quality enhancement within the lake. Withdrawing warmer water from epilimnion resulted in the preservation of the cooler water in hypolimnion whereas withdrawal from thermocline and hypolimnion caused warming of the hypolimnetic water, coinciding with the results obtained from literature (Kennedy 1999). Since warming of the hypolimnion results in decrease in the thermal stability of the water column, decreased stability can promote vertical entrainment of nutrients in the epilimnion (Effler, et al. 1986). In Tahtali Reservoir, the hypolimnetic water became warmer when the water was extracted under thermocline.

Sustainable management of the water resources under climate change stress in today's world necessitates better understanding of the hydrodynamics in reservoirs. The

effect of climate change on hydrodynamics was simulated and observed that 10% increase in air temperatures would result in 7% increase in surface air temperatures. Due to the warming of water surface, stratification started at 1 m upper point in the water column. Decreasing amounts of rain caused increase in surface water temperatures between 20% and 25%.

The sedimentation volume estimated using numerical model was compared with the volume of the deposited sediments estimated by Universal Soil Loss Equation (USLE). Sediment yield estimated by USLE since the construction of reservoir (1995) was 19.6×10^{6} tons. The total deposited sediment rate (only carried by two rivers) was $2.0\text{x}10^{6}$ tons when simulated using the numerical model. Due to the model results, the deposited sediment by rivers was 1/10 of the total erosion rate of the basin. Model results indicated sedimentation zones corresponding to the deep regions of the lake provided valuable information about the capacity of the reservoir that will be used for future management of the reservoir.

This study investigated the effects of hydrodynamics, withdrawal, climate change and sediment deposition on stratification patterns of Lake Tahtali, where the results are applicable to many others in the world. The results will also guide further investigation in the lake such as modeling of water quality.

REFERENCES

Ambrosetti, W., Barbanti, L., Sala, N. 2003. Residence time and physical processes in lakes. *Journal of Limnology* 62 (1): 1-15.

Anohin, V.A., Imberger, J., Romero, J.R., Ivey, G.N. 2006. Effect of Long Internal Waves on the Quality of Water Withdrawn from a Stratified Reservoir. *Journal of Hydraulic Engineering ASCE*, 132(11): 1134-1145.

Appelgren, A., Bergstrom, U., Brittain, J., Gallego, Diaz E., Hakanson, L., Heling, R., Monte, L. 1996. An outline of a model-based expert system to identify optimal remedial strategies for restoring contaminated aquatic ecosystems. *The project MOIRA. ENEA, Report* RT/AMB/96/17.

Appt, J., Imberger, J., Kobus, H. 2004. Basin-scale motion in stratified Upper Lake Constance. *Limnology and Oceanography* 49(4): 919-933.

Arnold, J.G., Bircket, M.D., Williams, J.R., Smith, W.F., McGill, H.N. 1987. Modeling the effects of urbanization on basin water yield and reservoir sedimentation. *Water Resources Bull.,* 23(6), Amer. Water Resources Assoc., 1101-1107.

Bell, V.A., George. D.G., Moore, R.J., Parker, J. 2006. Using a 1-D mixing model to simulate the vertical flux of heat and oxygen in a lake subject to episodic mixing. *Ecological Modeling* 190: 41-54.

Bonnet, M., Poulin, M., Devaux, J. 2000. Numerical modeling of thermal stratification in a lake reservoir. Methodology and case study. *Aquatic Science* 62: 105-124.

Brooks, N.H., Koh, R.C.Y. 1965. Discharge of Sewage Effluent from a Line Source into a Stratified Ocean. *Intern. Assoc. for Hyd. Res. ,* IXth Congress, Leningrad, Paper 2.19.

Blumber, A.F. and Mellor, G.L. 1987. A description of a three dimensional coastal ocean circulation model. *In: N.S. Heaps (ed.).* Three dimensional coastal ocean models, American Geophysical Union, Washington, D.C., 1-16.

Blumber, A.F., Khan, L.A., St. John, J.P. 1999. Three dimensional hydrodynamic model of New York Harbor Region. *Journal of Hydraulic Engineering. ASCE* 125 (8): 799-815.

Çalışkan, A. and Elçi, Ş. 2007. Effects of Selective Withdrawal on Hydrodynamics of a Stratified Reservoir. Accepted to be published in *Water Resources Management* DOI: 10.1007/s11269-008-9325-x

Casamitjana, X., Serra, T., Colomer, J., Baserba, C., Pérez-Losada J. 2003. Effects of the water withdrawal in the stratification patterns of a reservoir. *Hydrobiologia* 504: 21-28.

Cesare, G.D., Boillat, J.L., Schleiss, J. 2006. Circulation in Stratified Lakes due to Flood-Induced Turbidity Currents. *Journal of Environmental Engineering* 132:11 (1508).

Cole, J.J., Caraco, N.F., Kling, G.W., Kratz, T.K.1994. Carbon dioxide supersaturation in the surface waters of lakes. *Science* 265: 1568-1570.

Collins, W., Gregory, R., Anderson, J. 1996. A digital approach to seabed classification. *Sea Technology* 37 (8): 83–87.

Debler, W.R. 1969. On the analogy between thermal and rotational hydrodynamic stability. *Journal of Fluid Mechanics* 24: 165-176.

DEU-SUMER. 2006. Final Report for Modeling for Climate Change Effects in the Gediz and Büyük Menderes River Basins.

Doğan, O. 2002. Türkiye yağışlarının erozyon oluşturma gücü ve üniversal toprak kaybı eşitliğinin yağış erozyon indis değerleri. *Köy Hizmetleri Genel Müdürlüğü, Ankara Araştırma Enstitüsü Müdürlüğü Yayınları*, Genel Yayın No:220, Rapor Seri No:120, Ankara.

Dortch, M. S. 1997. Water Quality Considerations in Reservoir Management. Water Resources Update. *Universities Council on Water Resources*, Southern Illinois, University Carbondale, IL.

Effler, S.W., Wodka, C.T., Driscoll, C., Brooks, M., Perkins & E. M. Owens. 1986. Entrainment base flux of phosphorus in Onondaga Lake, *ASCE. Journal of Environmental Engineering* 112: 617-622.

Elçi, Ş. 2004. Modeling of hydrodynamic circulation and cohesive sediment transport and prediction of shoreline erosion in Hartwell Lake SC/ GA. *PhD Thesis*.Georgia Institute of Technology, pp. 242.

Elçi, Ş. and Work, P.A. 2004. Field Observations for Definition of Hydrodynamic Circulation in Hartwell Lake, SC/ GA. in *Sixth International Conference on Advances in Civil Engineering (ACE 2004)*. Bogazici University, Istanbul, 6-8 October 2004, Vol. 2, edited by T. Ozturan, Istanbul Kansu Printing Office, 2004, 1228-1237.

Elçi, Ş., Work, P.A., Hayter, E.J. 2007. Influence of Stratification and Shoreline Erosion on Reservoir Sedimentation Patterns. *Journal of Hydraulic Engineering* 133 (3): 255-266.

Elçi, Ş., Bor, A., Calışkan A. 2008. Utilizing Acoustic Methods for Sedimentation Prediction. *Submitted to Environmental Monitoring and Assessment.*

Elwin, E.H. and Slotta, L.S. 1969. Entering streamflow effects on currents of a density stratified model reservoir. *Engineering Experiment Station Oregon State University,* Corvallis, U.S.A., Bulletin no. 44.

EPA 2006. Environmental fluid dynamics code.
http:// www.epa.gov /ATHENS/ wwqtsc/html/efdc.html
(accessed October, 2006).

Falconer, R.A., George, D.G., Hall, P. 1991. Three-dimensional numerical modeling of wind driven circulation in a shallow homogenous lake. *Journal of Hydrology* 124: 59-79.

Fan, J. and Morris, G. 1992. Reservoir sedimentation. I: Delta and density current deposits. *Journal of Hydraulic Engineering*. *ASCE* 118(3): 354-369.

Fischer, H.B., List, E.G., Koh, R.C. Y., Imberger, J. & Brooks, N. H. 1979. *Mixing in Inland and Coastal Waters.* Academic Press. New York, NY.

Galperin, B., Kantha, L. H., Hassid, S., and Rosati, A. 1988. A quasiequilibrium turbulent energy model for geophysical flows. *J. Atmospheric Sci.*, 45: 55–62.

Golson, K.F., Tsegaye, T.D., Rajbhandari, N.B., Green, T.H.., Coleman, T.L. 2000. Evaluating Modified Rainfall Erosivity Factors in the Universal Soil Loss Equation. *Geoscience and Remote Sensing Symposium Proceedings*. Honolulu, HI, USA. IGARSS IEEE 2000 International Vol:5. 2017-2020.

Graf, W. H. 1984. *Hydraulics of sediment transport.* Water Resources Publications Littleton, CO.

Guy, H.P., Simons, D.B., Richardson, E.V. 1966. Summary of alluvial channel data from flume experiments. *Professional Paper 462-I*. United States Geological Society, Washington, D.C.

Håkanson, L. 1996. A new, simple, general technique to predict seasonal variability of river discharge and lake temperature for lake ecosystem models. *Ecological Modeling* 88: pp. 157–181.

Hamrick, J.M. 1996. Users manual for the environmental fluid dynamic computer code. *Virginia Institute of Marine Science*. Special Report 328, 224 pp.

Harmancioglu, N.B. and Ozkul, S. 2008. Assessment of Global Warming at Basin Scale. *Geophysical Research Abstracts*, Vol. 10, EGU2008-A-12004.

Higginbottom, I., Hundley, A., Pauly, T. 1994. A Desktop Study of Some Acoustic Seabed Classification Systems. *Unpublished report by Sonar Data* Tasmania/Offshore Scientific Pty Ltd. 21 pp.

Hill, D.K. and Magnuson, J.J. 1990. Potential effects of global climate warming on the growth and prey consumption of Great Lakes fish. *Trans. Am. Fish Soc*. 119: 265-275.

Hondzo, M. and Stefan, H.G. 1991. Three case studies of lake temperature and stratification response to warmer climate. *Water Resources Research* 27 (8): 1837-1846, 1991.

Hotchkiss, R. H., and Parker, G. 1991. Shock fitting of aggradational profiles due to backwater. *Journal of Hydraulic Engineering* 117(9): 1129-1144.

Imberger, J. 1998. *Physical Processes in Lakes and Oceans*. AGU Coastal and Estuarine Studies. Volume 54.

IPCC 2001. Climate Change 2001: The Scientific Basis. *IPCC Third Assessment Report.* Cambridge: Cambridge University Press.

Ivey, GN. and Blake, S. 1985. Axisymetric withdrawal and inflow in a density-stratified container. *Journal of Fluid Mechanics* 161: 115-137.

Jin, K.R. and Ji, Z.G. 2005. Application and validation of three dimensional model in a shallow lake. *Journal of Waterway, Port, Coastal, Ocean Engineering*. *ASCE* 131 (5): 213-225.

Jin, K.R., Hamrick, J.H., Tisdale, T. 2000. Application of three-dimensional hydrodynamic model for Lake Okeechobee. *Journal of Hydraulic Engineering* 126(10): 758-771.

Johnson, B.H., Kim, K.W., Heath, R.E., Hsieh, B.B., Butler, H.L. 1993. Validation of Three-Dimensional Hydrodynamic Model of Chesapeake Bay. *Journal of Hydraulic Engineering* Vol:119, No:1.

Kennedy, R.H. 1999. Reservoir design and operation: limnological implications and management opportunities. In Tundisi, J.G.&M. Straskraba (eds), *Theoretical Reservoir Ecology and its Applications*. Backhuys Publishers. Leiden. The Nederlands. 1-28.

Krone, R.B. 1962. Flume studies of the transport of sediment in estuarial shoaling processes. *Hydr. Eng. Lab. And Sanitary Eng. Lab*., University of California, Berkeley, CA.

Leon, L.F., Lam, D., Schertzer, W., Swayne, D. 2005. Lake and climate models linkage: a 3-D hydrodynamic contribution. *Advances in Geosciences* 4: 57-62.

Lindenscmidt, K.E. and Hamblin, P.F. 1997. Hypolimnetic aeration in Lake Tegel, Berlin. *Water Research,* Volume 31, Issue 7, Pages 1619-1628.

Lo, K.F.A., 1994. Quantifying soil erosion for Shihmen Reservoir watershed, Taiwan. *Agricultural Sysyems*, 45, Elsevier, 105-116.

MacIntyre, S., James, O.S., Sarah, A.G., George, W.K. 2006. Physical pathways of nutrient supply in a small, ultraoligotrophic arctic lake during summer stratification. *Limnology and Oceanography* 51(2): 2006, 1107–1124.

Mahony, J.J. and Pritchard, W.G. 1981. Withdrawal from a reservoir of stratified fluid. *Proceedings of the Royal Society of London*. Series A, Mathematical and Physical Sciences, Volume 376, Issue 1767, pp. 499-523.

Manual on Sediment Management and Measurement. 2003. *World Meteorological Organization Operational Hydrology.* Report No. 47

Matzinger, A., Schmid, M., Veljanoska, S.E., Patceva, S., Guseska, D., Wagner, B., Müller, B., Sturm, M., Wüest, A. 2007. Eutrophication of ancient Lake Ohrid: Global warming amplifies detrimental effects of increased nutrient inputs, *Limnology and Oceanography* 52 (1): 338-353, 2007.

McLain, A.S., Magnuson, J.J., Hill, D.K. 1994. Latitudinal and longitudinal differences in thermal habitat for fishes influenced by climate warming: Expectations from simulations. *Int. Ver. Theor. Angew. Limnol. Verh*. 25: 2080- 2085.

Mehta, A.J., Carey, W.P., Hayter, E.J., Heltzel, S.B., Krone, R.B., McAnally, W.H., Jr., Parker, W.R., Schoellhamer, D., and Teeter, A.M. 1989. Cohesive sediment transport: Part 1 process description ; Part 2, Application. *Journal of Hydraulic Eng.,* 115(8): ASCE, 1076-1112.

Mellor, G. L. and Yamada, T. 1982. Development of a turbulence closure model for geophysical fluid problems. *Rev. Geophys. Space Phys.*, 20: 851–875.

Ministry of Agriculture and Rural Affairs, 2006. Universal Soil Loss Equation Manual for Turkey. *Tagem-BB-Topraks,* Institute publish number 225, Technical publish number 25, Tokat Soil and Water Resources Research Institute.

Minns, C.K. and Moore, J.E. 1992. Predicting the impact of climate change on the spatial pattern of freshwater fish yield capability in eastern Canadian lakes. *Clim. Change* 22: 327-346.

Monte, L., Hakanson, L., Brittain, J. 1997. Prototype models for the MOIRA computerized system. *ENEA, Report.* RT/AMB/97/5.

Odhiambo, B.K. and Boss, S.K. 2004. Integrated Echo Sounder, Gps, and Gis for Reservoir Sedimentation studies: Examples from Two Arkansas Lakes, *Journal of the American Water Resources Association.* Paper no: 02061.

Ottosson, F. and Abrahamsson, O. 1998. Presentation and analysis of a model simulating epilimnetic and hypolimnetic temperatures in lakes. pp. 26

Patterson, J.C., Hamblin, P.F., Imberger, J. 1984. Classification and dynamic simulation of the vertical density structure of lakes. *Limnology and Oceanography* 29 (4): 845-861.

Rueda, F.J. and Schladow, S.G. 2003. Dynamics of Large Polymictic Lake. II: Numerical Simulations. *Journal of Hydraulic Engineering* 129(2): 92-101.

Rueda, F.J., Schladow, S.G., Monismith, S.G., Stacey, M.T. 2003. Dynamics of Large Polymictic Lake. I: Field Observations. Journal of Hydraulic Engineering 129(2): 82-91.

Schladow, S.G., and Thompson, K.L. 2000. Winter thermal structure of Lake Tahoe. *Limnology and Oceanography*. American Chemical Society, Washington, DC.

Sheng, Y.P. 1984. A turbulent transport model of coastal processes. *Proc. 19th Int. Conf.On Coastal Eng., ASCE* 2380-2396.

Shuter, B.J. and Post, J.R. 1990. Climate, population, viability, and the zoogeography of temperature fishes. *Trans. Am. Fish Soc*. 119: 314-336.

Smolarkiewicz, P. K., and T. L. Clark, 1986.The multidimensional positive definite advection transport algorithm: further development and applications. *J. Comp. Phys.*, 67, 396-438.

Spiegel, R. H., and Imberger, J. 1980. The classification of mixed-layer dynamics in lakes of small to medium size. *Journal of Physical Oceanography* 10, pp. 1104-1121.

Soni, J.P. 1981. Laboratory Study of Aggradation in Alluvial Channels, *Journal of Hydrology* 49: 87-106.

Stasio, B.T., Hill, D.K., Kleinhans, J.M., Nibbelink, N.B., Magnuson, J.J. 1996. Potential effects of global climate change on small north-temperature lakes: Physics, fish, and plankton. *Limnology and Oceanography* 41(5): 1136-1149.

Stefan, H.G. and Fang, X. 1994. Dissolved oxygen model for regional lake analysis. *Ecol. Model* 71: 37-68.

Tetra Tech, 1999. Theoretical and computational aspects of sediment transport in the EFDC model. *Technical Rep. Prepared for U.S. Environmental Protection Agency*, Tetra Tech, Inc., Fairfax, Va.

The Ministry of Environment and Forestry. 2007. Fist National Communication of Turkey on Climate Change. Report, Implemented by United Nations Development Program (UNDP), Turkey, Edited by Günay Apak and Bahar Ubay.

Tucker, G.E. and Slingerland, R. 1997. Drainage basin responses to climate change. *Water Resources Research* Vol. 33, No:8: Pages 2031-2047.

Urick, R. J. 1983. Principles of Underwater Sound, Peninsula Publishing, Los Altos.

Walesh, S.G. and Monkmeyer, P.L.1970. Withdrawal of a viscous density-stratified fluid from the bottom of a reservoir. *Preprint of a paper presented at the National Water Resources Engineering meeting,* ASCE, Memphis, Tennessee.

Wood, I.R. 2001. Extensions to the theory of selective withdrawal. *Journal of Fluid Mechanics* 448: 315-333.

Wood, I.R. and Binney, P. 1976. Selective withdrawal from a Two-Layered Fluid. Research Report. Department of Civil Engineering, Univ. of Canterbury, Christchurch, New Zealand.

Yang, Z., Khangaonkar, T., DeGasperi, C., Marshall, K. 2000. Three-dimensional modeling of temperature stratification and density-driven circulation in Lake Billy Chinook, Oregon. *Proc. 6th Int. Conf, Estuarine and Coastal Modeling, ASCE* 411-425.